



University of Kentucky  
UKnowledge

---

University of Kentucky Doctoral Dissertations

Graduate School

---

2008

## BENZENE-1,3-DIAMIDOETHANETHIOL (BDETH2) AND ITS METAL COMPOUNDS

Kamruz Md Zaman

*University of Kentucky*, kmzama2@uky.edu

[Right click to open a feedback form in a new tab to let us know how this document benefits you.](#)

---

### Recommended Citation

Zaman, Kamruz Md, "BENZENE-1,3-DIAMIDOETHANETHIOL (BDETH2) AND ITS METAL COMPOUNDS" (2008). *University of Kentucky Doctoral Dissertations*. 644.  
[https://uknowledge.uky.edu/gradschool\\_diss/644](https://uknowledge.uky.edu/gradschool_diss/644)

This Dissertation is brought to you for free and open access by the Graduate School at UKnowledge. It has been accepted for inclusion in University of Kentucky Doctoral Dissertations by an authorized administrator of UKnowledge. For more information, please contact [UKnowledge@lsv.uky.edu](mailto:UKnowledge@lsv.uky.edu).

ABSTRACT OF DISSERTATION

Kamruz Md Zaman

The Graduate School  
University of Kentucky

2008

BENZENE-1,3-DIAMIDOETHANETHIOL (BDETH2) AND ITS METAL  
COMPOUNDS

---

ABSTRACT OF DISSERTATION

---

A dissertation submitted in partial fulfillment of the requirement for the degree of Doctor  
of Philosophy in the College of Arts and Science at the University of Kentucky

By

Kamruz Md Zaman

Lexington, Kentucky

Director: Dr. David A. Atwood, Professor of Chemistry

Lexington, Kentucky

2008

Copyright © Kamruz Md Zaman 2008

## ABSTRACT OF DISSERTATION

### BENZENE-1,3-DIAMIDOETHANETHIOL (BDETH<sub>2</sub>) AND ITS METAL COMPOUNDS

There is a global need to find a permanent and readily implemented solution to the problem of heavy metal pollution in aqueous environments. A dithiol compound, benzene-1,3-diamidoethanethiol (BDETH<sub>2</sub>), also known as *N,N'*-bis(2-mercaptoethyl) isophthalamide or *N,N'*-bis(2-mercaptoethyl)-1,3-benzenedicarboxamide, capable of binding divalent metal ions, has been synthesized and characterized. A broad range of BDET-metal compounds, spanning the periodic chart, has been prepared and characterized by IR, MS, EA, Raman, XAFS and TGA. The characteristics of the BDET-M compounds were determined through secondary reactions. In an effort to derivatize BDET-M compounds through alkylaluminum a new cyclic compound, 1,3-bis(4,5-dihydrothiazolo)benzene, has been synthesized by refluxing BDETH<sub>2</sub> in the presence of AlMe<sub>3</sub>.

Mineral coating studies have been performed and it was found that coating with BDET prevents metal leaching. XPS studies indicated that covalent bonds exist between BDET and metals at the mineral surfaces.

BDETH<sub>2</sub> is not water soluble and must be used as an ethanolic solution to precipitate metals from water. In an effort to find similar ligands that are water-soluble another dithiol compound, *N,N'*-bis(2-mercaptoethyl)oxalamide (MOA), and a monothiol compound, *N*-mercaptoethyl-furoylamide (MFA), have been synthesized. Each was found to precipitate Cd, Hg and Pb from water, to varying degrees. Some metal compounds of MOA, MFA and dithiothreitol (DTT), a water-soluble dithiol compound have been prepared and characterized. These compounds provide insight into the properties of the BDET-M compounds. For example, it was shown that insolubility in water is a common feature of thiol compounds and is not unique to BDET-M compounds.

KEYWORDS: BDETH<sub>2</sub>, BDET-M, XAFS, AMD, XPS.

Kamruz Md Zaman

---

July 31, 2008

---

BENZENE-1,3-DIAMIDOETHANETHIOL (BDETH2) AND ITS METAL  
COMPOUNDS

By

Kamruz Md Zaman

Dr. David A. Atwood

---

Director of Dissertation

Dr. Robert B. Grossman

---

Director of Graduate Studies

July 31, 2008

---



DISSERTATION

Kamruz Md Zaman

The Graduate School  
University of Kentucky

2008

BENZENE-1,3-DIAMIDOETHANETHIOL (BDETH2) AND ITS METAL  
COMPOUNDS

---

DISSERTATION

---

A dissertation submitted in partial fulfillment of the  
requirement for the degree of Doctor of Philosophy in the  
College of Arts and Science at the University of Kentucky

By

Kamruz Md Zaman

Lexington, Kentucky

Director: Dr. David A. Atwood, Professor of Chemistry

Lexington, Kentucky

2008

Copyright © Kamruz Md Zaman 2008

## DEDICATION

This dissertation is dedicated to my late parents

Mr. Abdul Wahed Sarker

And

Mrs. Ayesha Akhter Begum

Who always inspired me to pursue higher education

## ACKNOWLEDGEMENTS

I would like to thank my research supervisor, Dr. David A. Atwood, for his guidance and help in completing my doctoral program in chemistry at the University of Kentucky. I would also like to thank the other members of my graduate committee, Dr. J. Selegue, Dr. E. DeMoll and Dr. M. Mullen, for their suggestions and assistance. I would also like to thank my wife, Jewel, who always stood by me and extended her support to me in times of hardship. I would like to mention my daughter, Mahin, who always inspires me to do something special. Finally, I would like to thank my brothers and sisters for their encouragement and support.

## TABLE OF CONTENTS

Acknowledgements.....	iii
List of Tables.....	vii
List of Figures.....	viii
List of Files.....	x
Chapter 1: Introduction	
1.1 Statement of Purpose.....	1
1.2 Metal and Metalloid Contaminants in the Environment.....	2
1.2.1 Iron.....	3
1.2.2 Cobalt.....	4
1.2.3 Nickel.....	5
1.2.4 Copper.....	6
1.2.5 Cadmium.....	6
1.2.6 Mercury.....	7
1.2.7 Lead.....	9
1.2.8 Arsenic.....	9
1.3 Methods for Removing Heavy Metals.....	10
1.3.1 Phytoremediation.....	11
1.3.2 Constructed Wetlands.....	13
1.3.3 Bioremediation.....	14
1.3.4 Activated Carbon Adsorption.....	17
1.3.5 Adsorbents from Agricultural and Forest Wastes.....	17
1.3.6 Ion-exchange Resins.....	18
1.3.7 Polythiol-functionalized Alumina Membranes.....	19
1.3.8 Nanoporous Adsorbent Materials.....	19
1.3.9 Crown Thioethers.....	21
1.3.10 Polymeric Chelating Fibers.....	22
1.3.11 Tunable Biopolymers.....	22
1.3.12 Extraction from Aqueous Solutions.....	24
1.3.12.2 Surfactants.....	24
1.3.13 Chemical Precipitation.....	25
1.4 Conclusions.....	44
Chapter 2: Metal Compounds of BDETH <sub>2</sub>	
2.1 Overview.....	46
2.2 Alkali and Alkaline Earth Metal Thiolates.....	47
2.2.1 Alkali Metal Thiolates.....	48
2.2.2 Alkali Metal Compounds of BDETH <sub>2</sub> .....	49
2.2.3 Alkaline Earth Metal Thiolates.....	53
2.2.4 Alkaline Earth Metal Compounds of BDETH <sub>2</sub> .....	54

2.2.5	Conclusions.....	55
2.3	Transition Metal Thiolates.....	56
2.3.1	Transition Metal Complexes of BDETH <sub>2</sub> .....	57
2.3.2	Conclusions.....	60
2.4	Main Group Metal Thiolates.....	61
2.4.1	Cadmium Complexes.....	62
2.4.2	Mercury Complexes.....	63
2.4.3	Tin Complexes.....	64
2.4.4	Lead Complexes.....	66
2.4.5	Arsenic Compounds.....	68
2.4.6	Main Group Compounds of BDETH <sub>2</sub> .....	71
2.5	Attempted Metallation of BDET-Metal Compounds.....	85
2.6	Experimental.....	87
2.6.1	General Considerations.....	87
2.6.2	Syntheses.....	88
2.6.3	Leaching Studies.....	97
Chapter 3: Attempted Alkylaluminum		
3.1	Overview.....	99
3.2	Synthesis and Characterization.....	101
3.3	Experimental.....	106
3.4	Conclusions.....	107
Chapter 4: <i>N,N'</i> -Bis(2-mercaptoethyl) oxalamide (MOA)		
4.1	Overview.....	109
4.2	Synthesis and Characterization.....	109
4.3	Experimental.....	114
4.4	Conclusions.....	117
Chapter 5: Metal Compounds of Dithiothreitol (DTT)		
5.1	Overview.....	119
5.2	Synthesis and Characterization.....	120
5.3	Experimental.....	124
5.4	Conclusions.....	127
Chapter 6: <i>N</i> -Mercaptoethylfuroylamide (MFA)		
6.1	Overview.....	128
6.2	Synthesis and Characterization.....	128
6.3	Experimental.....	132
6.4	Conclusions.....	136
Chapter 7: Mineral Coating Study		
7.1	Overview.....	137
7.2	Results and Discussion.....	142
7.2.1	Cinnabar.....	142
7.2.2	Realgar.....	144

7.2.3 Sphalerite.....	146
7.2.4 Galena.....	147
7.2.5 Covellite.....	148
7.2.6 Pyrite.....	150
7.2.7 Chalcopyrite.....	152
7.3 Examination of the BDET-coated Mineral Surface.....	153
7.4 Experimental.....	160
7.4.1 General Considerations.....	160
7.4.2 Sample Preparation.....	161
7.4.3 Analytical Techniques.....	162
7.5 Conclusions.....	163
 Chapter 8: Conclusions and Suggestions for Future Work	
8.1 Conclusions.....	166
8.2 Future Work.....	168
 References.....	171
 Vita.....	188

## LIST OF TABLES

Table 1.1, Results of Cd(II) and Cu(II) binding by PyDET.....	35
Table 1.2, Crystallographic data for BDETH <sub>2</sub> .....	38
Table 1.3, ICP and CVAA results of BDETH <sub>2</sub> with Pb(II) and Hg(II).....	41
Table 1.4, Results of gold ore leaching studies.....	43
Table 1.5, Results of BDET-Fe leaching.....	43
Table 2.1, FEFF parameters derived for cinnabar (hexagonal HgS).....	81
Table 2.2, FEFF parameters derived for BDET-Hg based on cinnabar parameters..	81
Table 2.3, Results of leaching studies for BDET-Cd, BDET-Hg and BDET-Pb.....	83
Table 3.1, Crystallographic data table for compound <b>15</b> .....	105
Table 5.1, Crystallographic data table for compound <b>23</b> .....	123
Table 7.1, Heavy metal leaching of coal samples, uncoated and BDET-coated.....	142
Table 7.2, XPS core level shifts of mineral sulfide binding with BDETH <sub>2</sub> .....	155

## LIST OF FIGURES

Figure 1.1, SDTC: metal binding and generation of toxic byproducts.....	30
Figure 1.2, Metal binding by STC.....	31
Figure 1.3, Metal binding by TMT.....	31
Figure 1.4, Computer drawing of PyDET.....	34
Figure 1.5, Proposed structure of a PyDET metal complex.....	34
Figure 1.6, Crystal structure of BDETH <sub>2</sub> .....	38
Figure 1.7, Intermolecular hydrogen bonding in BDETH <sub>2</sub> .....	39
Figure 1.8, ORTEP view of [Hg(SCH <sub>2</sub> CH <sub>2</sub> NH <sub>2</sub> ) <sub>2</sub> ](Cl) <sub>2</sub> .....	41
Figure 2.1, A compound containing two S-Na bonds.....	49
Figure 2.2, Proposed structures of alkali and alkaline earth metal BDET-Metal compounds.....	56
Figure 2.3, Proposed structure for the transition metal compounds of BDETH <sub>2</sub> .....	61
Figure 2.4, Molecular structure of [Cd(SCH <sub>2</sub> CH <sub>2</sub> NH <sub>2</sub> ) <sub>2</sub> ].....	62
Figure 2.5, View of the unit cell of [Cd(SCH <sub>2</sub> CH <sub>2</sub> NH <sub>2</sub> ) <sub>2</sub> ].....	63
Figure 2.6, Crystal structure of [Hg(S-2,4,6- <i>i</i> Pr <sub>3</sub> C <sub>6</sub> H <sub>2</sub> ) <sub>2</sub> ].....	64
Figure 2.7, Crystal structure of Sn(CEE) <sub>2</sub> .....	65
Figure 2.8, Crystal structure of [MeSn{N(CH <sub>2</sub> CH <sub>2</sub> CH <sub>2</sub> S)} <sub>3</sub> ] <sub>2</sub> .....	66
Figure 2.9, a) Crystal structure of Pb(SCH <sub>2</sub> CH <sub>2</sub> NH <sub>2</sub> ) <sub>2</sub> ; b) Packing diagram showing NH···S hydrogen bonds.....	67
Figure 2.10, Molecular structure of [Pb <sub>2</sub> Cl(SCH <sub>2</sub> CH <sub>2</sub> NH <sub>2</sub> ) <sub>3</sub> ].....	68
Figure 2.11 Structure of As <sub>2</sub> S <sub>3</sub> (C <sub>6</sub> H <sub>5</sub> ) <sub>2</sub> .....	69
Figure 2.12, Crystal structure of 2-iodo-1,3,2-dithiarsolane.....	70
Figure 2.13, a) Mercury binding to sulfurs, polymeric; b) monodentate gold binding; c) bidentate gold binding.....	77
Figure 2.14, Sulfur XANES spectra for HgS, BDET-Hg and BDETH <sub>2</sub> .....	78
Figure 2.15, a) Hg L <sub>III</sub> -edge XANES spectra for HgS and BDET-Hg; b) first derivative Hg L <sub>III</sub> -edge XANES spectrum.....	79
Figure 2.16, a) EXAFS oscillations isolated from the XAFS spectrum and displayed as $k^3\chi$ vs $k$ ; b) Radial structure function obtained by applying a Fourier transform to the $k^3\chi$ spectra shown in panel a....	80
Figure 2.17, Comparison of the FEFF model function and data for (a) the Hg-S shell in RSF back-transformed to k-space for cinnabar, HgS; (b) the Hg-S shell in RSF back transformed to k-space for BDET-Hg; and (c) the total k-space EXAFS oscillations for BDET-Hg.....	82
Figure 2.18, Proposed structures for main group compounds of BDETH <sub>2</sub> .....	85
Figure 3.1, Hypothetical product of reaction between BDET-M and AlMe <sub>3</sub> .....	99
Figure 3.2, Alkylaluminum of a Schiff-base ligand.....	100
Figure 3.3, Hypothetical products of reaction between BDETH <sub>2</sub> and AlMe <sub>3</sub> .....	101
Figure 3.4, Amino-thiol cyclization.....	103
Figure 3.5, Crystal structure of 1,3-bis(4,5-dihydrothiazolo) benzene.....	105
Figure 3.6, Simplified mechanism for the formation of 1,3-bis(4,5-dihydrothiazolo)benzene.....	108
Figure 4.1, Product of intramolecular cyclization of MOA.....	112

Figure 4.2, Proposed structures of MOA-Metal compounds.....	118
Figure 5.1, Dithiothreitol (DTT).....	119
Figure 5.2, Crystal structure of the disulfide form of DTT.....	123
Figure 5.3, Proposed structures of DTT-Metal compounds.....	127
Figure 7.1, ICP analysis for cinnabar (HgS) leaching study.....	144
Figure 7.2, ICP analysis for realgar (AsS) leaching study.....	145
Figure 7.3, ICP analysis for sphalerite (ZnS) leaching study.....	147
Figure 7.4, ICP analysis for galena (PbS) leaching study.....	148
Figure 7.5, ICP analysis for covellite (CuS) leaching study.....	150
Figure 7.6, ICP analysis for pyrite (FeS <sub>2</sub> ) leaching study.....	151
Figure 7.7, ICP analysis for chalcopyrite (CuFeS <sub>2</sub> ) leaching study.....	153
Figure 7.8, Photoelectron spectra of the N 1s orbital of (a) BDET as an unbound ligand; and coordinated to (b) PbS and (c) FeS <sub>2</sub> .....	156
Figure 7.9, Photoelectron spectra of the S 2p orbital of fresh (a) PbS; (b) FeS <sub>2</sub> ; (c) unbound BDET; and the complexes of (d) PbS-BDET; and (e) FeS <sub>2</sub> -BDET.....	158
Figure 7.10, Photoelectron spectra of (a) the Pb 4f orbitals (left-hand panel); (b) Fe 2p orbitals (right-hand panel) bound and unbound to BDET...	158
Figure 7.11, Postulated covalent bonding between BDET and metals in minerals....	165

## LIST OF FILES

File Name: KZ Dissertation. pdf (1.5 MB)

# CHAPTER 1

## INTRODUCTION

### 1.1 Statement of Purpose

The objective of this dissertation research was to synthesize a ligand that will bind heavy metals in aqueous environments, to fully characterize the resulting precipitates, and to study the basic chemistry of the metal compounds that formed. It was hypothesized that a ligand containing a soft thiol group will covalently bond with divalent metal cations that are soft or borderline Lewis acids. Since the divalent heavy metal cations are soft in nature it was envisioned that a ligand containing thiol group(s) might effectively remove them from water. The ligand chosen to test this hypothesis was benzene-1,3-diamidoethanethiol (BDETH<sub>2</sub>), also known as *N,N'*-bis(2-mercaptoethyl)-isophthalamide or *N,N'*-bis(2-mercaptoethyl)-1,3-benzenedicarboxamide.

Several investigations with BDETH<sub>2</sub> were carried out prior to this work.<sup>1-10</sup> BDETH<sub>2</sub> was found to be effective in binding heavy metals such as Hg and Pb under laboratory conditions. It also proved capable of binding 1) mercury from gold mining effluent, 2) metals under acid mine drainage conditions, 3) mercury from contaminated soil, and 4) lead from lead battery recycling plant waste water. The results of these investigations will be discussed in the last part of this chapter.

The previous work focused on applications rather than the basic chemistry of BDETH<sub>2</sub> and the BDET-metal compounds. It is clear, however, that knowledge of the composition and characteristics of the BDET-M compounds is critical if the ligand is to be utilized commercially. Thus, the research involved the synthesis and characterization

of a broad range of BDET-M compounds spanning the periodic chart. The prevention of metal leaching by coating coal and sulfur-containing minerals with BDETH<sub>2</sub> was demonstrated. Unsuccessful attempts were made to synthesize a water-soluble analogue of BDETH<sub>2</sub> and derivatize it by introducing a polar group into its aromatic backbone. Another dithiol compound, *N,N'*-bis(2-mercaptoethyl) oxalamide (MOA), and a monothiol compound, *N*-mercaptoethyl-furoylamide (MFA), capable of binding divalent metals, were synthesized and characterized. Some metal compounds of MOA, MFA and dithiothreitol (DTT), a water-soluble dithiol, were synthesized and characterized. A new cyclic compound, 1,3-bis(4,5-dihydrothiazolo)benzene, was prepared from BDETH<sub>2</sub> in an effort to derivatize it with AlMe<sub>3</sub>. This work provides a complete understanding of the chemistry of the BDET-M compounds.

## 1.2 Metal and Metalloid Contaminants in the Environment

Environmentally important metals are generally divided into three different categories.<sup>11</sup> In the first category belong metals like sodium, potassium and calcium. They are considered macro-nutrients in the biosphere. Iron, copper and zinc belong to the second category, called micro-nutrients. Some metals such as cadmium, mercury, lead and arsenic have no known biological function and are generally considered toxic. These are in the third category and are of particular environmental concern.

Cadmium, lead, mercury and arsenic are soft Lewis acids.<sup>12a,12b</sup> They have affinity for soft Lewis bases, such as the sulfhydryl side chain of cysteine, an amino acid. The toxic effects of heavy metals result, in part, due to their bonding with the cysteine

residues in proteins.<sup>13</sup> However, the actual physiological consequences vary from metal to metal.

Although the metals themselves cause environmental pollution, speciation may also create forms with differing toxicity. Organometallic compounds and simple inorganic salts often greatly differ in toxicity. For example, organomercury and organolead compounds are more toxic than inorganic compounds of lead and mercury.<sup>14</sup> The reverse is true for arsenic; organoarsenics are less toxic than inorganic arsenics. Arsenic(V) has been found to be much less toxic than arsenic(III).<sup>15,16</sup> Arsenolipids, which are almost non-toxic, are stored in the tissues of fish and shellfish.<sup>17</sup> The following sections will discuss the chemistry of some metals and metalloids with particular focus on their speciation in water and the form of the element that BDETH<sub>2</sub> is expected to bind.

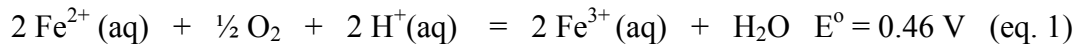
### 1.2.1 Iron

In water systems (both natural waters and their sediments) iron exists in various oxidation states: metallic iron (iron metal), ferrous iron {Fe(II)}, and ferric iron {Fe(III)}. The presence or absence of dissolved oxygen (DO) determines the oxidation state of iron existing in a particular aquatic system. The redox reactions in which iron participates are also largely dependent on the presence of dissolved oxygen.<sup>18</sup>

Bacterial oxidation of particulate organic matter makes the sediments of most bodies of anoxic (i.e. without oxygen) water systems. Iron exists in the sediments of such anoxic environments in the reduced form, ferrous iron {Fe(II)}. It is often found as iron sulfide.

In oxic (i.e. oxygen-containing) water systems iron exists in the oxidized form, ferric iron {Fe(III)}. In these systems it exists as Fe(OH)<sub>3</sub> and Fe<sub>2</sub>O<sub>3</sub>, either particulate or colloidal.

Aqueous solutions of Fe(II) in the absence of complexing anions contain the blue-green ion [Fe(H<sub>2</sub>O)<sub>6</sub>]<sup>2+</sup>, which is oxidized in acid solutions as shown in equation 1.<sup>19</sup>



The hydrolysis of the pale purple ion [Fe(H<sub>2</sub>O)<sub>6</sub>]<sup>3+</sup> is complicated and condition dependent. The main equilibrium at lower concentrations is shown in equation 2.<sup>19</sup>



A small amount of Fe(OH)<sub>2</sub><sup>+</sup> may be formed but the second main species is believed to be the diamagnetic μ-oxo dimer (equation 3).<sup>19</sup>



Fe<sup>2+</sup> and Fe<sup>3+</sup> have been implicated in the generation of acid mine drainage. This will be discussed in detail in chapter 7.

### 1.2.2 Cobalt

In aqueous solutions cobalt exists in both Co(II) and Co(III) forms. In basic media Co<sup>2+</sup> exists as Co(OH)<sub>2</sub>, which may be pink or blue. It is amphoteric, dissolving in

concentrated hydroxide solutions to give a deep blue solution containing  $[\text{Co}(\text{OH})_4]^{2-}$  ions. Oxidation of  $[\text{Co}(\text{H}_2\text{O})_6]^{2+}$  to  $\text{Co}^{3+}$  is very unfavorable in aqueous solutions (equation 4).<sup>20</sup>



$[\text{Co}(\text{H}_2\text{O})_6]^{3+}$  can be generated by electrolytic or  $\text{O}_3$  oxidation of cold acidic perchlorate solutions of Co(II).  $[\text{Co}(\text{H}_2\text{O})_6]^{3+}$  lies in equilibrium with  $[\text{Co}(\text{OH})(\text{H}_2\text{O})_5]^{2+}$ .<sup>20</sup>

### 1.2.3 Nickel

Nickel has a tendency to complex with both inorganic and organic ligands in water systems. The green hexaaquanickel(II) ion,  $[\text{Ni}(\text{H}_2\text{O})_6]^{2+}$ , is present in aqueous solutions of Ni(II) when no other complexing agents are present.<sup>20</sup>  $\text{Ni}(\text{OH})_2$  and  $\text{Ni}(\text{OH})_3^-$  appear at highly basic pH.  $\text{Ni}(\text{OH})^+$  and  $\text{Ni}(\text{HCO}_3)^+$  may also be present in the pH range of 8-10.

Aqueous nickel is not readily hydrolyzed to the hydroxide under typical environmental conditions; significant formation of hydroxide complexes occur only under basic conditions ( $\text{pH} > 7$ ).

The speciation of nickel is greatly affected by the extent of formation of nickel complexes with the industrial reagents and natural organic ligands that are present in polluted aquatic systems. Humic acid solubilizes nickel from nickel carbonate by generating organo-metal complexes.<sup>21</sup>

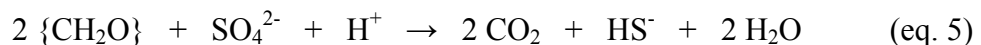
#### 1.2.4 Copper

In aqueous solutions copper exists as the aquo ion  $[\text{Cu}(\text{H}_2\text{O})_6]^{2+}$ .<sup>20</sup> In natural waters copper forms complexes with both inorganic and organic ligands. The complexes with  $\text{OH}^-$  and  $\text{CO}_3^{2-}$  are strong, but those with  $\text{Cl}^-$  and  $\text{SO}_4^{2-}$  are relatively weak. In acidic environments ( $\text{pH} < 7$ ),  $\text{Cu}(\text{II})$  is the dominant species. However, in a typical aqueous environment ( $\text{pH} = 6-8$ )  $\text{Cu}(\text{II})$ ,  $\text{Cu}(\text{OH})_2$ ,  $\text{CuHCO}_3$ ,  $\text{CuCO}_3$  and  $\text{CuOH}^+$  are found.<sup>19</sup>

#### 1.2.5 Cadmium

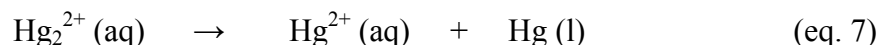
Most of the cadmium in sea water is present as chloride complexes such as  $\text{CdCl}^+$ ,  $\text{CdCl}_2$  and  $\text{CdCl}_3^-$ . Hydrolysis of  $\text{Cd}(\text{II})$  leads to species such as  $[\text{Cd}(\text{OH})(\text{H}_2\text{O})_5]^+$ .

Cadmium is also found in harbor sediments. However, cadmium concentrations in the anaerobic bottom layer of harbor water are low. Microbial reduction of sulfate produces sulfide as shown in equation 5. The sulfide precipitates cadmium as insoluble cadmium sulfide (equation 6) explaining why the sediment is high in Cd while the water has a low concentration.<sup>22</sup>

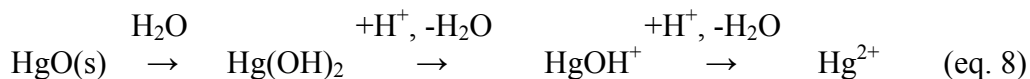


### 1.2.6 Mercury

In aqueous solutions mercury exists as the Hg(II) ion. Hydrated Hg(II) exists as  $[\text{Hg}(\text{H}_2\text{O})_6]^{2+}$ , with an octahedral geometry around the metal. The unusual  $^+\text{Hg}-\text{Hg}^+$  unit that is found in insoluble salts such as  $\text{Hg}_2\text{Cl}_2$  disproportionates in aqueous solution as shown in equation 7.<sup>14</sup>



Mercury(II) is a very soft Lewis acid.<sup>12</sup> It forms stable complexes with soft Lewis bases such as the sulfide anion. Mercury is found in nature as the sulfide mineral, called cinnabar. Precipitates of HgO form when the pH of an aqueous solution of Hg(II) is increased. HgO is highly soluble in neutral and acidic water. The solution may be viewed as an aqueous species of mercury(II) hydroxide,  $\text{Hg}(\text{OH})_2$ . The process is shown in equation 8.<sup>4</sup>



Attack on Hg(II) by methylcobalamin (i.e. Vitamin B<sub>12</sub>) leads to methylation. In methylcobalamin the central cobalt atom is bonded to a methyl group. Equation 9 represents the attack by the anionic methyl group of methylcobalamin on the electrophilic Hg(II).<sup>23</sup>

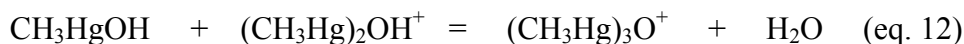
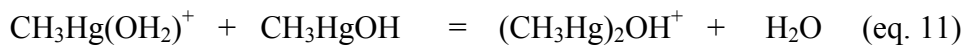


$\text{L}_5\text{Co}-\text{CH}_3$  = simplified methyl-cobalamin.

In general,  $\text{CH}_3\text{Hg}^+$  exists as  $\text{CH}_3\text{HgCl}$  although in shellfish it is also found as  $\text{CH}_3\text{HgSCH}_3$ . Further methylation at higher pHs leads to the formation of  $(\text{CH}_3)_2\text{Hg}$ .<sup>11</sup>

The methylmercury ion  $\text{CH}_3\text{Hg}^+$  is the primary source of toxic effects of mercury and mercury compounds in the environment.  $\text{CH}_3\text{Hg}^+$  and  $(\text{CH}_3)_2\text{Hg}$  are both more toxic than the free element or ion because they are more lipophilic. Organic derivatives of mercury are more hazardous than the simple inorganic salts because they are lipid soluble (and hence bioconcentrate) and are able to cross the blood-brain barrier, thereby causing the complex and irreversible neurological symptoms and disturbances associated with mercury intoxicants.<sup>24</sup>

The ion  $\text{CH}_3\text{Hg}^+$  is hydrated in aqueous solution. The following pH-dependent reactions lead to the formation of oxonium ions (equations 10-12):<sup>24</sup>



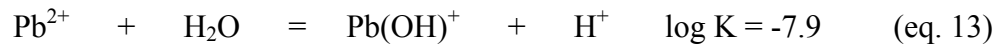
The mercury in the oxonium ions binds sulfur and selenium strongly. This high affinity for sulfur leads to complexation of mercury by cysteine and methionine units in peptides partially explaining the toxicity of  $\text{CH}_3\text{Hg}^+$ .

$\text{CH}_3\text{Hg}^+$  was detected in the waters of Minamata Bay close to the Japanese fishing village of Minamata. The largest episode of mercury poisoning in the history of mankind that took place there in 1956.<sup>25</sup> The mercury came from an acetaldehyde plant that used  $\text{Hg}^{2+}$  in the production of acetaldehyde from acetylene. Residual mercury found its way

into the Minamata Bay, was taken up by the fish and shellfish, and then bioconcentrated in the form of lipophilic methylmercury derivatives. Although on much smaller scales the presence of  $\text{CH}_3\text{Hg}^+$ . For example, a study of a series of Adirondack lakes in New York State found that in most lakes approximately 10% of the total mercury existed as  $\text{CH}_3\text{Hg}^+$ .<sup>26</sup>

### 1.2.7 Lead

The +2 oxidation state is prevalent in the common compounds of lead. In water  $\text{Pb}^{2+}$  undergoes partial hydrolysis according to equation 13.<sup>20</sup>



However, the speciation of lead(II) in aqueous solution involves several hydroxo-complexes.<sup>27</sup> Below pH 5.5,  $\text{Pb}^{2+}(\text{aq})$  predominates, but as the pH increases,  $\text{Pb}_4(\text{OH})_4^{4+}$ ,  $\text{Pb}_6(\text{OH})_8^{4+}$ , and  $\text{Pb}_3(\text{OH})_4^{2+}$  sequentially appear culminating in the precipitation of  $\text{Pb}(\text{OH})_2(\text{s})$ .

### 1.2.8 Arsenic

There are many arsenic forms of environmental significance including arsenious acids ( $\text{H}_3\text{AsO}_3$ ,  $\text{H}_2\text{AsO}_3^-$ ,  $\text{HAsO}_3^{2-}$ ), arsenic acids ( $\text{H}_3\text{AsO}_4$ ,  $\text{H}_2\text{AsO}_4^-$ ,  $\text{HAsO}_4^{2-}$ ), arsenites, arsenates, methylarsonic acid  $\{\text{CH}_3\text{OAs}(\text{OH})_2\}$ , dimethylarsenic acid  $\{(\text{CH}_3)_2\text{AsO}_2\text{H}\}$ , arsine ( $\text{AsH}_3$ ), dimethylarsine  $\{\text{HAs}(\text{CH}_3)_2\}$  and trimethylarsine  $\{\text{As}(\text{CH}_3)_3\}$ .

Arsenic(V) chemistry resembles that of phosphorus(V). In aqueous systems, it exhibits anionic behavior. In aerobic waters, arsenic acid predominates only at extremely low pH ( $< 2$ ); within pH 2–11 it is replaced by  $\text{H}_2\text{AsO}_4^-$  and  $\text{HAsO}_4^{2-}$ . Arsenious acid appears at low pH and under mildly reduced conditions, but it is replaced by  $\text{H}_2\text{AsO}_3^-$  at higher pHs.

### 1.3 Methods for Removing Heavy Metals

The development of new technologies to remove heavy metals such as cadmium, lead and mercury from the environment has attracted the attention of researchers for quite a long time now and remains an extremely active field. Most heavy metals are extremely toxic because, as ions or in certain compounds, they may be taken into living systems where they tend to combine with and inhibit the functioning of particular enzymes. Severe physiological or neurological effects may result from the presence of very small amounts of a toxic heavy metal (or metalloid) in the body. Both short-term exposure to high doses of a heavy metal or long-term exposure to lower levels can cause numerous health problems, including anemia and other blood disorders, damage to the nervous system and brain, kidney disease, reproductive impairments in men (impotence and sterility) and women (decreased fertility, abnormal menstrual cycles, and miscarriages), birth defects, mental retardation, behavioral disorders, and death in fetuses and young children, irreversible damage to the lungs, and shortness of breath and emphysema.<sup>28</sup>

The total annual global input of mercury to the environment from all sources including natural, anthropogenic, and oceanic emissions is estimated to be approximately

5500 tons.<sup>29,30</sup> Thus, mercury pollution will likely remain a serious long-term hazard to human health and environmental systems.

Various methods have been developed and are being used to remove heavy metals from the environment. These include phytoremediation, bioremediation, precipitation of metal ions with lime, sulfide, and other chemical reagents, cementation, solvent extraction, electrodeposition, treatment with ion exchange resins, carbon adsorption, membrane filtration, application of microorganisms and biomass, reverse osmosis, electrolysis, zeolite adsorption, and others.<sup>31-35</sup> Some of these methods are used for water purification as well. The following sections will discuss the methods currently being used for the removal of heavy metals from the environment.

### 1.3.1 Phytoremediation

Phytoremediation involves the cultivation of certain species of plants in a contaminated area where they absorb the environmental pollutants through their roots. This results in the detoxification and/or sequestration of the contaminant elements. This process can be conveniently divided into 1) phytoextraction, 2) rhizofiltration, and 3) phytostabilization.<sup>36</sup> In phytoextraction, plants transport and concentrate the toxic metals from the soils into the roots and shoots. In rhizofiltration the plant roots absorb, precipitate and concentrate toxic metals from polluted effluents. Phytostabilization sequesters heavy metals by using plants that can tolerate heavy metals in significant quantity

It has been demonstrated that some species of Indian Mustard (*Brassica juncea*) can accumulate Pb in roots and transport it to the shoots very effectively.<sup>37</sup> *B. juncea* is

also capable of concentrating Cd, Ni, Zn, and Cu in the shoots. In two later studies it was shown that the addition of synthetic chelating agents such as EDTA to the soils significantly increased lead transportation from the roots to the shoots of *B. juncea*.<sup>38</sup> Roots of Indian Mustard (*Brassica juncea*), Sunflower (*Helianthus annuus*), etc. were also shown to be effective in removing toxic metals such as Cu, Cd, Ni, Pb, and Zn from water systems.<sup>39</sup>

This process has been successful in cleaning up sites contaminated by a number of organic contaminants including TNT, PCP, and trichloroethylene and metals such as Cd, Ni, and Pb,<sup>40,41</sup> but it has not been successful with mercury because the metal is toxic to most plants. There are not many plants that can survive in areas contaminated with mercury long enough to effect remediation. However, Water hyacinth, a species found in South America and Southeast Asia has been introduced to the California coast recently.<sup>42</sup> This plant can safely absorb mercury and can accumulate up to 4435 ppb mercury in their roots and 852 ppb mercury in their shoots. It is believed that the mercury initially accumulates in the roots, where it is bound by carboxylate- containing molecules. It then partially migrates to the shoots, where it is more tightly bound by sulfur biochelates such as 2-mercaptobenzothiazole (MBT).<sup>43</sup> But a problem arises with the mercury-saturated plants, which must be treated as hazardous waste when harvested.

However, there are some bacteria that can defend themselves against mercury through a collection of genes known as the *mer* operon. These genes code for a series of enzymes that can demethylate organic mercury to form inorganic mercury, then reduce the inorganic mercury to elemental mercury, which is released. Through genetic engineering, biologists have now succeeded in transferring the operon to some species of

plants, including tobacco and yellow poplar.<sup>44,45</sup> Both species were shown to survive in mercury spiked solutions and to effect significant mercury removal. The mercury absorbed by the plants was converted to  $Hg^{\circ}$  and released, meaning that the plants did not become saturated and did not therefore need to be harvested. The primary problem with this approach is that the mercury “removal” releases the element into the atmosphere to eventually precipitate somewhere else. And a certain percentage of the precipitated mercury will presumably be methylated and find its way into the food chain, where it will be concentrated into higher predators and potentially threaten human life.

### 1.3.2 Constructed Wetlands

Constructed wetlands have been developed recently for heavy metal removal from water systems.<sup>46</sup> One such system was constructed in the summer of 2000, and consisted of four pairs of one-acre (0.4 ha) wetland cells. Water flowed from one cell to the next, then to the discharge point. The wetland cells, vegetated with *Scirpus californicus* (commonly known as California Bulrush), had a water retention time of approximately 48 hours. The wetland system effectively reduced total and dissolved Hg(II) in the water by 86%. It also reduced Pb(II) concentrations by 89% from the influent concentration. Mercury removal efficiency was found to improve with treatment cell maturation. The system is of low cost and the maintenance consists of checking vegetation growth and free flow of water through the system.

Wetlands laboratory simulations also demonstrated cadmium removal.<sup>47</sup> Influent were obtained by mixing a synthetic wastewater with  $CdCl_2 \cdot H_2O$  at four concentrations, 1, 5, 10, and 20 ppm, for the four experimental runs. The mean effluent cadmium

concentrations varied between 0.02 and 0.16 ppm. Cadmium removal efficiencies were 98.6–99.4% in free water surface, and 99.3–99.9% in the subsurface flow wetland systems.<sup>47</sup> The subsurface flow wetland showed slightly better performance than the free water surface wetland in terms of various pollutant removal. However, the two systems had similar performances in removing cadmium.

Another investigation performed in Jiangsu, China revealed that more than 90% of Cd, Pb and Zn can be removed by treatment in constructed wetlands vegetated with different plant species such as *Alternanthera philoxeroides* (commonly known as Alligatorweed), *Zizania latifolia* (commonly known as Manchurian wildrice), *Echinochloa crus-galli* (commonly known as Japanese millet), *Polygonum hydropiper* (commonly known as Water pepper), and related species.<sup>48</sup>

### 1.3.3 Bioremediation

Bioremediation uses microscopic organisms such as bacteria, and fungi to remove contaminant elements from water. It is very similar to phytoremediation. In nature there exist some bacteria that can convert inorganic and methyl mercury to elemental mercury through the *mer* operon. A system has been developed for the bioremediation of wastewater streams coming out of chlor-alkali plants.<sup>49,50</sup> The waste stream is enriched with a nutrient solution for the bacteria and diverted through a bioreactor containing a large colony of the organisms. The flow is regulated such that the water will remain approximately three hours in the reactor, which is also designed to retain the reduced mercury. The treated water then passes through an activated carbon filter to remove any mercury not captured by the bacteria. The elemental mercury can be recovered from the

reactor. This process is relatively cheap and has been shown to effectively remove mercury from the water streams. However, it does have some drawbacks. The mercury concentration in the incoming waste water must be regulated because the mercury will overwhelm the bacteria's defenses and kill them if it grows too high (over 9 ppm).<sup>49</sup> Also, this technique requires an extensive reactor setup and is therefore not suitable for *in situ* remediation.

Bacterial modification is another option. In this case it is not necessary to depend on the *mer* operon to detoxify mercury. The bacteria would not necessarily volatilize the pollutant and no reactor would be required to capture the elemental mercury released. This has also been attempted, by genetic engineering of the polyphosphate kinase (*ppk*) gene into some bacteria that already contained the mercury transport *mer* genes but not the reduction enzyme.<sup>51</sup> The *ppk* gene codes for the organism to create large amounts of linear orthophosphate polymers. This was engineered to replace the *merA* enzyme, so that when mercury levels grew dangerous within the bacteria, polyphosphate was synthesized. Apparently the phosphate chelated the mercury and prevented it from interfering with processes within the cell, granting the treated bacteria the ability to hyperaccumulate the metal without ill effects.

This is interesting because phosphate is not as good a ligand for mercury as thiolates and sulfides, and it is reasonable to think that bacteria that produced thiol compounds instead of polyphosphate might be even more effective. This also has been tried, by engineering into *E. Coli* the *mer* mercury transport genes and genes to express metallothionein, a cysteine rich, low molecular weight protein that is known to chelate heavy metals through its cysteine groups.<sup>52</sup> These were placed in a reactor and mercury

contaminated water was permitted to flow through. The bacteria removed mercury nearly quantitatively until saturation was reached. Although this was an excellent filter system, it did face problems similar to other filters, namely that it could be saturated and then would have to be replaced. Also, bioaccumulating bacteria are probably not a good choice for *in situ* remediation because they will become part of the local food chain and could actually increase the bioavailability of the mercury.

Marine microalga *Tetraselmis suecica* can be used in bioremediation processes in seawater polluted with cadmium.<sup>53</sup> It was observed that the cadmium removed was proportional to the concentration of this metal in the medium and it was dependent on the time of exposure. *T. suecica* removed 59.6% of cadmium after only six days when it was exposed to 6 ppm of culture and this percentage increased as cadmium decreased in the medium; the initial cell density used was only  $25 \times 10^4$  cells/mL. It was concluded that living microalgal cells of *T. suecica* with an initial cell density of  $25 \times 10^4$  cells/mL could act as an effective system for cadmium removal at cadmium concentrations up to 6 ppm.<sup>53</sup>

In another study twenty-four strains of marine microalgae were tested for cadmium removal and it was found that the marine green microalga *Chlorella* sp. NKG16014 showed the highest removal of cadmium with 48.7% after two weeks when this microalga with an initial cell density of  $5 \times 10^7$  cells/mL was exposed to 50  $\mu$ M cadmium (5.62 ppm).<sup>54</sup>

However, there has been little commercial exploitation of microalgal biosorption for metal removal or recovery processes.

#### 1.3.4 Activated Carbon Adsorption

Activated carbon adsorption is effective in removing mercury from water systems. In one study over 99% Hg(II) removal was demonstrated by 11 different brands of commercial activated carbon at pH 4-5.<sup>55</sup> However, activated carbons do not function efficiently at pH < 4 or > 9. It was also observed that total Hg(II) removal decreases in the presence of strong chelating agents like ethylenediaminetetraacetate (EDTA) due to the formation of mercury(II)-EDTA complexes. Later tests have shown that activated carbon is reasonably effective at purifying vapor streams.<sup>56,57</sup> Mercury (II) can also be successfully removed from water by coconut shell based activated carbon,<sup>58</sup> with the extent of removal of Hg(II) depending on sorbent dose, pH, and initial Hg(II) concentration. Mercury uptake increased from 72 to 100% with increase in pH from 2 to 10.

#### 1.3.5 Adsorbents from Agricultural and Forest Wastes

Removal of heavy metals from the environment can be accomplished by natural adsorbents from agricultural and forest waste byproducts.<sup>59,60</sup> These include peanut wastes,<sup>61,62</sup> onion skin,<sup>63</sup> maize,<sup>64</sup> rice husks,<sup>65</sup> bagasse pith,<sup>66</sup> cork wastes,<sup>67</sup> technical lignins,<sup>68,69</sup> conifer leaves,<sup>70</sup> and wood barks.<sup>71,72</sup> Removal of metal ions including Hg(II) from aqueous solution has been successfully demonstrated using *Pinus radiata* bark and tannins, chemically modified with an acidified solution of formaldehyde.<sup>73</sup> The

adsorption largely depended on the pH of the solution, and adsorption by modified bark increased from 72.6% at pH 1 to 75.9% at pH 5. When modified tannins were used, adsorption increased from 55.9% at pH 1 to 77.4% at pH 5.

#### 1.3.6 Ion-exchange Resins

Ion-exchange resins containing sulfur based groups are capable of removing mercury from water. The best known among them is commonly known as TMR (for Total Mercury Removal).<sup>74</sup> Supplied by Rohm and Haas, this resin is a styrene-divinylbenzene copolymer containing aryl thiol groups. It is capable of adsorbing nearly 0.7g of mercury per gram of resin. The resin can be regenerated by treatment with concentrated hydrochloric acid.

Trace heavy metal ions including mercury can be efficiently removed from drinking and ground water by using weakly basic anion exchangers.<sup>75</sup> Use of these ion exchangers was demonstrated both in the laboratory and at semi-industrial scales.

Recently a method has been developed in which Hg and Cd from drinking water sources can be removed by selectively extracting them with weakly basic resins.<sup>76</sup> The process is based on selective extraction resulting from Lewis acid-base interactions. The resin material exhibits high performance at neutral or basic pH. Humic acids present in water may create a minor problem by forming complex compounds with mercury and thus hindering diffusion. Some commercial resins functioning as ion exchangers reduce mercury levels to 34 ppb from waste waters with mercury content ranging from 70 to 90 ppm.<sup>77</sup>

### 1.3.7 Polythiol-functionalized Alumina Membranes

Polythiol-functionalized alumina membranes are attractive support materials because of their good chemical and thermal resistance.<sup>34</sup> Moreover, they possess the many surface hydroxyl groups necessary for ligand attachment. High capacity sorbents can be made by covalently attaching ligands with multiple binding sites, e.g. polythiols such as poly-S-benzyl-L-cysteine (PLC) and poly-L-glutamic acid (PLGA). Optimization of the ratio of ligand chain length/pore radius, and operating conditions resulted in significant improvement of sorption efficiency. Polythiol-functionalized membranes are characterized by high sorption capacities, high site accessibility, and fast sorption rates.<sup>34</sup>

### 1.3.8 Nanoporous Adsorbent Materials

A new class of high-performance, SiO<sub>2</sub>-based nano-porous functionalized sorbent materials with molecular recognition capability has been designed and developed by Pacific Northwest National Laboratory (PNNL).<sup>78</sup> These novel materials were created by combining synthetic nano-porous substrates with specifically-tailored pore sizes (2-10 nm) and very high surface areas (approximately 1000 m<sup>2</sup>/g) with self-assembled monolayers of well-ordered functional groups. These functionalized nano-porous sorbent materials have high affinity and specificity for targeted cations or anions, either free or complexed. They exhibit very high adsorption capability and are successful in removing inorganic pollutants from both surface and ground waters. Extensive tests were performed on one type of these functionalized nano-porous material called thiol-SAMMS (thiol self-assembled monolayers on mesoporous SiO<sub>2</sub>). Designed to remove heavy

metals including mercury, they exhibited highly favorable adsorption characteristics: exceptionally high metal loading (approximately 100-600 mg metal/g sorbent), very fast kinetics (> 99% adsorption in less than 1 minute of contact time), and significant specificity ( $K_d$  values ranging between 103-106 mL/g). Possessing unique ionic and molecular recognition characteristics, they proved to be far superior than other commercially available sorbents in removing heavy metals including Hg from polluted water and water streams. US EPA toxicity leaching characteristic tests showed that once specifically bonded, the pollutants remain immobilized on the nano-materials. Preliminary data suggests that use of these novel nanomaterials would significantly cut down on remediation costs due to their better performance characteristics compared to the conventional adsorbents such as resins and activated carbon.

#### 1.3.8.1 Multiwalled Carbon Nanotubes (MWCNTs)

The sorption of Pb(II), Cu(II) and Cd(II) onto multiwalled carbon nanotubes (MWCNTs) has been investigated.<sup>79</sup> Maximum sorption capacities of 77.08 mg/g for Pb(II), 24.49 mg/g for Cu(II) and 10.86 mg/g for Cd(II) were found at room temperature, pH 5.0 and metal ion equilibrium concentration of 10 mg/L. The metal-ion sorption capacities of the MWCNTs were 3-4 times larger than those of powder activated carbon and granular activated carbon that are commonly used as sorbents for water purification.

Nanoparticles having much larger surface areas (on a mass basis) than bulk particles and being amenable to functionalization with various chemical groups that increase their affinity towards target compounds are particularly attractive sorbents. However, the ability to provide large quantities of nanomaterials (by suppliers) is an

important issue in the commercialization of nanotechnology for heavy metal remediation. Another problem to is the lack of information about the environmental fate, transport and toxicity of nanomaterials.<sup>80</sup> Little is known about the hydrolytic, oxidative, photochemical and biological stability of nanomaterials in natural and engineered environmental systems.

### 1.3.9 Crown Thioethers

Several studies have demonstrated the utility of polymer pendant ligands for the extraction of different metal ions from water systems.<sup>81-83</sup> Crown thioethers in particular were shown to be very effective in remediating Hg(II) in water streams due to the high affinity of the sulfur crowns for the Hg(II) ion.<sup>84</sup> One representative member of this family is [17]aneS<sub>5</sub> attached to polystyrene-divinylbenzene through an amine linkage.<sup>85</sup> This polymer showed excellent extraction properties. Mercury removal rates of 97-99% was achieved after thirty minutes exposure to solutions of as high as 34 ppm mercury. Even in an extremely concentrated solution of 170 ppm mercury, the mercury removal rate was 91%. The increased hydrophilicity in acidic water due to the amine linker was considered to be the basis of the success of these compounds in binding mercury. The polymer could be regenerated by treatment with dithizone, but it increases the cost of this technique.

The free crown thioethers 12S4 (1, 4, 7, 10-tetrathiacyclododecane) and 9N3 (1, 4, 7-triazacyclononane) form both mono and bis complexes with Hg(II).<sup>86</sup> While binding to Hg(II) the 12S4 ligand forms a square planar (S<sub>4</sub>) complex and the 9N3 forms a distorted trigonal prismatic structure by sulfur and hexakis(amine) coordination

### 1.3.10 Polymeric Chelating Fibers

Two new classes of chelating fibers, polymercaptopropylsilsesquioxane (PMPS) and copper (II) ferrocyanide complexed with poly[1-(2-aminoethyl)-3-aminopropyl]-silsesquioxane (Cu-FC-PAEAPS) were reported to be effective in removing trace amounts of mercury well below parts per billion concentrations under a variety of conditions.<sup>29</sup> These polymeric chelating materials do not need complex synthetic procedures and expensive containment systems, unlike the powder form of mesoporous organosilica materials.

### 1.3.11 Tunable Biopolymers

Removal of Cd from dilute waste streams has been demonstrated by using tunable, metal-binding biopolymers prepared using elastin-like polypeptides composed of either one or two hexa-histidine clusters.<sup>87</sup> Structurally similar to elastin, a mammalian protein, the elastin-based biopolymers consist of the repeating pentapeptide (VPGVG) and undergo a reversible phase transfer from water-soluble form into aggregates as the temperature changes. The sequestered cadmium is easy to recover from the material.<sup>88</sup> However, it was found that the percentage of cadmium removal was modest (between 50 and 55%). It was partly due to the displacement of bound cadmium by zinc ions present in the soil. The use of histidine clusters offers no selectivity, and provides a narrow pH working range.

It is known that some metalloregulatory proteins like MerR and ArsR have high binding affinity for mercury and arsenic, respectively.<sup>89</sup> This fact was utilized to engineer tunable biopolymers for the selective removal of mercury.<sup>90</sup> MerR was fused to

an elastin-like polypeptide (ELP) to provide the biopolymer with high selectivity. Mercury was bound selectively by the biopolymer at an expected ratio of 0.5 mercury/biopolymer with minimal binding of competing metals like Cd, Ni and Zn that were present at 100-fold excess. Extraction of the sequestered mercury was performed without difficulty, allowing the biopolymer to be reused. Mercury in contaminated water could be reduced to concentrations below the required drinking water limits.

#### 1.3.11.1 Nanoscale Biopolymers

The emergence of genetic and protein engineering has made possible the construction of nanoscale materials that can be controlled precisely at the molecular level. The advent of recombinant DNA techniques has made it possible to create ‘artificial’ protein polymers with fundamentally new molecular organization. These nanoscale biopolymers are specially pre-programmed within a synthetic gene template. They can be controlled at the molecular level with high precision in terms of size, composition and function. It is now possible to specifically design protein-based nanobiomaterials possessing both metal-binding and tunable properties that can be used to selectively remove heavy metals from dilute solutions.<sup>91</sup> However, there is no report in the literature of the use of nanoscale biopolymers in remediating heavy metals from the environment.

### 1.3.12 Extraction from Aqueous Solutions

#### 1.3.12.1 Aqueous Biphasic Systems

One of the most commonly used biphasic systems utilizes water and polyethylene glycol (PEG).<sup>92</sup> Polyethylene glycol forms two phases in the presence of salts. Although metal ions can be directly extracted into the PEG-rich phase in the absence of a complexant, better selectivity is achieved by adding a water-soluble complexant. The advantage of using the biphasic PEG system is that it is inexpensive, non-flammable, and non-toxic. Although this technique has proven effective in binding different divalent metal ions including Cu, Ni, and Co, there is no data supporting extraction of Cd, Hg or Pb ions.

#### 1.3.12.2 Surfactants

Surfactants have been found to remove mercury from water systems.<sup>93</sup> Surfactants are molecules that possess both hydrophobic and hydrophilic end groups. In aqueous solution they form aggregates called micelles with the hydrophilic groups occupying the outer region. Surfactants act as extractants by transferring metal ions from an aqueous to an organic phase. The metal ions become encapsulated in the hydrophobic region of the micelle during extraction. About 85% of Cu was removed when a mixed surfactant system consisting of sodium dodecylsulfate (SDS)/Triton X-100 (alternatively called polyoxyethylene octyl phenyl ether) was used.<sup>93</sup> However, there is no data in the literature supporting removal of Cd, Hg or Pb using this technique.

#### 1.3.12.2.1 Biosurfactants

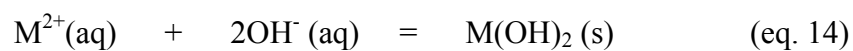
Surfactin, an anion biosurfactant produced by one of the most effective biosurfactants '*Bacillus subtilis*', has been shown to remove Cu(II) and Zn(II) from soil and sediments.<sup>94</sup> Investigations carried out with soil containing 890 mg/kg of Zn and 420 mg/Kg of Cu and sediments containing 1110 mg/Kg of Cu and 3300 mg/Kg of Zn showed that 0.25% surfactin/1% NaOH removed 25% of the Cu and 6% of the Zn from the soil and 15% of the Cu and 6% of the Zn from the sediments.<sup>94</sup>

The presence of two charges due to glutamic and aspartic amino acids as part of its peptide structure, its biodegradability, its effectiveness as a surfactant (low surface tension and critical micelle concentration (cmc) values), and its potential for in situ production present major advantages for using surfactin, while extensive adsorption onto the soil and the high concentrations (in the mM range) typically required to successfully extract soil-bound metals are serious problems of this technology.

#### 1.3.13 Chemical Precipitation

##### 1.3.13.1 Lime Precipitation

One of the earliest and most common technologies used for heavy metal removal is lime {Ca(OH)<sub>2</sub>} precipitation. This technology is based upon the precipitation of dissolved heavy metals by pH increase followed by settling of the precipitates.<sup>95</sup> The process for a typical divalent metal cation is shown in equation 14.



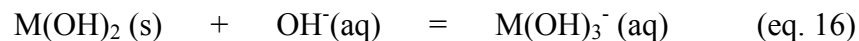
Sodium hydroxide (NaOH), or sodium carbonate (Na<sub>2</sub>CO<sub>3</sub>) can also be used. Some metal ions tend to produce basic salt precipitates, such as basic copper(II) sulfate, CuSO<sub>4</sub>· 3 Cu(OH)<sub>2</sub>, which is formed as a solid when hydroxide is added to a solution containing Cu<sup>2+</sup> and SO<sub>4</sub><sup>2-</sup> ions.

Sodium carbonate can be used to precipitate hydroxides {Fe(OH)<sub>3</sub>· x H<sub>2</sub>O}, carbonates (CdCO<sub>3</sub>), or basic carbonate salts {2 PbCO<sub>3</sub>· Pb(OH)<sub>2</sub>}. The carbonate anion produces hydroxide anions as a result of hydrolysis in water (equation 15).



The process of lime precipitation is simple and relatively inexpensive. Complete removal of metals such as Cu, Zn, Fe, Mn, Ni, and Co is possible.<sup>95</sup>

Since the minimum solubilities of the various metals do not occur at the same pH value, hydroxide precipitation of all the heavy metals cannot be considered a dependable technique.<sup>96</sup> Effective precipitation is prevented if complexing agents such as NH<sub>3</sub> and EDTA are present. Many metal hydroxides are amphoteric in nature and tend to dissolve at high pH values (equation 16).



Another major disadvantage of this method is the requirement of large doses of alkaline materials to increase and maintain pH values for extremely acidic water to above 6.5 for optimal metal removal.<sup>96</sup> Additionally, liming is often temporary and produces

secondary wastes, such as metal hydroxide sludges and gypsum, which are highly regulated and have costly disposal requirements.<sup>97</sup> The production of secondary wastes often proves to be a serious problem in the field treatment of Acid Mine Drainage (AMD), due to the continual need for dredging of downstream water basins and collection ponds to ensure that water quality is maintained for local water systems.

#### 1.3.13.2 Sulfide Precipitation

Most metal sulfides are very insoluble. Precipitation of the metal cation with sulfides can be utilized for the removal of heavy metals from aqueous waste streams. This may be accomplished by passing hydrogen sulfide into the solution containing the metal cation(s) (equation 17).<sup>11</sup>

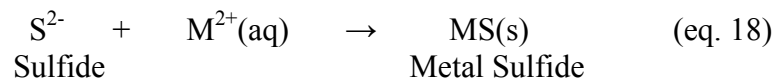


The chemical sludge containing precipitated sulfides must be collected and treated as hazardous waste. Precipitation is more efficient at high pH since sulfide is a basic anion. The pH is often raised by adding lime prior to treatment with H<sub>2</sub>S.

The biggest problem is that H<sub>2</sub>S is a toxic gas, so extreme care must be exercised while using it. Precipitation with different metal sulfides is a better, less problematic alternative.

As in the case of H<sub>2</sub>S, this precipitation process converts soluble metal compounds into relatively insoluble sulfide compounds through the addition of metal sulfide reagents such as sodium sulfide (Na<sub>2</sub>S), sodium hydrogensulfide (NaHS), ferrous sulfide (FeS), and calcium sulfide (CaS). Sulfides (S<sup>2-</sup>) and hydrogensulfides (HS<sup>-</sup>) are extremely

reactive with heavy metal ions over a wide pH range. Removal of Pb, Cu, Cr (+6), Ag, Cd, Zn, Hg, Ni, Tl, Sb, and V from wastewaters has been successfully demonstrated by sulfide precipitation (EPA, 1987). Metal sulfide precipitates often are physically removed from solution through coagulation, flocculation, clarification or filtration. The primary reactions involved in sulfide precipitation for a divalent metal cation is shown in equation 18.<sup>96</sup>



There are several advantages in this process. First, there is a high degree of metal removal, even at low pH values (pH = 2 - 3). Second, heavy metal removal is possible even with chelating agents present. Third, sulfide precipitation can be operated over a very wide pH range, typically from 2 to 12. However, there are some disadvantages associated with sulfide precipitation. First, utmost care is required to control release of the highly toxic H<sub>2</sub>S gas which can form under slightly acidic conditions. Second, sulfide may remain in the treatment effluent. Third, the process involves higher capital and operating costs than hydroxide precipitation.

However, in a recent work it was found that the addition of NaOH at a pH of 4-5 as a first precipitation step, followed by filtration and further addition of Na<sub>2</sub>S to the filtered liquid at pH 7-8 as a second precipitation step, effectively removed heavy metals from sewage sludge and at a lower cost.<sup>98</sup>

### 1.3.13.3 Other Chemical Reagents

Removal of mercury by precipitation with a chemical reagent is an economical and potentially effective possibility. It has been found that chemical reagents containing sulfur atoms work best to bind toxic heavy metals. At present several reagents are commercially available for this purpose: sodium or potassium dimethyldithiocarbamate (SDTC), sodium thiocarbonate (STC), and the trisodium salt of 2,4,6-trimercaptotriazine (TMT).

#### 1.3.13.3.1 SDTC

Sodium or potassium dimethyldithiocarbamate (SDTC) has the trade name HMP-2000.<sup>99</sup> This compound forms insoluble precipitates with heavy metals, and can be easily removed from water. It is effective in removing mercury from mixed gold/mercury cyanide waste streams. The addition of SDTC to mercury contaminated water resulted in an immediate drop in the mercury level. However, within hours the mercury level rose again if the precipitates were not removed from the water, suggesting that mercury was being leached into the water. SDTC is also known to decompose into byproducts such as tetramethylthiuram, also known as thiram, that is a potent biocide. For example, in 1999 approximately 117 tons of fish over a 50-mile stretch from Anderson to Indianapolis, Indiana were killed as a result of an accidental release of over 1.5 million gallons of SDTC contaminated wastewater into the city's wastewater system by the Guide Corporation (an auto parts manufacturer in Anderson, IN).<sup>100</sup> The wastewater was eventually discharged into the White river. The SDTC is thought to have decomposed into toxic compounds, including thiram, killing the fish. Figure 1.1 illustrates the metal

binding property of SDTC as well as the generation of toxic byproducts through its decomposition.<sup>99</sup>

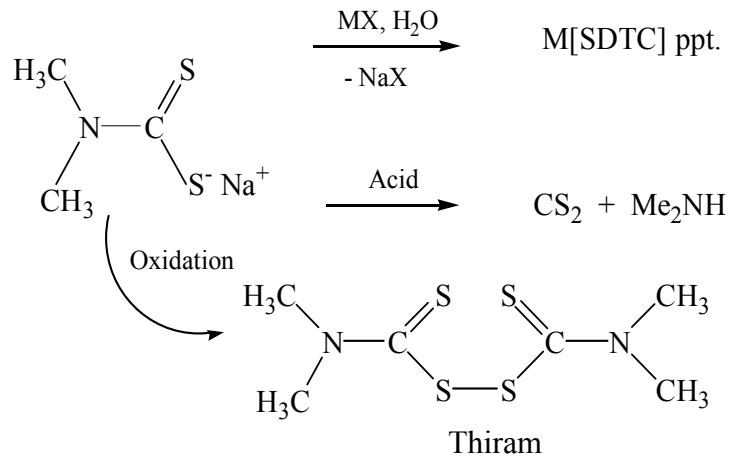


**Figure 1.1.** SDTC: metal binding and generation of toxic byproducts.<sup>99</sup>

#### 1.3.13.3.2 STC

The second most widely used chemical reagent for precipitating divalent heavy metals is sodium thiocarbonate (STC) with the trade name Thio-Red.<sup>99</sup> This compound has been claimed to precipitate heavy metals although not quite as effectively as SDTC, and not as a metal-ligand complex. However, there is once again a serious problem with the long-term stability of the resulting precipitates. It has been found that STC removes heavy metals through the formation of metal sulfides, not as the expected thiocarbonate complex and a byproduct of the reaction is carbon disulfide which is a volatile and toxic liquid (Figure 1.2).<sup>99</sup> Therefore, STC cannot be used for *in situ* remediation of contaminated sites.

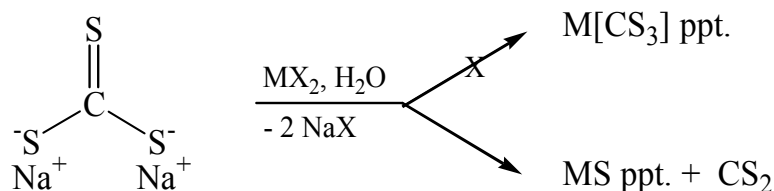


**Figure 1.2.** Metal binding by STC.<sup>99</sup>

### 1.3.13.3.3 TMT

Another chemical reagent that is commonly used for precipitating divalent and univalent heavy metals including mercury from water is the trisodium salt of 2,4,6-trimercaptotriazine (TMT). This ligand is even less effective for heavy metal precipitation than HMP-2000 or Thio-Red.<sup>99</sup> Furthermore, the resulting precipitates appear to go through multiple changes in form, releasing heavy metals in the process.<sup>101</sup>

Figure 1.3 shows TMT-metal bond formation.

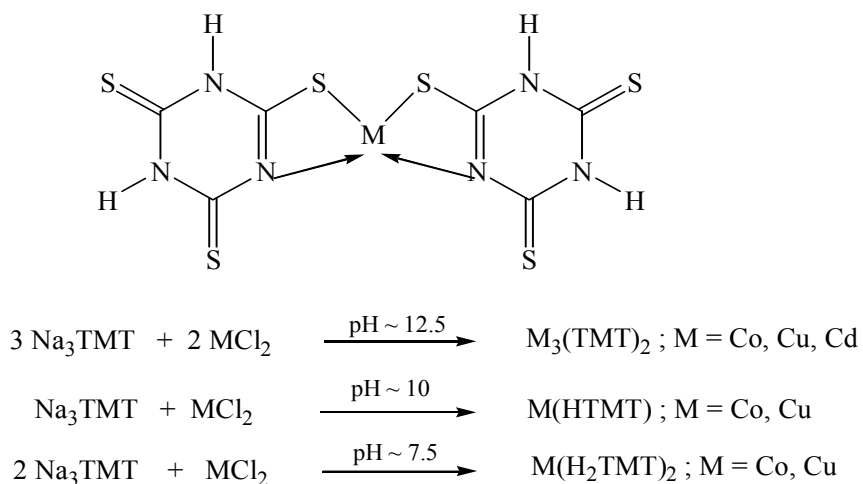


**Figure 1.3.** Metal binding by TMT.<sup>101</sup>

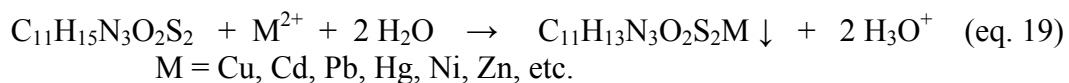
Although the exact mechanism by which these heavy metal TMT complexes decompose is not well understood, it is clear that the precipitates are not stable enough to



moderate to very strong as reflected in their bond enthalpies. The ligand-metal bonds are likely to be stable since the enthalpies of the formed metal-sulfur bonds are quite high.

#### 1.3.13.4.1 Pyridine-2,6-diamidoethanethiol (PyDETH<sub>2</sub>)

The first system that was developed and synthesized to bind heavy metals irreversibly is known as pyridine-2,6-diamidoethanethiol (PyDETH<sub>2</sub>) (Figure 1.4).<sup>103</sup> This ligand is capable of reducing heavy metal concentrations well below EPA discharge limits, produces precipitates that are insoluble under aqueous conditions, and stable over a wide range of pH, and do not produce secondary byproducts. For example, copper can be reduced by > 99.99% from a 50.00 ppm copper solution at pH 4.5 by using PyDETH<sub>2</sub> and cadmium can be reduced by 99.88% from a 50.00 ppm cadmium solution at pH 6.0.<sup>103</sup> Table 1.1 shows the results of copper and cadmium binding by PyDETH<sub>2</sub>. PyDETH<sub>2</sub> utilizes its sulfur and nitrogen atoms to stabilize the metal complexes that form when it binds heavy metals (Figure 1.5).<sup>103</sup> The reaction between the ligand and a divalent metal ion is shown in eq. 19.



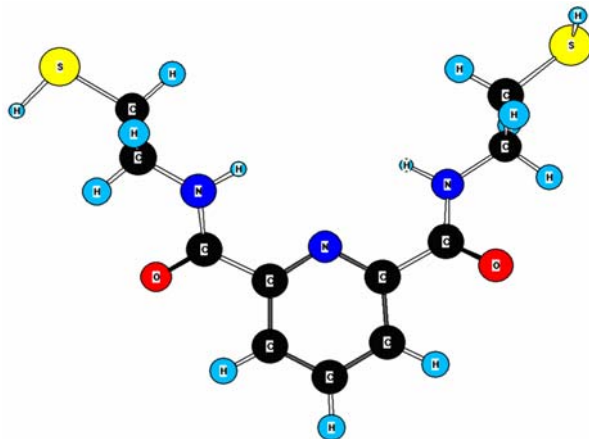


**Figure 1.4.** Computer drawing of PyDET.<sup>103</sup>

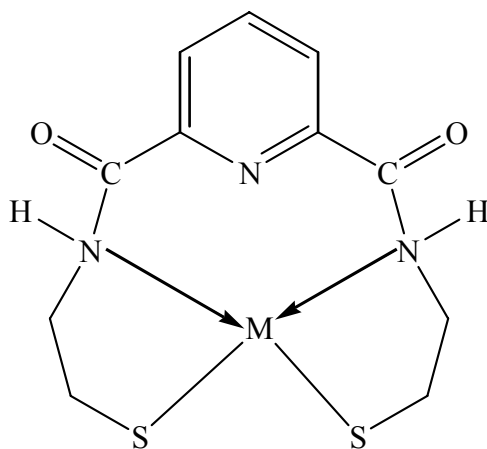


**Figure 1.5.** Proposed structure of PyDET metal compounds.<sup>103</sup>

**Table 1.1.** Results of Cd(II) and Cu(II) binding by PyDET.<sup>103</sup>

Metal	Initial Concentration (ppm)	Solution pH	Time (h)	Final concentration (ppm)	Maximum metal removed (%)
Cd	50.00	4.0	1	2.29	95.42
Cd	50.00	4.0	4	0.94	98.12
Cd	50.00	6.0	1	0.15	99.70
Cd	50.00	6.0	4	0.06	99.88
Cu	50.00	4.5	1	0.92	98.16
Cu	50.00	4.5	4	<0.0093	>99.98
Cu	50.00	6.0	1	1.34	97.32
Cu	50.00	6.0	4	<0.0093	>99.98

#### 1.3.13.4.2 Benzene-1,3-diamidoethanethiol (BDETH<sub>2</sub>)

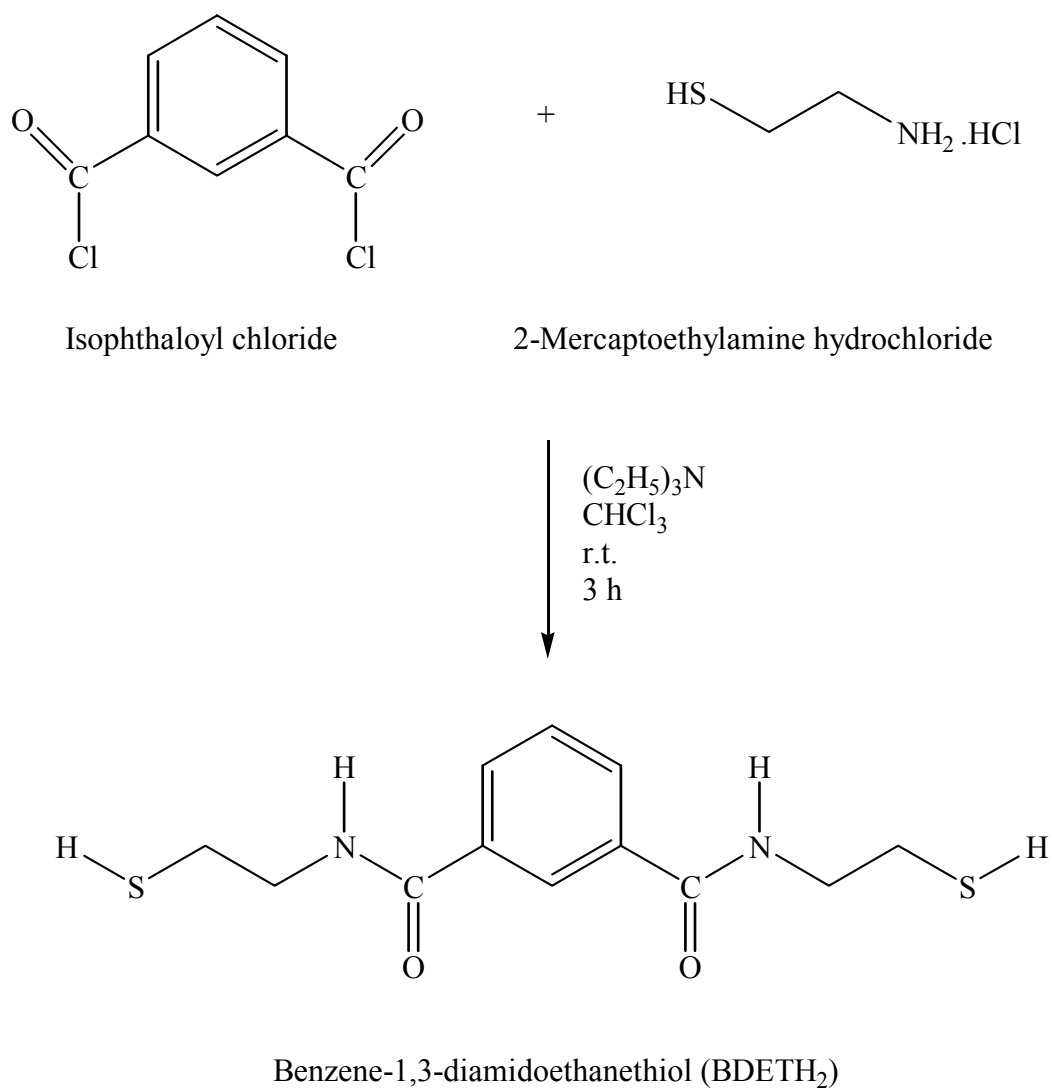
Immediately after the successful development and synthesis of PyDETH<sub>2</sub> another compound benzene-1,3-diamidoethanethiol (BDETH<sub>2</sub>) was developed.<sup>1</sup> The design of BDETH<sub>2</sub> follows Pearson's Hard-Soft Acid-Base (HSAB) interaction principle which states that hard acids will preferentially bond with hard bases and soft acids will preferentially bond with soft bases.<sup>12a,12b</sup> According to this theory, small size, high oxidation state, low polarizability, high electronegativity, low-energy Highest Occupied Molecular Orbitals (HOMO) or high-energy Lowest Unoccupied Molecular Orbitals (LUMO) are the characteristics of hard acids and hard bases. On the other hand, soft acids and soft bases are distinguished by large size, low or zero oxidation state, high polarizability, low electronegativity, high-energy HOMO (bases) or low-energy LUMO (acids). This theory helps to understand the predominant factors which drive chemical reactions. The products of metathesis reactions can be predicted using this theory. Results of this work clearly demonstrated that BDETH<sub>2</sub> is capable of binding divalent

heavy metals completely and irreversibly and without generating any secondary toxic waste. It was envisioned that this ligand would preferably interact and bond with soft metals, such as Hg(II) and Pb(II). The ligand was designed specifically to give a linear S-Hg-S geometry as seen in MerP proteins. Results from several investigations demonstrated that BDETH<sub>2</sub> is effective in removing metals under laboratory conditions and in actual applications.

#### 1.3.13.4.2.1 Synthesis and characterization

Benzene-1,3-diamidoethanethiol (BDETH<sub>2</sub>) was synthesized by combining isophthaloyl chloride with 2-mercaptoethylamine hydrochloride (also known as 2-aminoethanethiol hydrochloride, or cysteamine hydrochloride) (Scheme 1.2). White crystals were obtained upon crystallization from THF at -20 °C, M.p. 129-131 °C, yield 80.2 %.

In the infrared spectrum (KBr pellet) the bands at 3242, 2557, and 1640 cm<sup>-1</sup> were attributed to N-H stretching ( $\nu_{\text{NH}}$ ), S-H stretching ( $\nu_{\text{SH}}$ ), and C=O stretching ( $\nu_{\text{C=O}}$ ) respectively. Absence of bands between 500 and 400 cm<sup>-1</sup> due to S-S stretching and between 1070 and 1030 cm<sup>-1</sup> due to S=O stretching indicates that no oxidation of the S-H functionality is occurring. In the <sup>1</sup>H NMR the amide protons were shown as a broad singlet at 6.58 ppm, while the sulfhydryl (or thiol) protons exhibited a triplet at 1.44 ppm. In the <sup>13</sup>C NMR the signals at 169.1, 45.1, and 24.7 corresponded to the carbonyl carbon, methylene carbon adjacent to the amide nitrogen, and the methylene carbon next to the sulfhydryl (or thiol) group, respectively.



**Scheme 1.2.** Synthesis of Benzene-1,3-diamidoethanethiol (BDETH<sub>2</sub>)

The structure of BDETH<sub>2</sub> was confirmed by single crystal X-ray crystallographic analysis (Figure 1.6). It crystallizes in the orthorhombic space group *f*222. The molecule is flat, the amido and the sulfhydryl (or thiol) groups being coplanar with the aromatic ring. The crystallographic data for BDETH<sub>2</sub> are presented in Table 1.2.

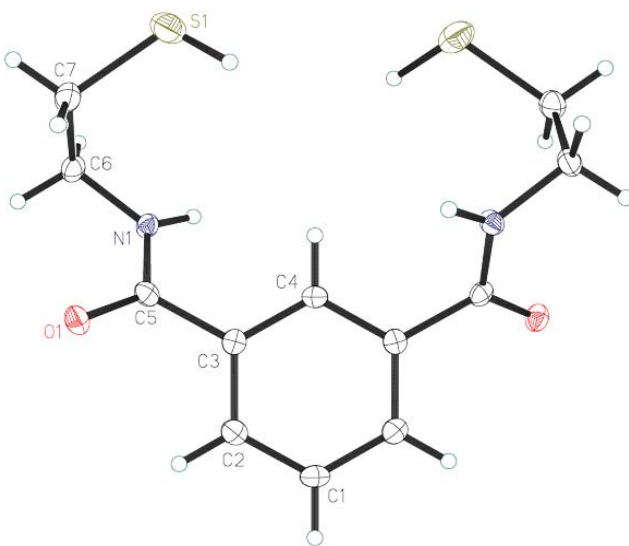


**Figure 1.6.** Crystal structure of BDETH<sub>2</sub>

**Table 1.2.** Crystallographic data for BDETH<sub>2</sub>

formula	C <sub>12</sub> H <sub>16</sub> N <sub>2</sub> O <sub>2</sub> S <sub>2</sub>
fw	284.39
crystal system	orthorhombic
space group	f222
a (Å)	15.5530(4)
b (Å)	17.3790(6)
c (Å)	9.9810(8)
α (deg)	90.00
β (deg)	90.00
γ (deg)	90.00
V (Å <sup>3</sup> )	2697.8(2)
Z	8
T (K)	90(2)
Radiation	MoKα (λ = 0.71073 Å)

There is intermolecular hydrogen bonding between the amide NH protons and oxygen of the amide C=O groups in BDETH<sub>2</sub> (Figure 1.8). Hydrogen bonding between amide NH and C=O groups has been observed in proteins and protein-ligand complexes.<sup>104,105</sup>

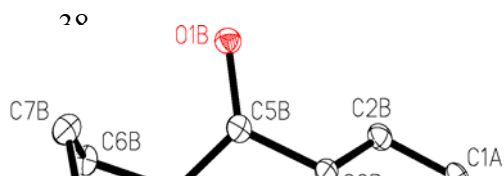


**Figure 1.7.** Intermolecular hydrogen bonding in BDETH<sub>2</sub>

The pK<sub>a</sub> of a typical thiol group lies between 10 and 11. The sulfur atom of a thiol is quite nucleophilic, rather more so than the oxygen atom of an alcohol. Thiols have been found to be reactive towards neutral complexes like [Pt(bipy)NO<sub>2</sub>Cl] (bipy = 2,2'-bipyridine) and cationic substrates like [Pt(terpy)Cl]<sup>+</sup> (terpy = 2,2'-6,2''-terpyridine) indicating their nucleophilicity.<sup>106</sup> Since it is well-known that extensive NH...S hydrogen bond networks are present in zinc fingers,<sup>107</sup> it is possible that such interactions are also present in BDETH<sub>2</sub>.

1.3.13.4.2.2 Reaction between BDETH<sub>2</sub> and a Divalent Metal Cation

The effectiveness of BDETH<sub>2</sub> in binding divalent heavy metals was examined by preparing a series of aqueous solutions of Hg(II) and Pb(II) at pH 4.0 and 6.0 and adding stoichiometric amounts (1:1 mole ratio) of solid BDETH<sub>2</sub>.<sup>1</sup> Table 1.3 shows the results of Hg(II) and Pb(II) binding by BDETH<sub>2</sub>.<sup>1</sup> It is evident from table 1.3 that BDETH<sub>2</sub> is capable of binding Hg(II) and Pb(II) very effectively. 99.9% of lead was removed from a

50.00 ppm aqueous solution within 6 hours at a pH of 4.0, whereas 99.97% of mercury removal occurred within 20 hours at pHs of 4.0 and 6.0 from a 50.00 ppm mercury solution.<sup>1</sup> It was also found that reductions to the EPA toxicity limit for lead (5 ppm) were accomplished within 1 hour for lead solutions at pHs 4.0 and 6.0 whereas the EPA limit for mercury (0.2 ppm) was reached for the solutions at pHs 4.0 and 6.0 within 6 hours. Subsequent leaching studies established that dissolved mercury has a strong tendency to displace Cd, Cu, Mn, Pb, and Zn from the BDET-metal compounds.<sup>2</sup>

The reaction that occurs between BDETH<sub>2</sub> and a divalent metal cation can be shown by equation 20.



The mercury environment is linear with the mercury atom bonded to the two sulfur atoms of the ligand (discussed further in chapter 2). This environment is seen, for instance, in the compound formed between the ammonium salt of cysteamine (a component of BDETH<sub>2</sub>) and mercury, [Hg(SCH<sub>2</sub>CH<sub>2</sub>NH<sub>3</sub>)<sub>2</sub>](Cl)<sub>2</sub> (Figure 1.8).<sup>108</sup> The Hg-S(1) and Hg-S(2) bond distances in this compound are 2.3330(9) and 2.3380(9) Å respectively, and S(1)-Hg-S(2) bond angle is 168.5393 (3) °. In contrast, the Hg-S bond distance found in BDET-Hg is 2.42 Å.

**Table 1.3.** ICP and CVAA results of BDETH<sub>2</sub> with Hg(II) and Pb(II).<sup>1</sup>

Metal	Original M(II) conc. (ppm)	Solution pH	Time (h)	Final M(II) conc. (ppm)	% Metal removed
-------	----------------------------	-------------	----------	-------------------------	-----------------

Hg	50.00	4.00	1	1.96	96.08
Hg	50.00	4.00	6	1.65	96.70
Hg	50.00	4.00	20	0.93	98.14
Hg	50.00	6.00	1	0.50	99.00
Hg	50.00	6.00	6	0.13	99.74
Hg	50.00	6.00	20	0.09	99.81
Pb	50.00	4.00	1	0.10	99.80
Pb	50.00	4.00	6	0.05	99.90
Pb	50.00	4.00	20	0.05	99.90
Pb	50.00	6.00	1	0.31	99.38
Pb	50.00	6.00	6	0.22	99.56
Pb	50.00	6.00	20	0.13	99.74

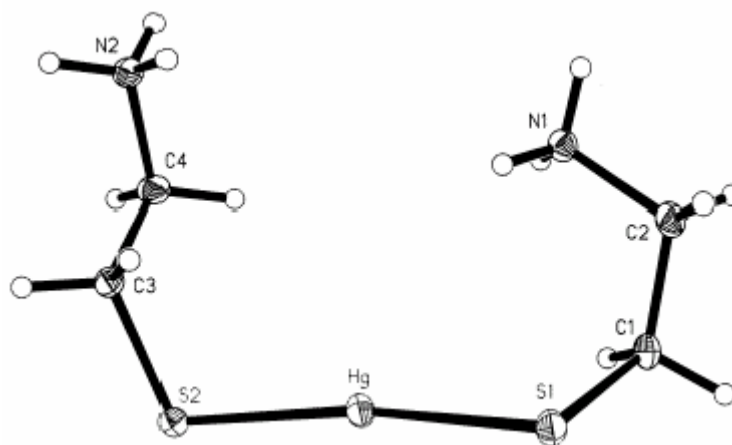


**Figure 1.8.** ORTEP view of  $[\text{Hg}(\text{SCH}_2\text{CH}_2\text{NH}_3)_2]^{2+}$ .<sup>108</sup>

#### 1.3.13.4.2.3 Gold Ore Column Studies

After it was successfully established that BDETH<sub>2</sub> completely precipitates soft heavy metals from aqueous solution under a wide variety of conditions, samples collected from an active gold-mining site in South America were treated with the sodium salt of this ligand. Addition of 0.01 vol % (v/v) 0.5 M BDET to the leaching solution during the final pass through the column (glass, 41 x 5 cm) reduced the mercury concentration from 0.998 to 0.470 ppm. When the BDET volume was increased to 0.30% (v/v) of the leaching solution the concentration of mercury was reduced to 0.001 ppm (Table 1.4).<sup>3</sup>

It is possible that the high concentrations of other metal-cyano complexes present in the solution required the addition of extra quantities of BDET in order to precipitate mercury completely within the leaching columns. In another study on mercury removal from heap leach solutions following the column leaching procedure it was necessary to increase the BDET dosage from the 1:1 stoichiometric ratio (BDET to Hg) to higher values in order to compensate for high copper concentrations.<sup>3</sup> Even at a BDET volume of 0.30% (v/v) of the leaching solution the gold and silver concentrations coming out of the gold-cyanide process remained virtually unchanged.<sup>4</sup> This can be attributed to the fact that gold and silver under these conditions exist as [Au(CN)<sub>2</sub>]<sup>-</sup> and [Ag(CN)<sub>2</sub>]<sup>-</sup> anions while Hg exists as neutral, water-soluble Hg(CN)<sub>2</sub> (9.3 g/100 mL of water)..

#### 1.3.13.4.2.4 Acid mine drainage

In order to explore the utility of BDET for binding metals under acid mine drainage (AMD) conditions, an abandoned coal mine in Pikeville, Kentucky, USA was selected for study. Treatment of the mine effluent reduced Fe concentrations to

< 0.009 ppm from an initial concentration of 2.70 ppm and that of Mn from 0.913 ppm to < 0.001 ppm.<sup>5</sup> In a leaching study of BDET-Fe aqueous iron concentrations remained consistent for the BDET treated AMD samples for 30 days (Table 1.5).<sup>5</sup>

**Table 1.4.** Results of gold ore leaching studies.<sup>3</sup>

Metal	Initial conc.(ppm)	Metal:BDET <sup>2-</sup> ratio	Time (week)	Final metal conc.(ppm)
Cd	0.274	1 : 1	1	0.273
Cd	0.274	1 : 10	1	<0.005
Cd	0.274	1 : 100	1	<0.005
Cu	135	1 : 1	1	135
Cu	135	1 : 10	1	134
Cu	135	1 : 100	1	134
Au	94.1	1 : 1	1	93.4
Au	94.1	1 : 10	1	90.3
Au	94.1	1 : 100	1	89.6
Pb	0.122	1 : 1	1	0.122
Pb	0.122	1 : 10	1	<0.02
Pb	0.122	1 : 100	1	<0.02
Ag	39.8	1 : 1	1	40.5
Ag	39.8	1 : 10	1	37.6
Ag	39.8	1 : 100	1	37.4
Hg	34.5	1 : 1	1	4.05
Hg	34.5	1 : 10	1	0.005
Hg	34.5	1 : 100	1	<5x10 <sup>-5</sup>

**Table 1.5.** Results of BDET-Fe leaching.<sup>5</sup>

Time (d)	pH	BDET-Fe (mg)	Bound Fe (mg)	Leached Fe (mg)
1	0.0	1000	165.3	9.75
1	4.0	1000	165.3	5.11
1	6.5	1000	165.3	2.96
7	0.0	1000	165.3	16.7
7	4.0	1000	165.3	8.36
7	6.5	1000	165.3	3.79
30	0.0	1000	165.3	16.7
30	4.0	1000	165.3	8.36
30	6.5	1000	165.3	3.79

#### 1.3.13.4.2.5 Immobilization of mercury in soil

Mercury contaminated soil samples were collected from the Appalachia Region of Eastern Kentucky, USA and tested with the sodium salt of BDETH<sub>2</sub>. 99.6% of the mercury in the soil samples could be immobilized from an average initial concentration of around 10 mg of mercury per gram of soil (mg Hg/g soil) and that the mercury-ligand compound showed no detectable leaching from pH 0.0-10.0 after 30 days. It was also found that the EPA digestion technique (for the detection of mercury from solid or semisolid waste) was unable to entirely free the mercury from the BDET-Hg compound.<sup>5</sup>

#### 1.3.13.4.2.6 Lead battery recycling effluent

The potassium salt of BDETH<sub>2</sub> was applied to field samples collected from an operating lead battery recycling facility (LBRS) which generates waste water containing lead with concentrations ranging from 2 to 300 ppm at an average pH of 1.5. More than 99.4% of lead could be removed within 15 minutes starting with an average initial concentration of 3.61 ppm using a stoichiometric 1:1 molar dose of BDET<sup>2-</sup> ligand to metal contaminants present in the LBRS waste solutions.<sup>7</sup> Moreover, the BDET-Pb precipitates remained stable to leaching studies during 30-day leaching periods.

### 1.4 Conclusions

It is evident that all the methods and technologies that exist for the remediation of heavy metals from the environment have some advantages and disadvantages. The choice of an appropriate technology will depend on the types, locations, and nature of the water to be remediated. No single technology will be relevant to each circumstance. While

large scale use of some of these techniques are limited by high operating costs, others need optimum processing conditions like pH. Chemical precipitation has proven to be relatively easy and cost-effective. However, many precipitants like trimercaptotriazine (TMT), potassium/sodium thiocarbonate (STC), and sodium dimethyldithiocarbamate (SDTC) have been found to leach heavy metals back into the environment after a short period of time and often decompose to produce toxic substances.<sup>99</sup> Liming requires large doses of alkaline materials to increase and maintain pH values from typically 4.0 to above 6.5 for optimal metal removal. Additionally, liming is often temporary and produces secondary wastes, such as metal hydroxide sludges and gypsum, which are highly regulated and have costly disposal requirements. With sulfide precipitation utmost care is required to control release of the highly toxic H<sub>2</sub>S gas. Also, there exists a problem of residual sulfide in treatment effluent. More importantly, the process involves higher capital and operating costs. The dithiol ligand, benzene-1,3-diamidoethanethiol (BDETH<sub>2</sub>), has proven to be an ideal reagent for removing divalent metals from water. It has been found to effectively bind heavy metals such as Hg and Pb under laboratory conditions. More importantly, the ligand has proven effective in solving some important environmental problems such as removing mercury from gold mine effluent, and metals under acid mine drainage conditions, immobilizing mercury in contaminated soil and precipitating lead from lead battery effluent.

## CHAPTER 2

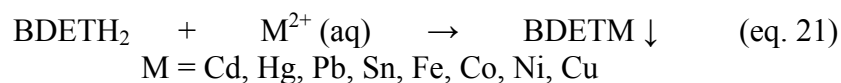
### Metal Compounds of BDETH<sub>2</sub>

#### 2.1 Overview

BDETH<sub>2</sub> removes soft heavy metals from water under a variety of conditions. However, this early work was driven by applications in metal removal from acid mine drainage, mercury from soil, water, and gold mining effluent, and lead battery recycling effluent. The chemical identity of the metal compounds that were formed in these applications was not determined. This chapter will describe the synthesis and full characterization of the compounds that form between BDETH<sub>2</sub> and the metals Cd, Hg, and Pb. Additionally, the chapter will contain an exploration of the compounds that form between BDETH<sub>2</sub> and Group 1 and 2 elements and various common transition metals. The goal will be to provide a complete understanding of how BDETH<sub>2</sub> interacts with the broadest possible range of cations.

The discussion of the metal complexes of BDETH<sub>2</sub> has been broken down into three different categories: 1) alkali and alkaline earth metal compounds, **2-5**, 2) transition metal compounds, **6-9**, and 3) main group metal compounds, **10-14**.

The syntheses of most divalent metal complexes of BDETH<sub>2</sub> were accomplished by one general method using aqueous metal salt solutions (equation 21). Divalent metal salts were used in the syntheses in accordance with our hypothesis which says that a ligand containing a soft thiol group will react with divalent metal cations that are soft or borderline Lewis acids. In the case of monovalent metals the reactions that were run in aqueous solutions are shown by equation 22.



For the preparation of the lithium and magnesium compounds the reactions were conducted under nitrogen since the reagents are air and moisture sensitive. The products were also handled under nitrogen since they were likely to be moisture-sensitive.

In a typical reaction an aqueous salt solution of a metal was added to an ethanolic solution of BDETH<sub>2</sub>. Although, in general, precipitates formed immediately, for BDETNa<sub>2</sub>, BDETK<sub>2</sub>, BDETCO, and BDETNi the reaction mixtures had to be stirred overnight and for BDETAsOH the reaction mixture was stirred for 7 days.

The following sections will describe the methods used for the preparation of metal thiolates and their structures, and the syntheses and characterization of BDET-metal compounds. The discussions will present the similarities and differences between different metal thiolates and the BDET metal compounds.

## 2.2 Alkali and Alkaline Earth Metal Thiolates

The bonding in alkali and alkaline earth thiolates is thought to be covalent with a high ionic component based on studies conducted with MSH, MSH<sup>+</sup>, and M(SH)<sub>2</sub> (M = Li, Na, K, Be, Mg, and Ca).<sup>109</sup> The alkali metal-sulfur bond is ionic with almost no charge transfer. Considerable charge transfer toward the metal are displayed in Mg-S and Be-S bonds and there is evidence for the presence of covalent character in the bond

between Be and S. Connections of elements of lower electronegativity to the metal center decrease the degree of ionicity.

Apart from covalency considerations the structural chemistry of the metal thiolate compounds are influenced by ligand size and charge density of the metal. Sterically demanding ligands and/or strongly coordinating or multidentate bases generally yield monomeric species. Reduction in ligand size and the use of weaker bases result in the formation of higher aggregates.

### 2.2.1 Alkali Metal Thiolates

Reactions between thiols and different reagents such as *n*-BuLi and metal hydrides have been used for the preparation of metal thiolates. Lithium thiolates have been most conveniently prepared by combining the thiol compounds with *n*-BuLi (equation 23).<sup>110</sup> The reactions have been reported to proceed smoothly with the liberation of butane.



In the case of sodium and potassium, the reaction of thiols with the corresponding hydrides has been found to be the most convenient route. The presence of a suitable Lewis donor facilitates the reaction.<sup>110</sup> Equation 24 illustrates the formation of alkali metal thiolates from alkali hydrides.



Monomeric and dimeric formulations are the most common structural features observed for lithium thiolates. Monomeric thiolates are formed when bulky ligands are used in the presence of excess donor as demonstrated by  $\text{Li}(\text{THF})_3\text{SMes}^*$  ( $\text{Mes}^* = 2,4,6\text{-}t\text{-Bu}_3\text{C}_6\text{H}_2$ ).<sup>111</sup> Four-coordinate metal centers with one metal-ligand interaction are characteristics of these compounds. Higher aggregates form when ligand bulk is reduced as in the dimer  $[\text{Li}(\text{THF})_2\text{SCPh}_3]_2$ .<sup>112</sup> In the literature there has also been a report of a dilithium salt,  $\text{LiS}(\text{-R-})\text{SLi}$  {where  $\text{R} = (\text{CH}_2)_2, (\text{CH}_2)_3, \text{CH} = \text{CH}, \text{etc.}$ }.<sup>113</sup> The heavier members of the alkali metal family like Na and K also display the same characteristics as observed for the lithium thiolates. A compound containing two S-Na bonds along with two ONa bonds has been reported in the literature (Figure 2.1).<sup>114</sup>

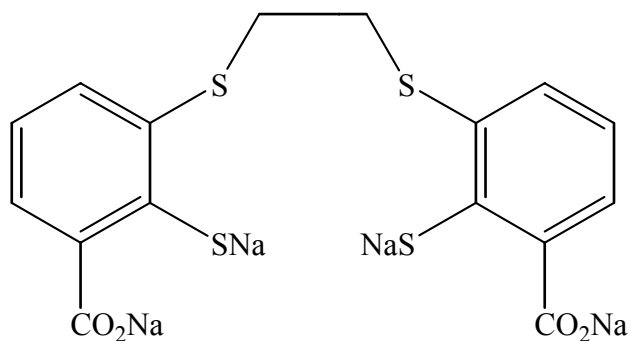


**Figure 2.1.** A compound containing two S-Na bonds.<sup>114</sup>

## 2.2.2 Alkali Metal Compounds of BDETH<sub>2</sub>

### 2.2.2.1 Synthesis and characterization

Compound **2** ( $\text{BDETLi}_2$ ) was prepared by combining  $\text{BDETH}_2$  with two equivalents of *n*-butyllithium under nitrogen. The compound formed immediately after addition of *n*-BuLi solution to the THF solution of  $\text{BDETH}_2$ . Compounds **3** ( $\text{BDETNa}_2$ ) and **4** ( $\text{BDETK}_2$ ) were prepared in the air by adding aqueous solutions of NaOH and

KOH (two equivalents) to stirred ethanolic solutions of BDETH<sub>2</sub>. For **3** and **4**, precipitates formed after the reaction mixtures were stirred overnight. While compound **2** was slightly yellowish, **3** and **4** were both white although the filtrates were light yellow. Yields for all of the reactions were quantitative. Compounds **3** and **4** were found to be very stable in air, light, and water. While compound **2** melted at 154-158 °C, compound **3** and compound **4** decomposed at temperatures of 205 °C and 210 °C, respectively. They were found to be insoluble in common laboratory solvents/solvent systems such as water, methanol, ethanol, water/methanol, water/ethanol, dimethylsulfoxide, dimethylsulfoxide/water, dimethylformamide, acetone, ethyl acetate, tetrahydrofuran, diethyl ether, acetonitrile, acetonitrile/water, 10% acetic acid, toluene, chloroform, dichloromethane, hexane, petroleum ether, nitromethane, and nitrobenzene. However, compound **2** was slightly soluble in dimethylsulfoxide.

Attempts to prepare the Na salt of BDETH<sub>2</sub> using NaOMe or *t*-BuONa, and the K salt using *t*-BuOK produced results (by melting point and IR) similar to that obtained using NaOH and KOH indicating that the thiol protons are labile and easily replaced by Na and K under a variety of conditions.

Infrared spectroscopy data showed that the peak at 2557 cm<sup>-1</sup> due to S-H stretching ( $\nu_{\text{SH}}$ ) was absent from the spectra of the metal compounds indicating that the protons of the thiol groups in BDETH<sub>2</sub> were displaced by the metals and the metals formed bonds with the S atoms. There were no bands corresponding to S-S stretching (between 500 and 400 cm<sup>-1</sup>) and S=O stretching (between 1070 and 1030 cm<sup>-1</sup>) indicating that no oxidation of the products occurred. Raman spectra were obtained for compounds **2** - **4** and the peaks at 316, 292 and 278 cm<sup>-1</sup> were assigned to Li-S, Na-S and K-S

stretches, respectively. These assignments were made considering that most vibrations attributable to the bonds within the ligand are over  $400\text{ cm}^{-1}$ . Metal-sulfur vibration frequencies fall below  $400\text{ cm}^{-1}$  and metal-sulfur vibration frequencies assume smaller numbers with increase in atomic mass of the element. In general, assignments of stretches to metal-sulfur bonds are very difficult because of overlapping bands that may arise from other sources including ligand stretches.

In the  $^1\text{H}$  NMR spectrum for compound **2**, the signal at 8.92 ppm may be attributed to the amide proton. The aromatic protons were displayed at 8.39, 7.96 and 7.60 ppm. The methylene protons were observed at 3.61 and 2.92 ppm. In the  $^{13}\text{C}$  NMR spectrum, the carbonyl carbon signal was observed at 166.1 ppm. The aromatic carbon peaks were found at 134.6, 129.9, 128.4 and 126.2 ppm. The methylene protons were displayed at 37.0 ppm.

In the EI mass spectrum for compound **2** the peak at  $m/z$  208 may be attributed to an intramolecular rearrangement with the loss of a fragment from the molecule. This happens when the carbonyl carbon of one side arm of the compound is attacked by the sulfide residing at the end of the other side arm. The peak at  $m/z$  282 may be due to the loss of two Li atoms from the two side arms of the molecule. Similarly, in the mass spectra for compounds **3** the peaks at  $m/z$  305 may be assigned to  $[\text{M}^+ - \text{Na}]$ . The base peak at  $m/z$  208 may be attributed to an intramolecular rearrangement with loss of a fragment from the molecule as in the case of **2**. In the mass spectrum for **4** the peak at  $m/z$  321 may be assigned to  $[\text{M}^+ - \text{K}]$ . The peak at  $m/z$  208 may be due to an intramolecular rearrangement with concomitant loss of a fragment from the molecule as in the case of **2** and **3**.

Single crystal X-ray analysis could not be performed since no appropriate solvent was found to grow crystals suitable for study. Attempts to grow crystals of compound **2** by liquid diffusion remained unsuccessful.

Thermogravimetric analysis (TGA) was performed in both air and nitrogen at heating rates of 10 °C/min. There were no distinct plateaus in the thermograms indicating that the compounds decompose without producing any stable intermediate to be used for structure determination. This is not surprising since the thermogram of BDETH<sub>2</sub> itself does not provide any information about its composition or structure. The ligand is stable up to 238 °C at which point it begins to lose weight in a regular fashion. The weight loss of 91.04% (between 238 and 388 °C) does not correspond to any structural feature of the compound.

The thermogram for **2**, under both N<sub>2</sub> and air, indicates that the compound is stable up to 273 °C after which it begins to lose weight. The weight losses of 63.3% between 273 and 418 °C, and 24.35% between 418 and 920 °C do not correspond to any structural feature of the compound. The thermogram for **3** shows that the compound is fairly stable up to 238 °C after which it begins to lose weight. The weight losses of 38.41% between 238 and 342 °C, and 19.21% between 342 and 494 °C are not of any diagnostic value. The thermogram for **4** indicates that the compound is stable up to 253 °C after which it begins to lose weight. The weight losses of 59.8% between 253 and 380 °C, 9.8% between 380 and 496 °C, and 27.0% between 496 and 604 °C do not correspond to any structural feature of the compound.

Elemental analyses indicated that the formulations are correct for BDETLi<sub>2</sub>, BDETNa<sub>2</sub> and BDETK<sub>2</sub>. For example, the calculated and experimental values for **2** (anal. calcd. for C<sub>12</sub>H<sub>14</sub>N<sub>2</sub>S<sub>2</sub>O<sub>2</sub>Li<sub>2</sub>) agree quite well. While the calcd. values are C, 48.7; H, 4.76; N, 9.46, the experimental values are C, 48.2; H, 5.39; N, 9.17, respectively. The elemental analysis data found experimentally for the other compounds, BDETNa<sub>2</sub> and BDETK<sub>2</sub> also agree well with the calculated values. These values are given in the Experimental Section.

### 2.2.3 Alkaline Earth Metal Thiolates

Alkane elimination has been widely used for preparing magnesium thiolates containing a wide variety of ligands and donors (equation 25).<sup>110</sup>



Low solubility and a tendency towards polymerization are common features in magnesium thiolate compounds with small ligands due to the high ionic component of the metal-ligand bond. Therefore, use of sterically demanding ligands and strong donors are very common in magnesium thiolate chemistry.

The first reported monomeric magnesium thiolate compound, Mg(S-2,6-Mes<sub>2</sub>C<sub>6</sub>H<sub>3</sub>)<sub>2</sub> (Mes = 2, 4, 6-Me<sub>3</sub>C<sub>6</sub>H<sub>2</sub>) was prepared using the very bulky terphenyl ligand, 2,6-Mes<sub>2</sub>C<sub>6</sub>H<sub>3</sub>.<sup>115</sup> Later, the formation of the four-coordinate, monomeric species Mg(Et<sub>2</sub>O)<sub>2</sub>(SMes\*)<sub>2</sub><sup>116</sup> and Mg(THF)<sub>2</sub>{N(SiMe<sub>3</sub>)<sub>2</sub>} (S-2,4,6-<sup>t</sup>Bu<sub>3</sub>C<sub>6</sub>H<sub>2</sub>)<sup>117</sup> were reported. The dimeric [Mg(STriph)<sub>2</sub>]<sub>2</sub> (Triph = 2,4,6-Ph<sub>3</sub>C<sub>6</sub>H<sub>2</sub>) was synthesized by utilizing the steric bulk of Triph and arene-magnesium interactions.<sup>116</sup>

## 2.2.4 Alkaline Earth Metal Compound of BDETH<sub>2</sub>

### 2.2.4.1 Synthesis and characterization

BDETMg, compound **5**, was prepared by reacting BDETH<sub>2</sub> with one equivalent of Bu<sub>2</sub>Mg in THF under nitrogen. Cloudiness appeared immediately after addition of the Bu<sub>2</sub>Mg solution to the THF solution of BDETH<sub>2</sub>. However, the reaction mixture was stirred overnight to ensure completion of the reaction. Compound **5** was faint yellow and formed in quantitative yield with a melting point of 202 °C (dec). Compound **5** was found to be stable in air, light, and water. It was found to be insoluble in common laboratory solvents/solvent systems like water, methanol, ethanol, water/methanol, water/ethanol, dimethylsulfoxide, dimethylsulfoxide/water, dimethylformamide, acetone, ethyl acetate, tetrahydrofuran, diethyl ether, acetonitrile, acetonitrile/water, 10% acetic acid, toluene, chloroform, dichloromethane, hexane, petroleum ether, nitromethane, nitrobenzene, etc.

Infrared spectroscopy data showed that the peak at 2557 cm<sup>-1</sup> due to S-H stretching (νSH) was absent from the spectrum of the metal compound indicating that the protons of the thiol groups in BDETH<sub>2</sub> were displaced by the metal and the metal formed bonds with the S atoms.

No solution NMR experiment could be performed with these compounds because of lack of solubility in NMR solvents. Likewise, single crystal X-ray analysis could not be performed since no appropriate solvent was found to grow crystals suitable for study.

In the mass spectrum for compound **5** the peak at m/z 306 may be assigned to M<sup>+</sup>. The peak at m/z 282 may be attributed to [M<sup>+</sup> - Mg]. The base peak at m/z 208 may be

attributed to an intramolecular rearrangement with loss of a fragment from the molecule as in the case of the alkali metal metal compounds of BDETH<sub>2</sub>.

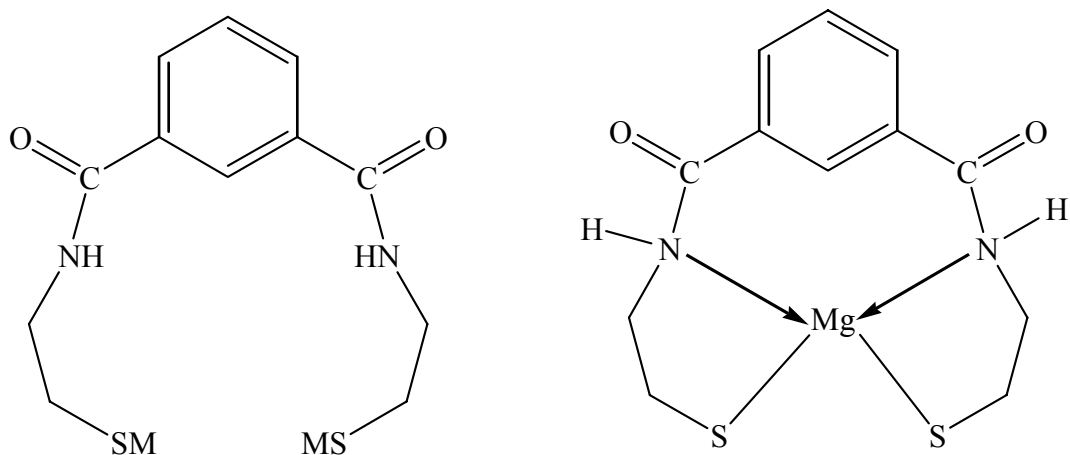
Thermogravimetric analysis (TGA) was performed under a flow of air at a heating rate of 10 °C/min. The thermogram for **5** shows that the compound is fairly stable up to 243 °C before it begins to lose weight. The weight losses of 38.7% between 243 and 393 °C, and 15.9 % between 393 and 595 °C are not of any diagnostic value. The absence of distinct plateaus in the thermogram indicates that the compound decomposes without producing any stable intermediate to be used for structural feature determination.

The elemental analysis agreed with the formulation BDETMg. The calculated and experimental values for **5** (anal. calcd. for C<sub>12</sub>H<sub>14</sub>N<sub>2</sub>S<sub>2</sub>O<sub>2</sub>Mg) agree quite well. While the calcd. values are C, 47.0; H, 4.60; N, 9.13, the experimental ones are C, 46.9; H, 4.37; N, 8.79 respectively.

### 2.2.5 Conclusions

Based on the results of the current investigation bi-metallic salt structures, very similar to LiS-(R)-SLi (where R = (CH<sub>2</sub>)<sub>2</sub>, (CH<sub>2</sub>)<sub>3</sub>, or CH = CH)<sup>113</sup> and {(CO<sub>2</sub>Na)C<sub>6</sub>H<sub>3</sub>(SNa)S}<sub>2</sub>,<sup>114</sup> are suggested for the alkali metal compounds, However, in the literature there is evidence for a two-coordinate lithium thiolate compound, [LiSC<sub>6</sub>H<sub>3</sub>-2,6-Mes<sub>2</sub>]<sub>2</sub>(Et<sub>2</sub>O)<sub>2</sub><sup>118</sup> and a host of compounds with tetrahedral geometry around the metal center (see the discussion above). A four-coordinate and tetrahedral structure of BDETH<sub>2</sub> around the central metal atom is proposed for BDET-Mg. Two sulfur and two nitrogen atoms coming from the two side arms of BDETH<sub>2</sub> complete the

coordination around the central metal atom. Figure 2.2 illustrates the possible structures of the bi-metallic alkali metal compounds and tetrahedral alkali earth BDET compound.



M = Li, Na, K

(a)

(b)

**Figure 2.2.** Proposed structures of BDET-M Compounds: a) alkali metal compounds, b) Mg compound

### 2.3 Transition Metal Thiolates

Several synthetic routes including i) salt metathesis, ii) protolysis of M-O, M-N, or M-C bonds, and iii) electrochemical syntheses have been followed for the preparation of transition metal thiolates.<sup>119</sup> Salt metathesis is the most common procedure (equation 26).



X = halide,  $\text{BF}_4^-$ ,  $\text{ClO}_4^-$ ; R = alkyl, aryl; B = base

Iron thiolates, both homoleptic and heteroleptic, comprise mono-, bi-, and tetra-nuclear species. The coordination number in these compounds is generally four although higher coordination numbers have been reported. However, in the mixed sulfide-thiolate complexes the coordination number is always four.<sup>120</sup> In natural systems like iron-sulfur proteins iron is present with a four-coordinate geometry.

The coordination chemistry of cobalt with mono- and bifunctional thiolate ligands, both in the presence or absence of sulfide, is dominated by the tendency to form tetrahedral  $MS_4$  units similar to that of iron.<sup>120</sup> But unlike iron, cobalt does not exist in oxidation states higher than +2 in thiolate and sulfide-thiolate compounds.

In general divalent nickel is present in nickel thiolate and mixed sulfide-thiolate complexes. The divalent  $d^8$  nickel in these compounds is characterized by square-planar  $MS_4$  units, in contrast to iron and cobalt complexes. These compounds have a tendency to form condensed species, in both protic and aprotic solvents.<sup>120,121</sup>

Cu (II) compounds in nature tend to be four-coordinate as in plastocyanin, a distorted tetrahedral structure with Cu (II) bound to two sulfurs from methionine and cysteinate and two nitrogen histidines.<sup>122</sup> With simple saturated or aromatic thiolates copper forms characteristic tetranuclear complexes of the type  $[Cu_4(SR)_6]^{2-}$  (R = alkyl, or aryl) with a cage-like tetrahedro- $Cu_4$ -octahedro- $(\mu-S)$  structure as in  $[Cu_4(SC_6H_5)_6]^{2-}$ .<sup>123</sup>

### 2.3.1 Transition Metal Compounds of BDETH<sub>2</sub>

#### 2.3.1.1 Synthesis and characterization

BDETFe (**6**), BDETCo (**7**), BDETNi (**8**) and BDETCu (**9**) were prepared by combining aqueous solutions of the metal salts at pH 6.5 with stirred solutions of

BDETH<sub>2</sub> in ethanol or THF. In the case of compounds **6** and **9** precipitates formed immediately after the addition of the aqueous or ethanolic solution of the metal salts to the stirred alcoholic solutions of BDETH<sub>2</sub> whereas the reaction mixtures were stirred overnight to obtain precipitates of compounds **7** and **8**. Compound **6** was slightly yellowish, compound **7** was pinkish-purple, compound **8** was brown, and compound **9** was turquoise blue. Yields of the products ranged from 69% for compound **6** to 100% for compound **9**. The compounds were found to be very stable in air, light, and water. All of the compounds decomposed at temperatures ranging from 162 °C for compound **6** to 210 °C for compound **8**. The compounds were found to be insoluble in the same laboratory solvents/solvent systems used for **2** – **5**.

Infrared spectroscopy data show that the peak at 2557 cm<sup>-1</sup> due to S-H stretching ( $\nu$ SH) is absent from the spectra of the metal complexes indicating that the protons of the thiol groups in BDETH<sub>2</sub> were displaced by the metals and the metals formed bonds with the S atoms. In the spectra there were no peaks for either S-S stretching (between 500 and 400 cm<sup>-1</sup>) or S=O stretching (between 1070 and 1030 cm<sup>-1</sup>) indicating that no oxidation of the compounds occurred.

Raman bands at 178, 106, 173 cm<sup>-1</sup> for compounds **6**, **8** and **9** can not be correlated to any coordination pattern as evidenced in the literature. The assignments of the peaks were made on the basis that metal-sulfur stretches are found below 400 cm<sup>-1</sup> and peaks due to the ligand fall over 400 cm<sup>-1</sup>. No discernible peak was observed for **7**.

No solution NMR experiment could be performed with these compounds due to lack of solubility in NMR solvents. Similarly, single crystal X-ray analysis could not be performed since no appropriate solvent was found to grow crystals suitable for the study.

In the EI mass spectrum for compound **6** the base peak at  $m/z$  208 is due to intramolecular rearrangement with the loss of a fragment as seen in the alkali and alkaline earth metal compounds of BDETH<sub>2</sub>. In the mass spectrum for compound **7** the peak at  $m/z$  282 may be assigned to  $[M^+ - Co]$  and the base peak at  $m/z$  208 may be due to intramolecular rearrangement with the loss of a fragment as in **6**. In the mass spectrum for compound **8** the peak at  $m/z$  282 may be assigned to  $[M^+ - Ni]$  and the peaks at  $m/z$  58, 60, and 62 may be attributed to the stable isotope peaks of Ni. In the mass spectrum of compound **9** the peaks at  $m/z$  63 and 65 may be attributed to the stable isotope peaks of Cu.

The thermograms for the compounds did not show any distinct plateaus indicating that the compounds decomposed without producing any stable intermediates. For example, the thermogram for **6** indicates that the compound is stable up to 259 °C after which it begins to lose weight. The weight losses of 85.7% between 259 and 389 °C, and 3.38% between 389 and 531 °C do not relate to any stable intermediate. The thermogram for **7** shows that the compound is fairly stable up to 283 °C after which it begins to lose weight. The weight losses of 70.95 % (between 283 and 372 °C) and 7.61% (between 372 and 493 °C) do not correspond to any structural feature of the compound. The thermogram for **8** shows that the compound is stable up to 99 °C after which it begins to lose weight. The weight losses of 3.21% (between 99 and 261 °C), 40.59% (between 261 and 407 °C) and 29.60% (between 407 and 415 °C) do not correspond to any structural feature of the compound. The thermogram for **9** shows that the compound is stable up to 108 °C after which it begins to lose weight. The weight losses of 6.13% (between 108 and 287 °C), 54.05% (between 287 and 454 °C), 9.12% (between 454 and

512 °C) and 6.77% (between 512 and 766 °C) do not correspond to any structural feature of the compound.

The experimental and the calculated values of elemental analysis data agree quite well indicating that the formulations BDETFe, BDETCo, BDETNi and BDETCu are correct. For example, for **7** (anal. calcd. for  $C_{12}H_{14}N_2S_2O_2Co$ ) the calculated and experimental values were as follows: Calcd. C, 42.2; H, 4.1; N, 8.2; S, 19.1 and Found C, 41.6; H, 4.0; N, 8.3; S, 18.8. The elemental analysis data found experimentally for the other compounds, namely, BDET-Fe, BDET-Ni and BDET-Cu also agree with the calculated values. These values are given in the Experimental Section 2.6.2.

### 2.3.2 Conclusions

IR, Raman, MS and EA, and evidence presented in the literature support four-coordinate distorted tetrahedral geometries for Fe, Co and Cu and square planar geometry for Ni in the transition metal compounds of BDETH<sub>2</sub>. It was mentioned earlier that metal thiolate compounds of iron, cobalt and copper as reported in the literature are mostly four-coordinate and tetrahedral. Nickel thiolate compounds are largely square planar. In the BDET-metal compounds two sulfur and two nitrogen atoms coming from the two side arms of BDETH<sub>2</sub> complete the coordination around the central metal atom. It is most probable that the compounds are polymeric. Figure 2.3 represents possible structures of the compounds.

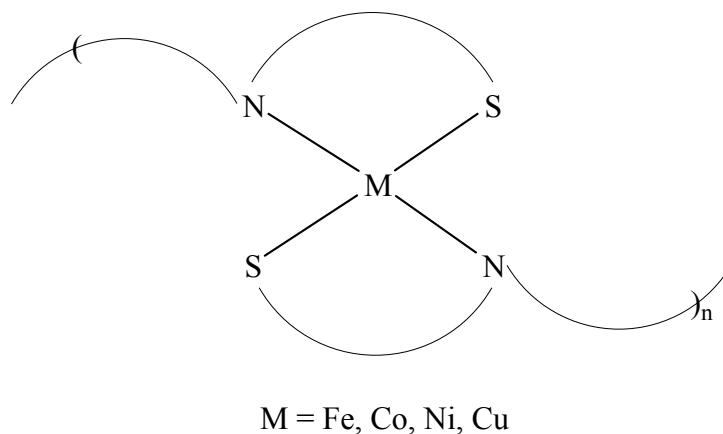


**Figure 2.3.** Proposed structure of transition metal compounds of BDETH<sub>2</sub>.

#### 2.4 Main Group Metal Thiolates

The main group thiolates display a large variety of coordination numbers and geometries around the metal centers caused by the lack of ligand field stabilization energy. A tendency to form polynuclear aggregates of tetrahedral building blocks is characteristic of their reactive behavior.<sup>120</sup> Reactivity of complexes of some of these elements, Hg and Pb in particular, may be influenced by ‘relativistic effects’ which are due to the high speeds of electrons when they move near a heavy nucleus.<sup>124</sup> A consequence of the relativistic effects is reduction in the separation of 6s - 5d orbital energies resulting from the stabilization of s orbitals and destabilization of the d orbitals.

The preparative methods for the synthesis of main group thiolates and sulfide thiolates of main group metals are similar to those used for the transition metals. They typically involve the reaction between thiolate anions (or corresponding thiolate-sulfide mixtures) and the dihalides in solvents such as methanol. Arsenic(III) thiolate compounds have been synthesized by reacting arsenic(III) halides (mainly chlorides) with thiols.

### 2.4.1 Cadmium Complexes

The synthesis and structural characterization of a stable mononuclear tetrahedral cadmium thiolate  $[\text{Cd}(\text{SPh})_4]^{2-}$  with a  $\text{CdS}_4$  core was reported in 1978.<sup>125</sup> The  $\text{CdS}_4$  units are distorted tetrahedra. The deviations from  $T_d$  symmetry are evident in the small  $\text{S}_1\text{-Cd-S}_2$   $\{98.7(2)^\circ\}$  and  $\text{S}_3\text{-Cd-S}_4$   $\{(108.5(2)^\circ)\}$  bond angles. The average Cd-S bond length is 2.56 Å.

More recently, the synthesis and characterization of  $[\text{Cd}(\text{SCH}_2\text{CH}_2\text{NH}_2)_2]$  (Figure 2.4) has been reported.<sup>126</sup> The compound was prepared by combining  $\text{HCl} \cdot \text{NH}_2\text{CH}_2\text{CH}_2\text{SH}$  with  $\text{CdCO}_3$  in the presence of  $\text{NaOH}$ . The compound consists of discrete  $[\text{Cd}(\text{SCH}_2\text{CH}_2\text{NH}_2)_2]$  molecules with intermolecular  $\text{NH} \cdots \text{S}$  hydrogen bonds (Figure 2.5).<sup>126</sup> In the structure cadmium is pentacoordinate, bonded to three sulfur and two nitrogen atoms yielding a distorted square pyramidal geometry. Two cadmium atoms, related by a center of inversion, constitute a dimeric structure. The Cd-S bond distances, varying between 2.492 to 2.735 Å, are comparable to related sulfur-bridged compounds (2.537-2.713 Å).

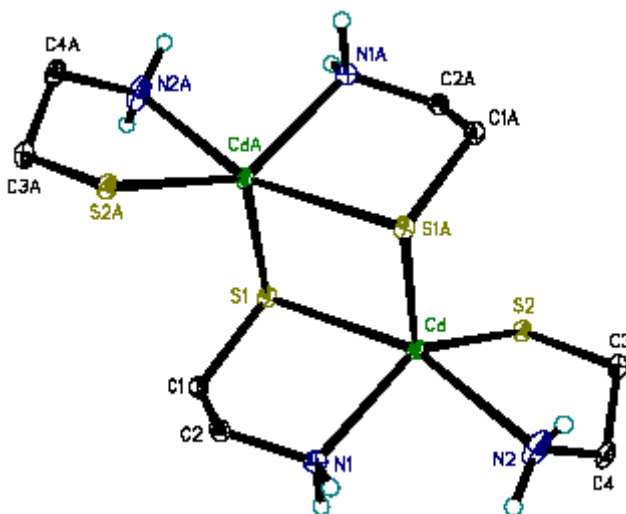


**Figure 2.4.** Molecular structure of  $[\text{Cd}(\text{SCH}_2\text{CH}_2\text{NH}_2)_2]$ .<sup>126</sup>

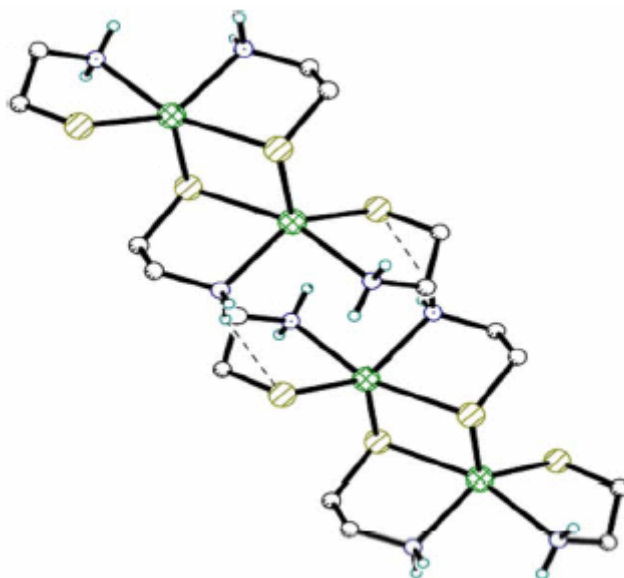


**Figure 2.5.** View of the unit cell of  $[\text{Cd}(\text{SCH}_2\text{CH}_2\text{NH}_2)_2]$  showing hydrogen bonding interaction.<sup>126</sup>

#### 2.4.2 Mercury Complexes

One of the first reported mononuclear Hg(II) thiolate complex is  $[\text{Hg}(\text{S}-2,4,6\text{-}i\text{Pr}_3\text{C}_6\text{H}_2)_2]$  (Figure 2.6).<sup>127</sup> It was obtained by reacting two equivalents of  $\text{LiS}-2,4,6\text{-}i\text{Pr}_3\text{C}_6\text{H}_2$  with  $\text{HgCl}_2$ . The structure consists of a linear two-coordinate Hg(II).

$[\text{Hg}\{\text{S}(\text{CH}_2\text{CH}_2\text{NH}_3)_2\}(\text{Cl})_2]$  (Figure 1.8), another mononuclear Hg(II) compound with a linear geometry for Hg, was prepared by combining  $\text{HCl} \cdot \text{NH}_2\text{CH}_2\text{CH}_2\text{SH}$  with  $\text{HgCl}_2$  in water.<sup>108</sup>

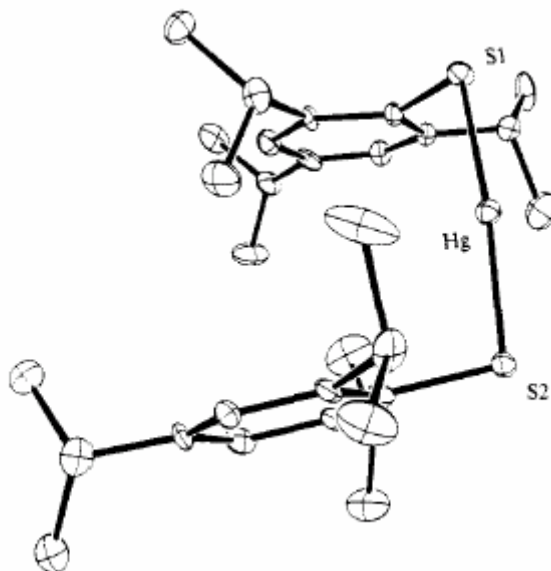


**Figure 2.6.** Crystal structure of  $[\text{Hg}(\text{S}-2,4,6\text{-}i\text{Pr}_3\text{C}_6\text{H}_2)_2]$ .<sup>123</sup>

### 2.4.3 Tin Complexes

Tin forms thiolates in the di- and tetravalent states with tetra, penta-, hexa-, and octacoordination.<sup>128</sup> The synthesis and characterization of  $\text{Sn}(\text{CEE})_2$  (HCEE = L-cysteine ethyl ester) (Figure 2.7), a tetra-coordinate Sn(II) thiolate, has been reported in the literature.<sup>129</sup> It was prepared by combining L-cysteine ethyl ester hydrochloride with tin dichloride dihydrate in deionized water in the presence of potassium carbonate. The four ligand coordination sites and the ‘open’ equatorial site occupied by the Sn(II) lone pair give a distorted four-coordinate pyramidal geometry to the overall structure. The Sn(II) ion coordinates to the two ligands through the amine nitrogen and the thiolate sulfur atom. No interaction between the ester group of the CEE ligand and the metal ion is observed.

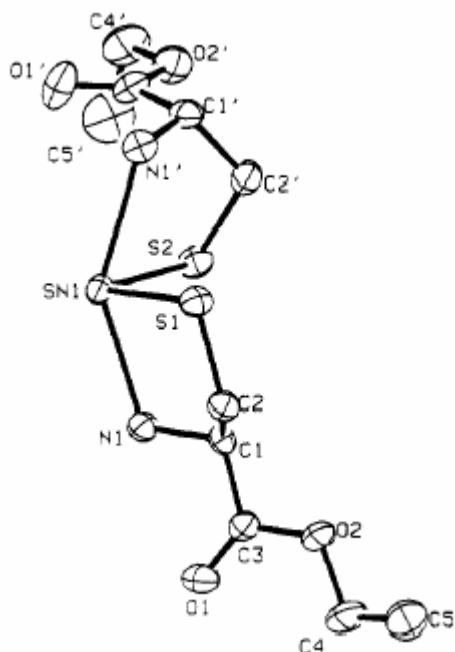


**Figure 2.7.** Crystal structure of  $\text{Sn}(\text{CEE})_2$  (HCEE = L – cysteine ethyl ester).<sup>129</sup>

A centrosymmetric dinuclear Sn(IV) thiolate compound,  $[\text{MeSn}\{\text{N}(\text{CH}_2\text{CH}_2\text{CH}_2\text{S})_3\}]_2$ , was synthesized by combining the tetradentate ligand  $\text{N}(\text{CH}_2\text{CH}_2\text{CH}_2\text{SH})_3$  with  $\text{MeSnCl}_3$ .<sup>130</sup> The structure (Figure 2.8) contains two tetrahedrally coordinated Sn(IV) atoms and two bridging thiolato groups. One interesting feature of the structure is that two of the ligand arms coordinate to one tin atom, while the third ligand arm is coordinated, in a bridging fashion, to a second tin atom. Neither the central nitrogen atom nor the pyridine solvent molecules are coordinated. Thus an almost perfect  $\text{SnCS}_3$  tetrahedron is formed.

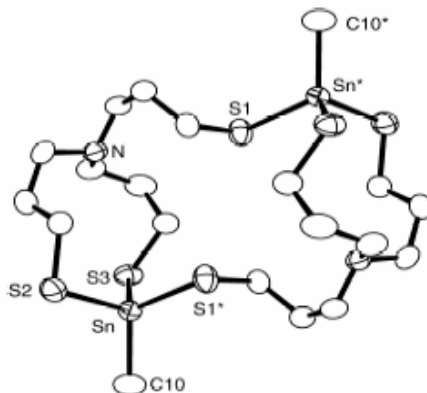


**Figure 2.8.** Crystal structure of  $[\text{MeSn}\{\text{N}(\text{CH}_2\text{CH}_2\text{CH}_2\text{S})_3\}]_2$ .<sup>130</sup>

#### 2.4.4 Lead Complexes

In its thiolate complexes lead has been found to exist only as Pb(II),<sup>128</sup> presumably due to the inert pair effect observed in heavier group 14 elements. The inert pair effect is a consequence of relativistic effects displayed by heavy atoms like mercury, lead, etc.<sup>124</sup> The coordination geometry around Pb(II) may be tetra-, penta-, and hexa-coordinate.<sup>128</sup>

A tetra-coordinate lead(II) thiolate compound,  $\text{Pb}(\text{SCH}_2\text{CH}_2\text{NH}_2)_2$  (Figure 2.9), was synthesized by the reaction of PbO with  $[\text{HSCH}_2\text{CH}_2\text{NH}_3]\text{Cl}$  and NaOH.<sup>131</sup> A pseudo trigonal bipyramidal configuration with a stereochemically active lone pair is a result of the Pb atom forming two covalent Pb-S and two intramolecular dative Pb $\cdots$ N bonds. There are no intermolecular Pb $\cdots$ Pb contacts in the molecule, and also no molecular symmetry elements are present. However, intermolecular N-H $\cdots$ S hydrogen bonds are present {Figure 2.9(b)}.

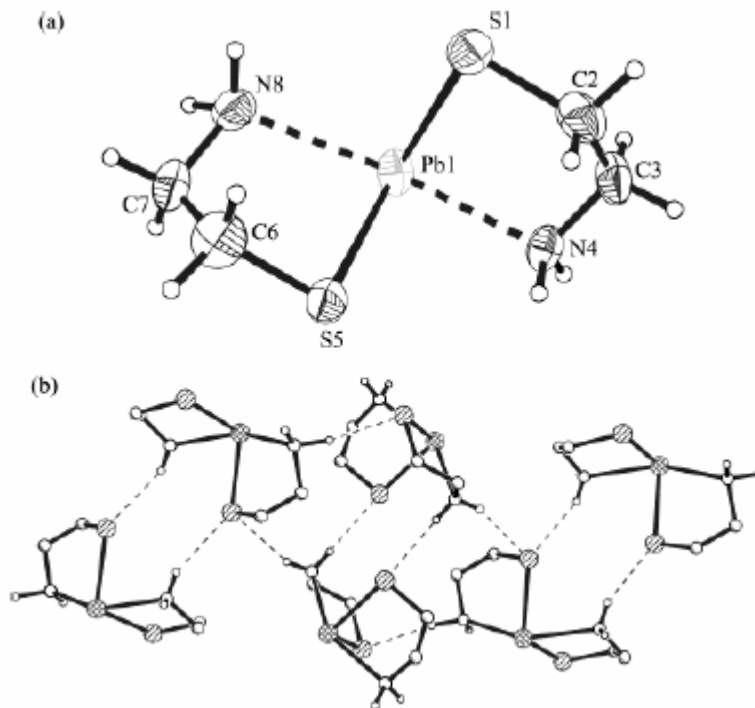


**Figure 2.9.** a) Crystal structure of  $\text{Pb}(\text{SCH}_2\text{CH}_2\text{NH}_2)_2$ .<sup>131</sup> b) Packing diagram showing N-H...S hydrogen bridges.<sup>131</sup>

Recently, the synthesis and characterization of  $[\text{Pb}_2\text{Cl}(\text{SCH}_2\text{CH}_2\text{NH}_2)_3]$ , a compound with both four- and five-coordinate Pb, has been reported.<sup>126</sup> The compound was prepared by combining  $\text{HCl} \cdot \text{NH}_2\text{CH}_2\text{CH}_2\text{SH}$  with  $\text{Pb}(\text{CH}_3\text{COO})_2 \cdot 3 \text{H}_2\text{O}$  in the presence of aqueous NaOH. The Pb atoms in the structure (Figure 2.10)<sup>126</sup> possess stereochemically active lone pairs giving the four-coordinate Pb a distorted square pyramidal geometry and the five-coordinate Pb an octahedral geometry. A planar four-membered  $\text{Pb}_2\text{S}_2$  ring is formed by the five-coordinate Pb atoms. A hydrogen bond is formed by the Cl bonded to the central Pb with the  $\text{NH}_2$  group of the tetracoordinate Pb. The sulfur of the tetracoordinate Pb of a second unit is involved in hydrogen bonding with the NH of the cysteamine attached to the core.

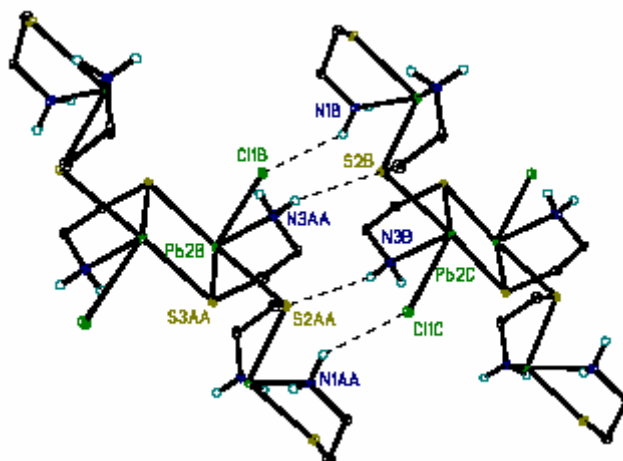


**Figure 2.10.** Molecular structure of  $[\text{Pb}_2\text{Cl}(\text{SCH}_2\text{CH}_2\text{NH}_2)_3]$ .<sup>126</sup>

#### 2.4.5 Arsenic Compounds

Only trivalent arsenic thiolate compounds have been reported in the literature.<sup>132,133</sup> This is expected because As(III) is a soft acid and binds preferentially with soft bases such as thiols. On the other hand, As(V) is a hard acid and usually does not bond with soft bases like thiols. In these compounds Arsenic(III) is found primarily with trigonal-pyramidal coordination geometry.<sup>132</sup> Some cases of tetrahedral geometry have also been reported in As(III) compounds containing non-sulfur groups.<sup>133</sup> This makes As(III) thiolates unique since this structural type is rarely seen in other thiolates, in particular those for transition metals. However, only a few As-S compounds have been structurally characterized. The list includes  $(\text{Me}_2\text{As})_2\text{S}_2$ ,<sup>134</sup>  $(\text{C}_6\text{H}_5)_2\text{As}_2\text{S}_3$  (Figure 2.11),<sup>135</sup> 5-Cl-1-O-4,6-S-5-arsaocane<sup>136</sup> and  $(\text{PhAsS})_4$ .<sup>137</sup>

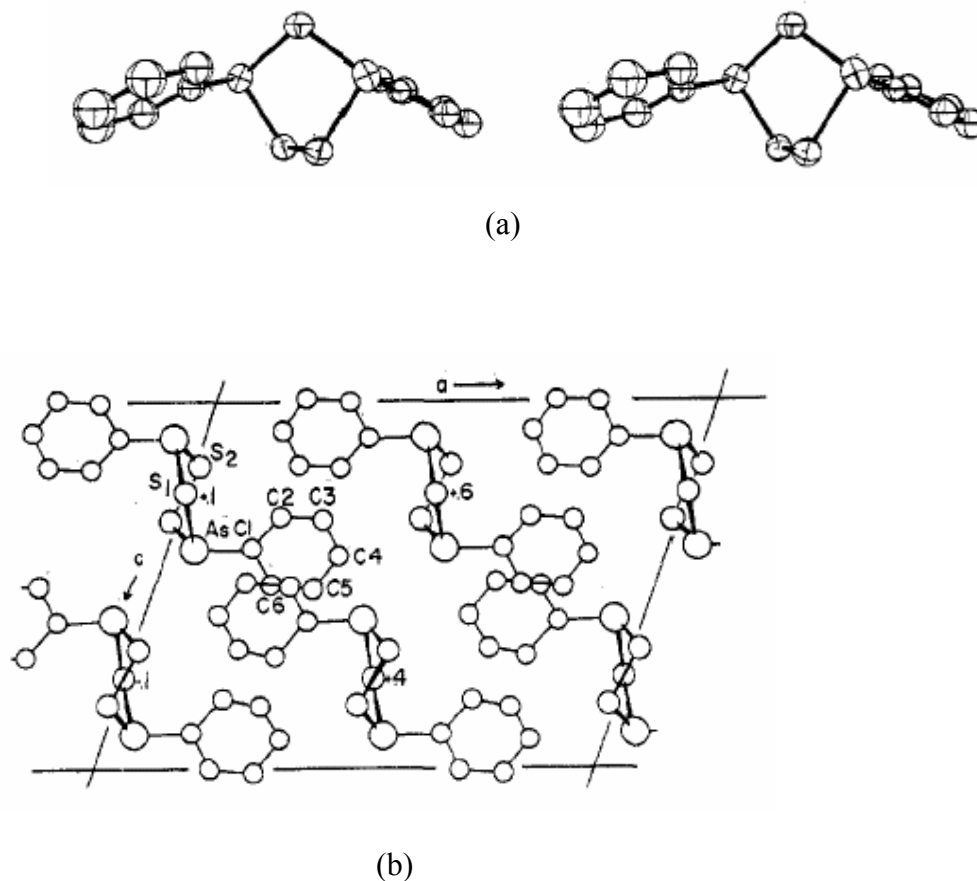


**Figure 2.11.** (a) An Ortep drawing of  $\text{As}_2\text{S}_3(\text{C}_6\text{H}_5)_2$ , (b) unit cell projection of  $\text{As}_2\text{S}_3(\text{C}_6\text{H}_5)_2$  on the  $xz$  axis.<sup>135</sup>

$(\text{C}_6\text{H}_5)_2\text{As}_2\text{S}_3$ , diphenyldiarsenic trisulfide, was prepared by treating a solution of phenylarsenic acid successively with aqueous ammonia, hydrogen sulfide gas, and concentrated hydrochloric acid.<sup>138</sup> Slow evaporation of a chloroform-octane mixture yielded needle-like crystals. A five-membered, nonplanar arsenic-sulfur ring with the sequence  $-\text{As}-\text{S}-\text{As}-\text{S}-\text{S}-$  constitutes the structure of the molecule. Each arsenic atom is bonded to one phenyl ring. The  $\text{As}-\text{S}(2)'$  and  $\text{As}-\text{S}(1)$  bond distances are 2.252 (5) and 2.253 (4) Å, respectively, and the  $\text{S}(2)-\text{S}(2)'$  bond length is 2.036 (6) Å. The  $\text{S}(1)-\text{As}-\text{S}(2)'$ ,  $\text{S}(2)'-\text{As}-\text{C}(1)$  and  $\text{S}(1)-\text{As}-\text{C}(1)$  bond angles are 98.4 (1), 99.7 (5), and 101.3 (4)°,

respectively. The As-S-As and As-S-S bond angles are  $107.47(7)^\circ$  and  $101.1(1)^\circ$  respectively.

In a later work N. A. Rey et al. proposed the molecular structures of As(III)-glutathione complexes as having trigonal pyramidal geometry around arsenic.<sup>139</sup>

The synthesis and characterization of two isomeric, self-assembled arsenic-thiolate macrocycles,  $As_2L_2Cl_2$  ( $H_2L = \alpha, \alpha'$ -dimercapto-*p*-xylene) was reported by Vickaryous et al.<sup>140</sup> Crystals of  $As_2L_2Cl_2$  were obtained by adding  $AsCl_3$  to a solution of  $H_2L$  in  $CHCl_3$  followed by slow diffusion of pentane into the solution.<sup>140</sup> The geometry around As in these complexes was found to be trigonal pyramidal. The As-S bond lengths ranged from 2.2180(8) to 2.2252(8) Å and the S-As-S bond angles were  $87.09(3)$  and  $90.32(9)^\circ$ .

This unique structural feature has also been demonstrated in halo-dithiarsenic and arsenic trithiolate compounds.<sup>141,142</sup> The crystal structure of 2-iodo-1,3,2-dithiarsolane (Figure 2.12)<sup>141</sup> containing two molecules in its asymmetric unit illustrates one such structure.

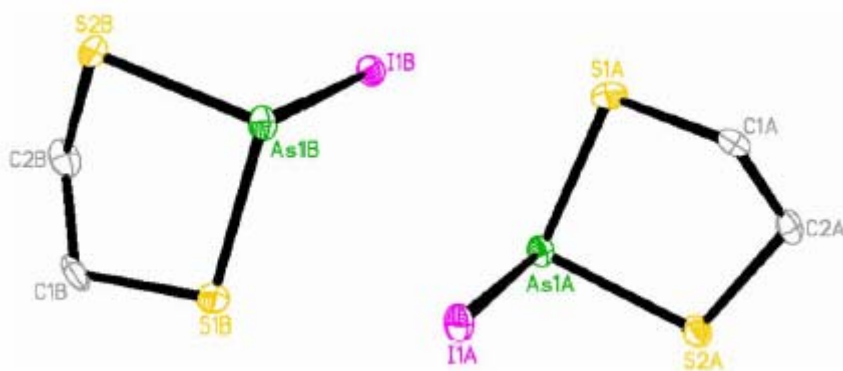


**Figure 2.12.** Crystal structure of 2-iodo-1,3,2-dithiarsolane.<sup>141</sup>

## 2.4.6 Main Group Compounds of BDETH<sub>2</sub>

### 2.4.6.1 Synthesis and characterization

#### 2.4.6.1.1 Synthesis

In a typical reaction an aqueous salt solution of a metal was added to an ethanolic solution of BDETH<sub>2</sub>. In all cases, except for BDET-AsOH, precipitates formed immediately after combination of the two solutions; in the case of BDET-AsOH the reaction mixtures had to be stirred for 7 days for the completion of the reaction. When sodium arsenite and sodium arsenate were combined with BDETH<sub>2</sub> solutions in 1:1 or 1:2 stoichiometric ratios, the desired product was not obtained. But, when a six fold excess of BDETH<sub>2</sub> was used both arsenite and arsenate gave almost identical products. Compounds **10** (BDET-Cd), **11** (BDET-Hg), **12** (BDET-Sn) and **14** (BDET-AsOH) were white, while compound **13** (BDET-Pb) was yellow. Yields of the products ranged from 65% for compound **10** to 100% for compound **13** and **14**. The compounds were found to be very stable in air, light, and water. None possessed reversible melting points; they decomposed at temperatures ranging from 156 °C to 210 °C.

#### 2.4.6.1.2 Characterization

BDETH<sub>2</sub> was designed to provide a linear S-M-S geometry in binding and precipitating mercury, while providing two strong covalent bonds, along with additional coordination by the nitrogens, to give at least a four-coordinate bonding environment for Cd, Sn and Pb and, a trigonal pyramidal geometry around As with bonds to the sulfur atoms of BDETH<sub>2</sub> and a hydroxyl group. The following discussion will present the complete characterization data for the BDET compounds of Cd, Sn, Hg, Pb and As.

Infrared spectroscopy data obtained for all five compounds show that the peak at  $2557\text{ cm}^{-1}$  due to S-H stretching ( $\nu\text{SH}$ ) is absent from the spectra indicating that the protons of the thiol groups in  $\text{BDETH}_2$  were displaced by the metals and the metals formed bonds with the S atoms. There were no peaks corresponding to S-S stretching (between  $500$  and  $400\text{ cm}^{-1}$ ) and S=O stretching (between  $1070$  and  $1030\text{ cm}^{-1}$ ) indicating that no oxidation of the compounds occurred.

Raman spectroscopy exhibited metal-sulfur stretches for all of the compounds. For example, the band at  $205\text{ cm}^{-1}$  in compound **10** was attributed to Cd-S. This is similar to values found in the literature for  $\nu\text{Cd-S}$  in tetrahedral cadmium compounds like  $\text{Cd}(\text{TAA})_2$  (TAA= monothioacetylacetonate)<sup>143</sup> and  $[\text{Cd}(\text{Et}_2\text{dtc})_2]_2$  (  $\text{Et}_2\text{dtc}$  = diethyldithiocarbamate).<sup>144</sup> The band at  $293\text{ cm}^{-1}$  for compound **11** can be attributed to a linear Hg-S bond and is similar to others reported in the literature.<sup>145</sup> For example, for the Hg-S bands in  $\text{Hg}(\text{SMe})_2$  the values  $297$ ,<sup>146</sup>  $295$ ,<sup>147</sup> and  $298$ <sup>148</sup>  $\text{cm}^{-1}$  have been reported. The band at  $352\text{ cm}^{-1}$  for **12** may be assigned to Sn-S stretching for a tetrahedral  $\text{BDET-Sn}$  compound although there is no evidence in the literature to support this. This assignment was made on the assumption that metal-sulfur stretches are found below  $400\text{ cm}^{-1}$  and that no band was observed below  $400\text{ cm}^{-1}$  in the spectrum for the ligand alone. The band at  $164\text{ cm}^{-1}$  for **13** was assigned to  $\nu\text{Pb-S}$ . This value is similar to values for  $\nu\text{Pb-S}$  reported in the literature for tetrahedral lead compounds like  $(\text{C}_6\text{H}_5)_3\text{PbSC}_6\text{H}_5$ .<sup>149</sup> Similarly, the band at  $379\text{ cm}^{-1}$  for **14** may be attributed to a As-S stretching of a trigonal pyramidal  $\text{BDET-AsOH}$  compound. However, there is no evidence in the literature to support this.

The compounds, except compound **13**, were found to be insoluble in over twenty-two common laboratory solvents/solvent systems such as water, methanol, ethanol, water/methanol, water/ethanol, etc. Compound **13** was very slightly soluble in DMSO. Therefore, no solution NMR experiments could be performed with these compounds. Attempts to run  $^1\text{H}$  NMR in DMSO with compound **13** yielded a spectrum with broad peaks that were very hard to interpret. No interpretable peaks were obtained in the case of  $^{13}\text{C}$  NMR.

In the EI mass spectroscopic data for BDET-Cd (**10**) the peak at  $m/z$  282 corresponds to  $[\text{M}^+ - \text{Cd}]$  while the peaks at 112, 111, and 110 correspond to the isotope peaks of Cd. In the spectrum for BDET-Hg (**11**) peaks at  $m/z$  204 - 198 correspond to the isotopic peaks of Hg. The peak at 282 corresponds to  $[\text{M}^+ - \text{Hg}]$ . In the spectrum for BDET-Sn (**12**) the peaks at  $m/z$  401 and 282 correspond to  $\text{M}^+$  and  $[\text{M}^+ - \text{Sn}]$  respectively, while the peaks at 120, 116 and 115 correspond to the isotope peaks of Sn. Similarly, in the spectrum for BDET-Pb (**13**) the peaks at  $m/z$  208, 207, and 206 correspond to the isotope peaks of Pb. The peak at 282 corresponds to  $[\text{M}^+ - \text{Pb}]$ . In the mass spectrum of BDET-AsOH (**14**) the peaks at  $m/z$  373 and 282 were attributed to  $[\text{M}^+ - \text{H}]$  and  $[\text{M}^+ - \text{AsOH}]$  respectively. The base peak at  $m/z$  208 results from intramolecular cyclization with the loss of a fragment from the molecule.

Efforts were made to run solid-state NMR since it has been reported in the literature that  $^{199}\text{Hg}$  MAS solid state NMR could be utilized to determine the coordination geometry of Hg-containing compounds from the shielding anisotropic shifts.<sup>145</sup> The anisotropic shift for tetrahedral Hg is small ( $< 1200$  ppm), for trigonal is intermediate (1200 – 1400 ppm), and for linear is large ( $> 4000$  ppm). The  $^{199}\text{Hg}$  MAS

solid state NMR for BDET-Hg resulted in a spectrum with no detectable  $^{199}\text{Hg}$  signal. Linear Hg compounds tend to feature high anisotropic shifts that are large and broad, often to the point of being undetectable. In the literature there is evidence that Hg signals are not observed for Hg-thiolates containing linear Hg-S bonds.<sup>145,150,87</sup> In one study it was reported that no Hg signals were obtained in the solid-state  $^{199}\text{Hg}$  NMR of  $\text{Hg}(\text{Ph})_2$ ,  $\text{CH}_3\text{HgO}_2\text{CCH}_3$ , or  $\text{PhHgO}_2\text{CCH}_3$ .<sup>150</sup> This was attributed to excessive sideband patterns ( $\gg 125$  KHz) which result from the large shift anisotropy expected for linear compounds. Similarly,  $^{199}\text{Hg}$  NMR signals for  $[\text{Hg}(18\text{S}6)](\text{PF}_6)_2$  (18S6 = 1,4,7,10,13,16(hexathiacyclooctadecane) were not observed due to the identical length (2.689(2) Å) of all six Hg-S bonds.<sup>87</sup> The lack of a  $^{199}\text{Hg}$  NMR signal provided indirect evidence that compound **11** contained a linear S-Hg-S bonding unit. By comparison, the solution structure of the MerP protein, where Hg is bound by two cysteine groups,<sup>151</sup> the geometry of the S-Hg-S bond was found to be  $177^\circ$  with a solution  $^{199}\text{Hg}$  NMR shift of -816 ppm.<sup>152,153</sup> It is important to note that BDETH<sub>2</sub> provides the same binding environment and geometry for Hg as the MerP protein. However, no signals were also detected for **10** and **13** in the  $^{113}\text{Cd}$  and  $^{207}\text{Pb}$  MAS solid state NMR. This can be attributed to the lack of any proton near the metal center resulting in very long relaxation times, and not to the presence of a linear S-M-S (M = Cd, Pb) bond since these compounds are expected to be ligated in a  $T_d$  geometry by the BDET ligand. No solid state NMR experiment was performed with the Sn and As compounds.

The coordination geometries of many model compounds have also been examined.<sup>145,154</sup> The most common primary coordination number for Hg(II) is 2. These compounds have covalent bond lengths that vary between 2.316 and 2.361 Å and bond

angles that vary between  $180.0^\circ$  and  $167.4^\circ$ .<sup>134</sup> Recently, it was demonstrated that a linear compound,  $[\text{Hg}\{\text{S}(\text{CH}_2)_2\text{NH}_3\}_2](\text{Cl})_2$ , is formed when  $\text{HgCl}_2$  reacts with cysteamine hydrochloride.<sup>108</sup> Cysteamine forms the side chains of BDETH<sub>2</sub>. The observed Hg – S bond lengths are 2.333(9) and 2.338(9) Å. And the S-Hg-S bond angle is  $168.53(3)^\circ$ . Distortions from linearity are generally caused by longer secondary bonding interactions found in the solid state.

Thermogravimetric analyses (TGA) were conducted to gain further information on the stability and composition of the compounds. The thermogram for **10** shows that the compound is fairly stable up to  $77^\circ\text{C}$  after which it begins to lose mass. The observed weight loss of 3.19 % between  $77$  and  $272^\circ\text{C}$  indicates that the compound may be hydrated, with slightly over half a molecule of  $\text{H}_2\text{O}$  present. However, the absence of broad bands at  $3415$  ( $\nu\text{OH}$ ) and  $1642\text{ cm}^{-1}$  ( $\delta\text{H}_2\text{O}$ ) in the IR spectrum and results of elemental analysis does not support this. The other weight losses for BDET-Cd indicate that the compound decomposes without producing any stable intermediates. The thermogram for **11** shows that the compound is very stable up to  $239^\circ\text{C}$ . No distinct plateau was observed in the thermogram indicating that the product decomposed without producing any stable intermediates. The observed weight losses of 13.76% (between  $239$  and  $303^\circ\text{C}$ ), and 62.32% (between  $303^\circ\text{C}$  and  $383^\circ\text{C}$ ) did not correspond to any structural feature of the compound. The weight losses simply indicate that the compound decomposes without producing any intermediates. The thermogram for **12** shows that the compound is stable up to  $82^\circ\text{C}$  after which it begins to lose weight. No distinct plateau was observed indicating that the compound decomposed without producing any stable intermediates. However, the residual weights of 45.34% and 24.95% at  $648$  and  $678^\circ\text{C}$

respectively may be attributed to SnS<sub>2</sub> and Sn indicating the presence of the atoms of Sn and S in the molecule. The thermogram for **13** shows that the compound is fairly stable up to 280 °C after which it begins to lose mass. The thermogram for compound **14** shows that it is stable up to 271 °C after which it begins to lose weight. The weight loss of 75.43% between 271 and 473 °C may be attributed to the loss of BDET from the molecule. The weight loss of 20.47% between 473 and 530 °C may be due to the loss of As from the molecule.

The weight losses observed indicate that the compounds decompose without producing any stable intermediates. This could be an indication that the compounds are polymeric rather than molecular (Figure 2.13a)<sup>8</sup>, an observation in keeping with the insolubility of the compounds.

This is further supported in the literature where BDETH<sub>2</sub> is used in passivating gold surfaces in self-assembled monolayers. In these studies the mode of bonding is either 'open' (Figure 2.13b) or with the two sulfurs bonded to two metals (Figure 2.13c).<sup>8</sup> For the present compounds, then, a bridging, polymeric structure where each sulfur is bonded to a separate metal is most likely.

The elemental analyses clearly indicate that the compound formulations BDETCd, BDETHg, BDETSn, BDETPb and BDETAsoH for **10**, **11**, **12**, **13** and **14** are correct. For **10** (anal. calcd. for C<sub>12</sub>H<sub>14</sub>N<sub>2</sub>S<sub>2</sub>O<sub>2</sub>Cd) the experimental values agreed very well with that of the calculated ones. While the calculated values for C, H and N were 36.5%, 3.58%, and 7.10%, respectively, the corresponding experimental values were 35.9%, 4.29%, and 6.94%. The elemental analysis data found experimentally for the other compounds,



at 2,472.0 eV, is similar to those observed<sup>155-157</sup> for aliphatic monosulfides containing C-S-H functional groups (thiols, mercaptans) and significantly removed from the peak position for the sulfide anion in HgS. BDET-Hg, which involves sulfur bonded between carbon and Hg(II), is appropriately intermediate in peak position between those for HgS and BDETH<sub>2</sub>.

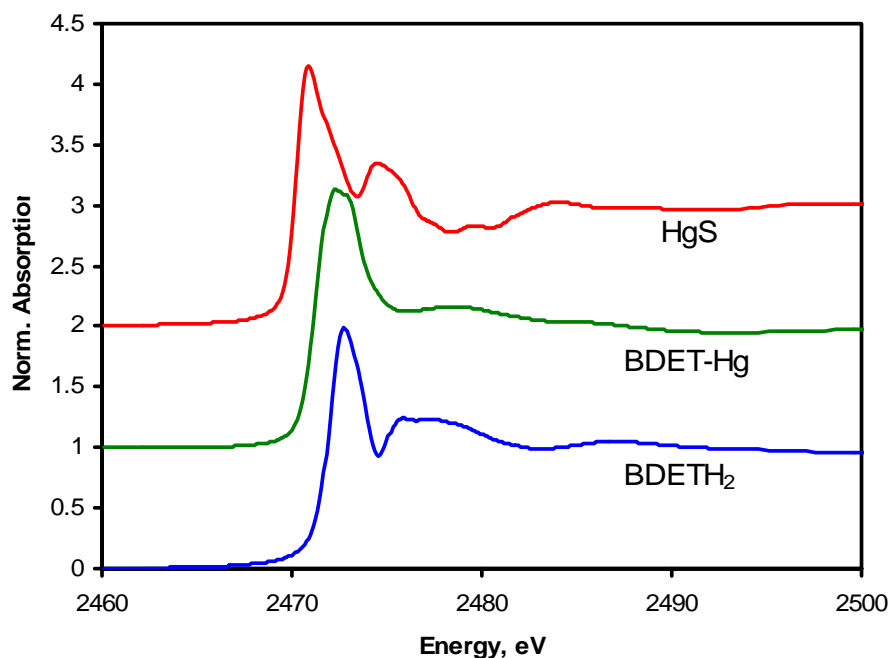


**Figure 2.14.** Sulfur XANES spectra for HgS, BDET-Hg and BDETH<sub>2</sub>.

Figure 2.15(a) shows the mercury L<sub>III</sub>-edge XANES spectra for both HgS (cinnabar) and BDET-Hg. The spectra are similar, although HgS has more pronounced fine structure as a consequence of the smaller and more regular unit cell and three-dimensionally ordered crystal structure.

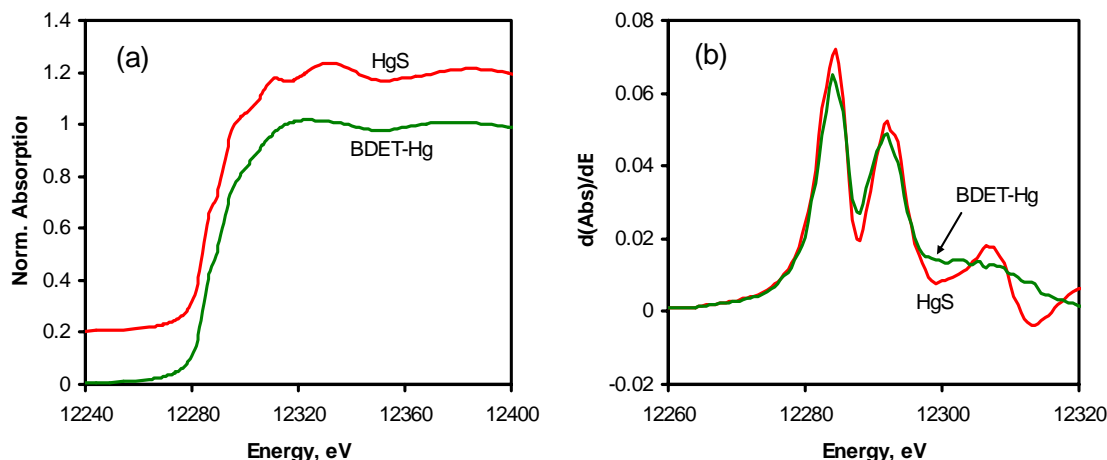


**Figure 2.15.** (a) Hg L<sub>III</sub>-edge XANES spectra for HgS and for the BDET-Hg; (b) first derivative Hg L<sub>III</sub>-edge XANES spectrum.

Figure 2.15(b) shows the first derivative XANES spectrum that accentuates the two inflection points on the rising edge in the XANES spectrum. A parameter known as the inflection point difference, or IPD, is defined as the separation in eV of the two prominent peaks that occur in the derivative XANES spectrum. This separation reflects the nature of the anion to which the Hg is bound.<sup>158,159</sup> Both HgS (cinnabar) and BDET-Hg have similar values for IPD:  $7.7 \pm 0.3$  eV for HgS and  $7.5 \pm 0.3$  eV for BDET-Hg reflecting the fact that Hg(II) is principally bound to sulfur atoms in both materials.

Figure 2.16 compares the EXAFS (extended X-ray absorption fine structure) region of the Hg XAFS spectra for HgS and BDET-Hg. Figure 2.16(a) shows the isolated EXAFS oscillations converted to a reciprocal space representation (k-space, in  $\text{\AA}^{-1}$ ) and weighted by  $k^3$ . As can be seen, these oscillations occur at regular intervals in k-space and the amplitude of the oscillations is significantly greater for HgS. The spacing of the oscillations is similar for both materials, although the two curves are offset from each other.

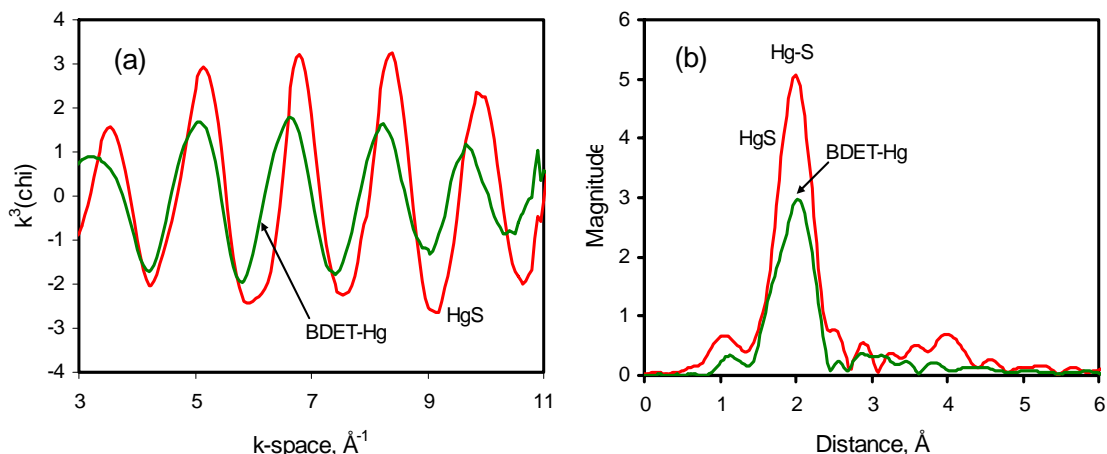


**Figure 2.16.** (a) EXAFS oscillations isolated from the XAFS spectrum and displayed as  $k^3(\chi)$  vs.  $k$ ; (b) Radial structure function obtained by applying a Fourier transform to the  $k^3\chi$  spectra shown in panel a. The single main peak represents the first Hg-S coordination shell, uncorrected for the phase shift.

The radial structure function (RSF) spectra shown in Figure 2.16(b) were obtained by applying a Fourier transform to the spectra in Figure 2.16(a). One main peak is observed in the RSF of both materials; it represents the first coordination shell between Hg and sulfur. The peak occurs at about the same position in both spectra, but its amplitude is almost twice as high in HgS than in BDET-Hg. By applying FEFF 6.0 fitting procedures<sup>160</sup> to the EXAFS region data, it is possible to estimate the bond distance,  $R$  in  $\text{\AA}$ , between Hg and S and the coordination number, CN, for the Hg. This was achieved by using HgS (cinnabar) as a model compound for the EXAFS data for BDET-Hg. Cinnabar has a distorted NaCl-type structure (space group,  $P 3_221$ ) and each  $\text{Hg}^{2+}$  cation is surrounded by two  $\text{S}^{2-}$  anions at a distance of 2.37  $\text{\AA}$  and the S-Hg-S bond angle is 172°. <sup>161</sup> The FEFF fitting can be achieved using the RSF ( $R$ ) or the  $k^3\chi$  spectrum ( $k$ ) or the back-transform of the major peak in the RSF, which separates the contribution of the Hg-S shell from the overall  $k^3\chi$  spectrum, ( $q$ ). FEFF least-squares fitting of cinnabar is summarized in Table 2.1.

**Table 2.1.** FEFF parameters derived for cinnabar (hexagonal HgS)

	$S_0^2$	$CN^1$	$e_0$	$R, \text{\AA}$	$\sigma^2$	$R_{\text{fact}}$
Crystallogr. <sup>17</sup>		2		2.37		
R (1.3-2.6 $\text{\AA}$ )	0.41	2	8.4	2.386	0.003	0.008
k (3 - 13 $\text{\AA}^{-1}$ )	0.41	2	8.2	2.385	0.003	0.044
q (Hg-S)	0.40	2	8.1	2.385	0.003	0.006
error (q)	$\pm 0.005$		$\pm 1.2$	$\pm 0.005$	$\pm 0.0006$	

<sup>1</sup> a value for CN of 2 was assumed for the fitting to derive values for  $S_0^2$ .

These values were then used to model the EXAFS region data for BDET-Hg. The resulting least-squares values are shown in Table 2.2. The comparison of data and fit returned by this procedure is shown in Figure 2.17, for cinnabar and BDET-Hg. Also indicated in figure 2.17 is the close correspondence of the k-space EXAFS spectrum for Hg in BDET-Hg and the k-space EXAFS spectrum derived from back-transform of the Hg-S shell in the RSF.

**Table 2.2.** FEFF parameters derived for BDET-Hg based on cinnabar parameters

	$S_0^2$	CN	$e_0$	$R, \text{\AA}$	$\sigma^2$	$R_{\text{fact}}$
R (1.3-2.6 $\text{\AA}$ )	0.41	2.15	5.4	2.42	0.008	0.024
k (3 - 13 $\text{\AA}^{-1}$ )	0.41	2.16	5.9	2.42	0.008	0.032
q (Hg-S)	0.40	2.08	5.9	2.42	0.008	0.020
error (q)		$\pm 0.25$	$\pm 1.6$	$\pm 0.01$	$\pm 0.001$	

<sup>1</sup> a value for  $S_0^2$  of 0.41 was assumed for the fitting to derive values for CN.

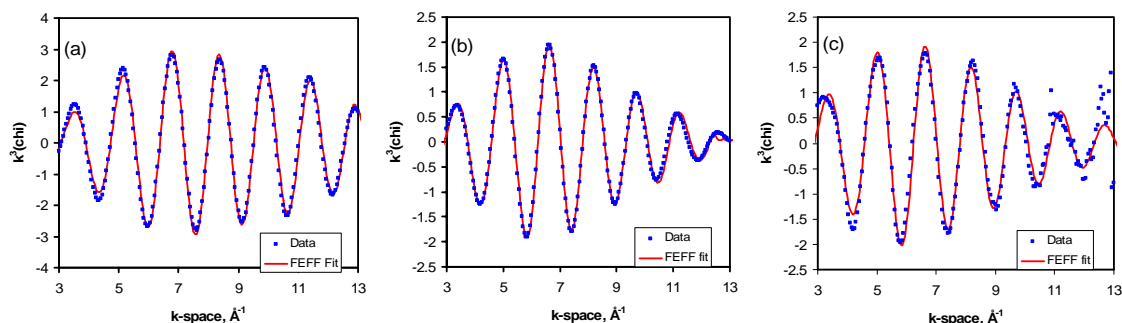


**Figure 2.17.** Comparison of FEFF model function and data for (a) the Hg-S shell in RSF back-transformed to k-space for cinnabar, HgS; (b) the Hg-S shell in RSF back-transformed to k-space for BDET-Hg; and (c) the total k-space EXAFS oscillations for BDET-Hg

The agreement among the different fitting bases, R, k, and q, is reasonable and within anticipated experimental errors. Interestingly, despite the apparent factor of almost 2 in amplitude of the Hg-S peaks in the RSF (Figure 2.16), the FEFF fitting indicates that the coordination number of Hg in both HgS and BDET-Hg are the same. The bond distance for the Hg-S bonds in BDET-Hg is about 0.04 Å longer and the Debye-Waller factor,  $\sigma^2$  is significantly higher; both of which will result in less amplitude in the RSF peak. The distance estimated for the Hg-S bonds in BDET-Hg is 2.42 Å, which falls in the range of values (2.34 – 2.53 Å) reported in the literature.<sup>161-163</sup>

The derived Hg-S bond distance is relatively long for two-coordinate Hg(II) in mercury-sulfur complexes and such elongation may indicate additional secondary interactions with other ligands.<sup>9</sup> More complex FEFF modeling was attempted to assess, in particular, the possibility that oxygen or carbon was in the first coordination sphere. However, such fitting did not improve the fits significantly nor did it provide any meaningful results. Hence, it can be concluded that, although such interactions may indeed be present to account for the longer Hg-S bond, they are not reflected in the

EXAFS data presumably because of their non-systematic nature. Such a result is more consistent with the BDET-Hg mercury complex being polymeric rather than crystalline.

XAFS experiments were attempted for the other BDET-M (M = Cd, Sn, Pb and As) compounds, but final results could not be obtained because no suitable reference compounds like pure CdS, SnS<sub>2</sub>, PbS and As<sub>2</sub>S<sub>3</sub> were available.

#### 2.4.6.3 Leaching Study

A leaching study was conducted to ascertain the stability of three BDET-M (M = Cd, Hg and Pb) compounds in harsh acidic conditions. These results clearly demonstrated that the BDET-M compounds are very stable and do not decompose under acidic conditions. This may be attributed to the hydrophobic nature of the ligand environment which would prevent access to the metal atoms by water soluble species such as H<sub>3</sub>O<sup>+</sup>. Table 2.3 summarizes the results of this study.

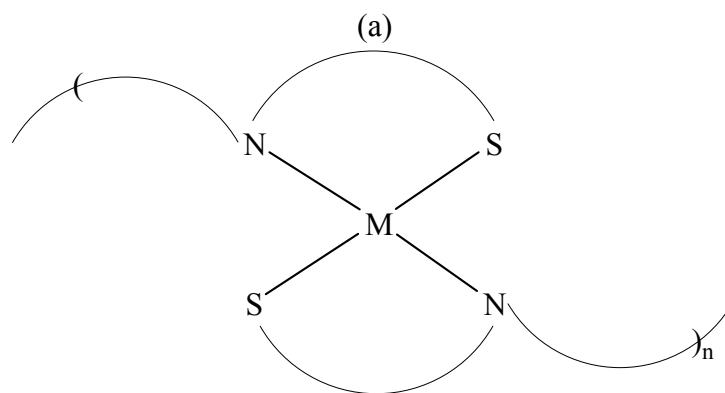
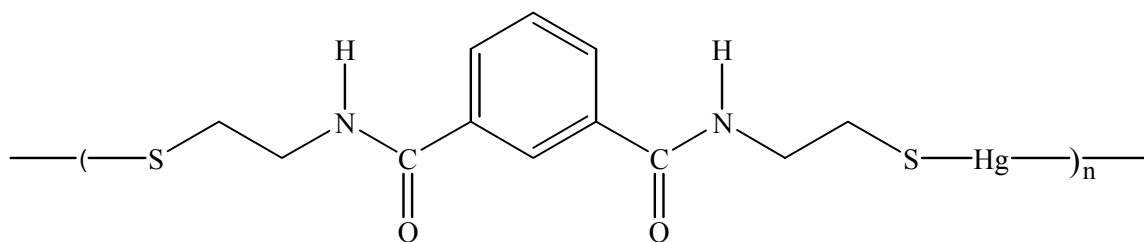
**Table 2.3.** Results of leaching studies for BDET-Cd, BDET-Hg and BDET-Pb

Metal	pH	Concentration (ppm)			
		1 d	7 d	14 d	28 d
Cd	1	<0.008 <sup>a</sup>	<0.008 <sup>a</sup>	<0.008 <sup>a</sup>	<0.008 <sup>a</sup>
Cd	3	<0.008 <sup>a</sup>	<0.008 <sup>a</sup>	<0.008 <sup>a</sup>	<0.008 <sup>a</sup>
Hg	1	<0.0005 <sup>b</sup>	<0.0005 <sup>b</sup>	<0.0005 <sup>b</sup>	<0.0005 <sup>b</sup>
Hg	3	<0.0005 <sup>b</sup>	<0.0005 <sup>b</sup>	<0.0005 <sup>b</sup>	<0.0005 <sup>b</sup>
Pb	1	<0.020 <sup>a</sup>	<0.020 <sup>a</sup>	<0.020 <sup>a</sup>	<0.020 <sup>a</sup>
Pb	3	<0.020 <sup>a</sup>	<0.020 <sup>a</sup>	<0.020 <sup>a</sup>	<0.020 <sup>a</sup>

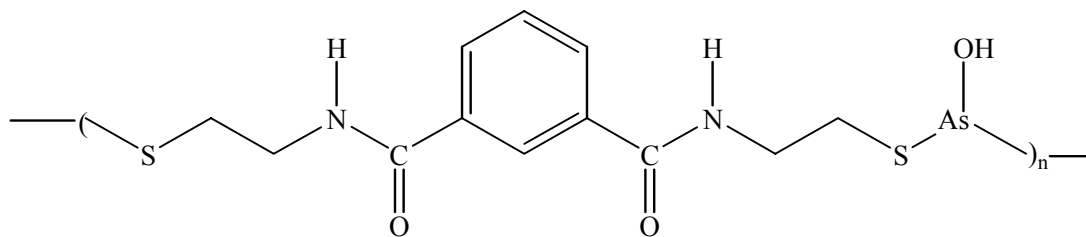
a-ICP-OES detection limit; b-CVAF detection limit

#### 2.4.6.4 Conclusions

Polymeric structures are proposed for the compounds. The results of the current study also support the presence of a linear coordination environment for BDET-Hg (**11**). It is likely that the BDET-Cd (**10**), BDET-Sn (**12**) and BDET-Pb (**13**) are four-coordinate and distorted tetrahedral and BDET-AsOH (**14**) is three-coordinate and trigonal pyramidal. In compound **11**, Hg is bonded to two sulfur atoms coming from the two side arms of BDETH<sub>2</sub>. Two sulfur and two nitrogen atoms coming from the two side arms of BDETH<sub>2</sub> complete the coordination around the central metal atom for compounds **10**, **12** and **13**. In compound **14**, As is bound to two sulfur atoms from the two side arms of BDETH<sub>2</sub>; -OH completes the coordination around As. Figure 2.18 illustrates the possible structures for **10**, **11**, **12**, **13** and **14**. However, it should be mentioned here that although Pb(IV) compounds have a tendency to be four-coordinate and tetrahedral, Pb(II) compounds exist as both discrete and polynuclear complexes exhibiting a broad range of coordination numbers, from 2 to 12.<sup>164</sup> It has also been reported that the most common coordination numbers are two [16% of all Pb(II) compounds reported in the CSD], four [24% of all Pb(II) compounds], and six [15% of all Pb(II) compounds]. Also, although majority of tin(II) thiolate compounds are tetrahedral, in the literature there is report of a two-coordinate bent tin(II) thiolate, Sn(SAr)<sub>2</sub> (Ar = C<sub>6</sub>H<sub>2</sub>Bu<sup>t</sup><sub>3</sub>-2,4,6).<sup>165</sup>



M = Cd, Sn, Pb  
(b)



(c)

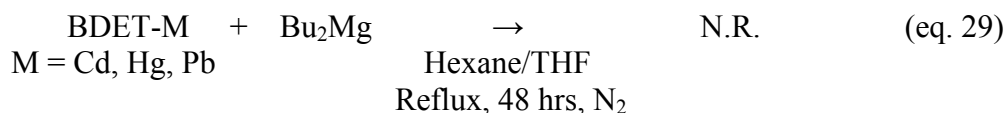
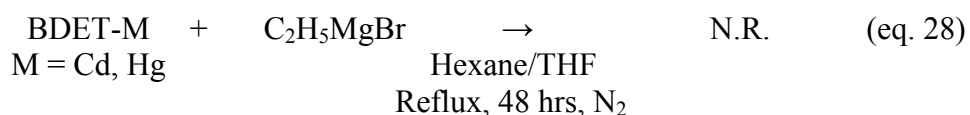
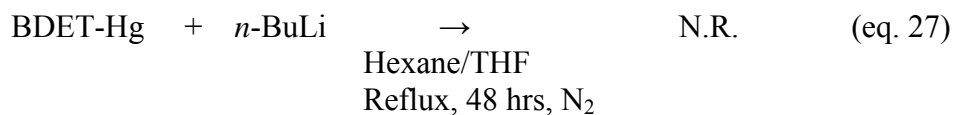
**Figure 2.18.** Proposed structures of main group compounds of BDETH<sub>2</sub>: (a) BDET-Hg, (b) BDET-M (M=Cd, Sn, Pb), (c) BDET-AsOH.

## 2.5 Attempted Metallation of BDET-Metal Compounds

Amido protons are moderately acidic ( $pK_a \sim 8$ ). It was thought the amido protons in the BDET-Metal are acidic as well and those protons could be abstracted by reacting the BDET-metal compounds with reagents like *n*-butyllithium (*n*-BuLi), ethylmagnesium bromide ( $C_2H_5MgBr$ ) and dibutylmagnesium ( $Bu_2Mg$ ) and thereby generating new

compounds soluble in polar solvents. This would facilitate growth of single crystals suitable for X-ray crystallographic study which, in turn, will give direct evidence for the structures of the BDET-Metal compounds.

Three BDET-M compounds, BDET-Hg, BDET-Cd, and BDET-Pb were treated with *n*-BuLi, C<sub>2</sub>H<sub>5</sub>MgBr and Bu<sub>2</sub>Mg under a variety of reaction conditions, but the reactions failed to yield the desired products despite the presence of acidic -NH protons in the BDET-M compounds and the fact that *n*-BuLi (pK<sub>a</sub> > 35), C<sub>2</sub>H<sub>5</sub>MgBr and Bu<sub>2</sub>Mg are good nucleophiles. It is assumed that the pK<sub>a</sub> of the amido protons in the BDET-Me compounds are much higher than 8. The presence of intermolecular hydrogen bonds between the -NH and the C=O groups may be a contributing factor as well. The attempted syntheses are shown in equations 27-29.



## 2.6 Experimental

### 2.6.1 General considerations

All chemicals were purchased from commercial sources and used without further purification. Solvents were of reagent grade. The following reagent grade materials were used for the synthesis of the BDET-Metal compounds: 1) isophthaloyl chloride (98% purity), 2) 2-mercaptoethylamine hydrochloride (98% purity), 3) triethylamine (99% purity), 4) *n*-BuLi (2.5 M in heptane), 5) NaOH (98%, pellets), 6) KOH (90%, flakes), 7) Bu<sub>2</sub>Mg (1.0 M in heptane), 8) Fe(CH<sub>3</sub>COO)<sub>2</sub> · 2H<sub>2</sub>O (99%), 9) Co(SO<sub>4</sub>) · H<sub>2</sub>O (99%), 10) Ni(CH<sub>3</sub>COO)<sub>2</sub> · 4H<sub>2</sub>O (99%), 11) Cu(CH<sub>3</sub>COO)<sub>2</sub> · H<sub>2</sub>O (98%), 12) CdCl<sub>2</sub> · H<sub>2</sub>O (99%), 13) HgCl<sub>2</sub> (99.5%), 14) SnCl<sub>2</sub> · 2H<sub>2</sub>O (99%), 15) Pb(CH<sub>3</sub>COO)<sub>2</sub> · 3H<sub>2</sub>O (99%), 16) NaAsO<sub>2</sub> (99%), 17) C<sub>2</sub>H<sub>5</sub>MgBr (1.0 M in THF), 18) Bu<sub>2</sub>Mg (1.0 M in heptane); all were purchased from Aldrich.

Elemental analyses were carried out at the Center for Applied Energy Research (CAER) at the University of Kentucky. Infrared spectra were recorded as KBr disks, using a Nicolet 320 FTIR spectrophotometer. Raman spectra were recorded at the Center for Applied Energy Research, University of Kentucky using a Nicolet FT-Raman 906 spectrometer ESP instrument. <sup>1</sup>H NMR spectra were run on a Varian INOVA 400 MHz instrument and <sup>13</sup>C NMR spectra were run on a Varian Gemini 200 MHz instrument. A Finnigan Incos 50 Quadrupole instrument was used for recording EI mass spectra. X-ray diffraction data were collected at 90 K on a Bruker-Nonius X8 Proteum diffractometer unit using Cu-Kα radiation and Nonius Kappa CCD diffractometer unit using Mo-Kα radiation, respectively from regular shaped crystals mounted in Paratone-N oil on glass

fibers. Thermogravimetric analyses were carried out on a TA instruments TGA 2950 thermogravimetric analyzer.

### 2.6.2 Syntheses

$C_{12}H_{16}N_2O_2S_2$  (**1**). To a stirred solution of  $HSCH_2CH_2NH_2 \cdot HCl$  (50.40 g, 0.4442 mol) in 700 mL of  $CHCl_3$  was added 40 mL (29.04 g, 0.2875 mol) of  $Et_3N$  and stirred for 15 minutes. To the resulting reaction mixture was added a solution of isophthaloyl chloride (30.20 g, 0.1488 mol) in 300 mL of  $CHCl_3$  and stirred for 15 minutes. Then another portion (40 mL) of  $Et_3N$  was added to the reaction mixture and stirred for 3 hrs. The reaction mixture was extracted with DI water (800 mL + 500 mL + 500 mL), the organic layer dried over anhydrous  $MgSO_4$ , and solvent removed under vacuum to yield 33.9 g (80.2%) of the product. Mp. 129-131 °C. IR (KBr) 3242 s (vNH), 3070 m {vC-H(Ar)}, 2936 m {vC-H(methylene)}, 2557 w (vSH), 1640 ss (vCO), 1542 ss ( $\delta$ NH), 1431 m (vC=C), 1319 m {in plane bending C-H(Ar)}, 1085 m (vC-S), 802m {out of plane bending C-H(Ar)}, 697 m {out of plane bending C-H(Ar)}  $cm^{-1}$ .  $^1H$  NMR ( $CDCl_3$ , 400 MHz)  $\delta$  1.44 (t, SH, 2H), 2.90 (m,  $CH_2SH$ , 4H), 3.71 (m, - $NHCH_2$ , 4H), 6.58 (s, -CONH, 2H), 7.56 (t, ArH, 1H), 7.98 (d, ArH, 2H), 8.21 (s, ArH, 1H).  $^{13}C$  NMR ( $CDCl_3$ , 200 MHz)  $\delta$  169.1 (CO), 136.1, 131.2, 129.8, 127.2 (ArC), 45.1 ( $NHCH_2$ ), 24.7 ( $CH_2S$ ). Anal. Calcd. for  $C_{12}H_{16}N_2O_2S_2$ : C, 50.7; H, 5.7; N, 9.9; S, 22.6. Found: C, 50.6; H, 5.9; N, 9.9; S, 22.7.

$BDETLi_2$  (**2**). To a solution of  $BDETH_2$  (1.42 g, 4.99 mmol) in 50 mL of THF was added *n*-BuLi in heptane (4.0 mL of 2.5 M solution, 10 mmol) under nitrogen. A yellowish precipitate formed immediately which was filtered by using a cannula. The

solid was vacuum-dried for 3 days to yield 1.48 g (100 %) of the product. Mp. 154-158 °C. Anal. Calcd. for  $C_{12}H_{14}N_2S_2O_2Li_2$ : C, 48.7; H, 4.76; N, 9.46. Found C, 48.2; H, 5.39; N, 9.17. IR (KBr) 3313 s (νNH), 3019 m {νC-H(Ar)}, 2964 m {νC-H(methylene)}, 2823 m {νC-H(methylene)}, 1638 ss (νCO), 1542 ss (δNH), 1263 m {in plane bending C-H(Ar)}, 801 m {out of plane bending C-H(Ar)}, 723 m {out of plane bending C-H(Ar)}  $cm^{-1}$ .  $^1H$  NMR (DMSO, 400 MHz) δ 2.92 (m,  $CH_2SH$ , 4H), 3.61 (m,  $-NHCH_2$ , 4H), 7.60 (t, ArH, 1H), 7.96 (d, ArH, 2H), 8.39 (s, ArH, 1H), 8.92 (s,  $-CONH$ , 2H).  $^{13}C$  NMR (DMSO, 200 MHz) δ 166.1 (CO), 134.6, 129.9, 128.4, 126.2 (ArC), 37.0 ( $CH_2$ ). Raman ( $cm^{-1}$ ): 316 (Li-S). MS m/z 208 (intramolecular rearrangement with loss of a fragment). The compound was found to be slightly soluble in dimethylsulfoxide, and dimethylformamide. However, it was found to be insoluble in other common laboratory solvents/solvent systems including water, methanol, methanol/water, ethanol, water/methanol, water/ethanol, acetone, dimethylsulfoxide/water, ethyl acetate, tetrahydrofuran, diethyl ether, acetonitrile, acetonitrile/water, chloroform, dichloromethane, hexanes, toluene, 10% acetic acid, etc.

BDETNa<sub>2</sub> (**3**). A solution of NaOH (0.34 g, 8.5 mmol) in 10 mL DI water was added to a stirred solution of BDETH<sub>2</sub> (1.20 g, 4.22 mmol) in 45 mL of 95% ethanol and stirred overnight. A white solid precipitate formed which was filtered under vacuum and dried in the air to yield 1.78 g (100%) of the product. Mp. 205 °C (dec). Anal. Calcd. for  $C_{12}H_{14}N_2S_2O_2Na_2$ : C, 43.9; H, 4.30; N, 8.57. Found C, 44.1; H, 3.92; N, 8.66. IR (KBr) 3300 s (νNH), 3074 m {νC-H(Ar)}, 2928 m {νC-H(methylene)}, 1638 ss (νCO), 1540 ss (δNH), 1384 m (νC=C), 1290 m {in plane bending C-H(Ar)}, 687 m {out of plane bending C-H(Ar)}  $cm^{-1}$ . Raman ( $cm^{-1}$ ): 292 (Na-S). MS m/z 305 [ $M^+ - Na$ ], 208

(intramolecular rearrangement with loss of a fragment). The compound was found insoluble in the same solvents as compound **2** plus dimethylsulfoxide, and dimethylformamide.

BDETK<sub>2</sub> (**4**). A solution of KOH (0.34 g, 6.1 mmol) in 10 mL DI water was added to a stirred solution of BDETH<sub>2</sub> (0.86 g, 3.0 mmol) in 30 mL of 95% ethanol and stirred overnight. White solid precipitate formed, which was filtered under vacuum and dried in the air to yield 1.08 g (100%) of the product. Mp. 210 °C (dec). Anal. Calcd. for C<sub>12</sub>H<sub>14</sub>N<sub>2</sub>S<sub>2</sub>O<sub>2</sub>K<sub>2</sub>: C, 40.0; H, 3.9; N, 7.8. Found C, 40.4; H, 4.2; N, 8.1. IR (KBr) 3298 s (νNH), 3067 m {νC-H(arom)}, 2925 m {νC-H(methylene)}, 1638 ss (νCO), 1536 ss (δNH), 1430 m (νC=C), 1290 m {in plane bending C-H(Ar)}, 688 m {out of plane bending C-H(Ar)} cm<sup>-1</sup>. Raman (cm<sup>-1</sup>): 278 (K-S). MS m/z 321 [M<sup>+</sup> - K], 208 (intramolecular rearrangement with loss of a fragment). The compound was found insoluble in the same solvents as compound **3**.

BDETMg (**5**): To a stirred solution of BDETH<sub>2</sub> (0.56 g, 2.0 mmol) in 50 mL of THF was added, dropwise, 1.0 mL (1.0 mmol) Bu<sub>2</sub>Mg (1.0 M in heptane) and stirred for 24 hours. Solvent was removed under vacuum and dried in air to yield 0.61 g (100%) of the product. Mp. 202 °C (dec). Anal Calcd. for C<sub>12</sub>H<sub>14</sub>N<sub>2</sub>S<sub>2</sub>O<sub>2</sub>Mg: C, 47.0; H, 4.60; N, 9.13; S, 20.9. Found C, 46.9; H, 4.37; N, 8.79; S, 20.6. IR (KBr) 3421m (νNH), 2926 s {νC-H(methylene)}, 1639 ss (νCO), 1534 ss (δNH), 1477 m (νC=C), 1273 m {in plane bending C-H(Ar)}, 698 m {out of plane bending C-H(Ar)} cm<sup>-1</sup>. MS m/z 306 [M<sup>+</sup>] and 282 [M<sup>+</sup> - Mg]. The compound was found to be insoluble in the same solvents as compound **3**.

BDETFe (**6**). A solution of  $\text{Fe}(\text{CH}_3\text{COO})_2 \cdot 2 \text{H}_2\text{O}$  (0.180 g, 1.00 mmol) in DI water (10 mL) was added to a stirred solution of BDETH<sub>2</sub> (0.284 g, 1.00 mmol) in 10 mL of THF and stirred. A slightly yellow precipitate formed immediately which was filtered under vacuum and dried in the air to yield 0.235 g (69% ) of the product. Mp. 162 °C (dec). Anal. Calcd. for  $\text{C}_{12}\text{H}_{14}\text{N}_2\text{S}_2\text{O}_2\text{Fe}$  : C, 42.6; H, 4.2; N, 8.3. Found C, 41.9; H, 4.5; N, 8.7. IR (KBr) 3295 s (νNH), 3067 m {νC-H(Ar)}, 2927 m {νC-H(methylene)}, 1639 ss (νCO), 1538 ss (δNH), 1478 m (νC=C), 1291 m (in plane bending C-H(Ar)), 692 m {out of plane bending C-H(Ar)} $\text{cm}^{-1}$ . Raman ( $\text{cm}^{-1}$ ): 178 (Fe-S). MS m/z 208 (intramolecular rearrangement with the loss of a fragment) The compound was insoluble in the same solvents as compound **3**.

BDETCo (**7**). To a stirred solution of BDETH<sub>2</sub> (0.72 g, 2.5 mmol) in 50 mL of 95% ethanol was added  $\text{CoSO}_4 \cdot \text{H}_2\text{O}$  (0.39 g, 2.5 mmol) solid and stirred overnight. The pinkish-purple precipitate that formed was filtered under vacuum and dried in the air to yield 0.85 g (99%) of the product. Mp. 209 °C (dec). Anal Calcd. for  $\text{C}_{12}\text{H}_{14}\text{N}_2\text{S}_2\text{O}_2\text{Co}$ : C, 42.2; H, 4.1; N, 8.2; S, 19.1. Found C, 41.6; H, 4.0; N, 8.3; S, 18.8. IR (KBr) 3328 s (νNH), 3062 m {νC-H(Ar)}, 2928 m {νC-H(methylene)}, 1643 ss (νCO), 1536 ss (δNH), 1384 m (νC=C), 1277 m {in plane bending C-H(Ar)}, 695 m {out of plane bending C-H(Ar)} $\text{cm}^{-1}$ . MS m/z 282 [ $\text{M}^+$  - Co] and 208 (intramolecular rearrangement with the loss of a fragment). The compound was insoluble in the same solvents as compound **3**.

BDETNi (**8**). To a stirred solution of BDETH<sub>2</sub> (0.72 g, 2.5 mmol) in 50 mL of 95% ethanol was added 0.62 g (2.5 mol)  $\text{Ni}(\text{CH}_3\text{COO})_2 \cdot 4 \text{H}_2\text{O}$  solid and stirred overnight to give a brown precipitate. The precipitate was filtered under vacuum and dried in the air to yield 0.86 g (100 %) of the product. Mp. 210 °C (dec). Anal. Calcd.

for  $C_{12}H_{14}N_2S_2O_2Ni$ : C, 42.2; H, 4.1; N, 8.2; S, 18.8. Found C, 41.7; H, 4.7; N, 8.0; S, 18.3. IR (KBr) 3298 s ( $\nu NH$ ), 3067 m  $\{\nu C-H(Ar)\}$ , 2925 m  $\{\nu C-H(methylene)\}$ , 1638 ss ( $\nu CO$ ), 1536 ss ( $\delta NH$ ), 1430 m ( $\nu C=C$ ), 1290 m  $\{\text{in plane bending } C-H(Ar)\}$ , 688 m  $\{\text{out of plane bending } C-H(Ar)\} cm^{-1}$ . Raman ( $cm^{-1}$ ): 106 (Ni-S). MS m/z 282 [ $M^+ - Ni$ ]; 58, 60, and 62 isotopic peaks of Ni. The compound was found insoluble in the same solvents as compound **3**.

BDETCu (**9**). A solution of  $Cu(CH_3COO)_2 \cdot H_2O$  (0.50 g, 2.5 mol) in DI water (10 mL) was added to a stirred solution of BDETH<sub>2</sub> (0.72 g, 2.5 mol) in 25 mL of 95% ethanol. A turquoise blue precipitate formed immediately which was filtered under vacuum and dried in the air to yield 0.57 g (66%) of the product. Mp. 184 °C (dec). Anal Calcd. for  $C_{12}H_{14}N_2S_2O_2Cu$ : C, 41.7; H, 4.1; N, 8.1. Found C, 41.3; H, 3.9; N, 7.8. IR (KBr) 3304 s ( $\nu NH$ ), 3068 m  $\{\nu C-H(Ar)\}$ , 2937 m ( $\nu C-H(methylene)\}$ , 1641 ss ( $\nu CO$ ), 1534 ss ( $\delta NH$ ), 1478 m ( $\nu C=C$ ), 1274 m  $\{\text{in plane bending } C-H(Ar)\}$ , 695 m  $\{\text{out of plane bending } C-H(Ar)\} cm^{-1}$ . Raman ( $cm^{-1}$ ): 173 (Cu-S). MS m/z 63 and 65 isotopic peaks of Cu. The compound was found insoluble in the same solvents as compound **3**.

BDETCd (**10**). A solution of  $CdCl_2 \cdot H_2O$  (0.92 g, 5.0 mmol) in DI water (10 mL) was added to a stirred solution of BDETH<sub>2</sub> (1.42 g, 5.00 mmol) in 50 mL of 95% ethanol. A white precipitate formed immediately which was filtered under vacuum and dried in the air to yield 1.28 g (65%) of the product. Mp. 196 °C (dec). Anal Calcd. for  $C_{12}H_{14}N_2S_2O_2Cd$ : C, 36.5; H, 3.58; N, 7.10. Found C, 35.9; H, 4.29; N, 6.94. IR (KBr) 3414 s ( $\nu NH$ ), 2926 m  $\{\nu C-H(methylene)\}$ , 1632 ss ( $\nu CO$ ), 1541 ss ( $\delta NH$ ), 1479 s ( $\nu C=C$ ), 1274 m  $\{\text{in plane bending } C-H(Ar)\}$ , 729 m  $\{\text{out of plane bending } C-H(Ar)\}$

$\text{cm}^{-1}$ . Raman ( $\text{cm}^{-1}$ ) 174 (Cd-S). MS  $m/z$  282 [ $\text{M}^+ - \text{Cd}$ ]; 112, 111, and 110 isotopic peaks of Cd. The compound was found insoluble in the same solvents as compound **3**.

BDETHg (**11**). A solution of  $\text{HgCl}_2$  (1.36 g, 5.00 mmol) in DI water (30 mL) was added to a stirred solution of BDETH<sub>2</sub> (1.42 g, 5.00 mmol) in 50 mL of 95% ethanol. A white precipitate formed immediately which was filtered under vacuum and dried in the air to yield 2.51 g (100%) of the product. Mp. 156 °C (dec). Anal Calcd. for  $\text{C}_{12}\text{H}_{14}\text{N}_2\text{S}_2\text{O}_2\text{Hg}$ : C, 29.8; H, 2.92; N, 5.80. Found C, 29.2; H, 2.44; N, 5.41. IR (KBr) 3300 s ( $\nu\text{NH}$ ), 3062 m { $\nu\text{C-H(Ar)}$ }, 2923 m { $\nu\text{C-H(methylene)}$ }, 1642 ss ( $\nu\text{CO}$ ), 1533 ss ( $\delta\text{NH}$ ), 1478 m { $\nu\text{C=C}$ }, 1275 m {(in plane bending C-H(Ar))}, 728m {out of plane bending C-H(Ar)}  $\text{cm}^{-1}$ . Raman ( $\text{cm}^{-1}$ ): 293  $\text{cm}^{-1}$  (Hg-S). MS  $m/z$  282 [ $\text{M}^+ - \text{Hg}$ ]; 204-198 isotopic peaks of Hg. The compound was found to be insoluble in the same solvents as compound **3**.

BDETSn (**12**). A solution of  $\text{SnCl}_2 \cdot 2 \text{H}_2\text{O}$  (1.12 g, 5.00 mmol) in 95% ethanol (25 mL) was added to a stirred solution of BDETH<sub>2</sub> (1.42 g, 5.00 mmol) in 50 mL of 95% ethanol. Voluminous white precipitate formed immediately which was filtered under vacuum and dried in the air to yield 1.63 g (81.4%) of the product. Mp. 210 °C (dec). Anal Calcd. for  $\text{C}_{12}\text{H}_{14}\text{N}_2\text{S}_2\text{O}_2\text{Sn}$ : C, 35.9; H, 3.52; N, 6.98. Found C, 35.2; H, 3.23; N, 6.71. IR (KBr) 3328 s ( $\nu\text{NH}$ ), 3062 m { $\nu\text{C-H(Ar)}$ }, 2928 m { $\nu\text{C-H(methylene)}$ }, 1643 ss ( $\nu\text{CO}$ ), 1536 ss ( $\delta\text{NH}$ ), 1277 {in plane bending C-H(Ar)}, 695 m {out of plane bending C-H(Ar)}  $\text{cm}^{-1}$ . Raman ( $\text{cm}^{-1}$ ): 352 (Sn-S). MS  $m/z$  401 [ $\text{M}^+$ ], 282 [ $\text{M}^+ - \text{Sn}$ ]; 120, 116 and 115 isotope peaks of Sn. The compound was found insoluble in the same solvents as compound **3**.

BDETPb (**13**). A solution of  $\text{Pb}(\text{CH}_3\text{COO})_2 \cdot 3 \text{H}_2\text{O}$  (0.95 g, 2.5 mmol) in DI water (10 mL) was added to a stirred solution of BDETH<sub>2</sub> (0.71 g, 2.5 mmol) in 25 mL of 95% ethanol. A yellow precipitate formed immediately which was filtered under vacuum and dried in the air to yield 1.14 g (93.3%) of the product. Mp. 178 °C (dec). Anal Calcd. for  $\text{C}_{12}\text{H}_{14}\text{N}_2\text{S}_2\text{O}_2\text{Pb}$ : C, 29.4; H, 2.88; N, 5.72. Found C, 28.9; H, 2.76; N, 5.67. IR (KBr) 3318 s (νNH), 3079 m {νCH(Ar)}, 2887 m {νCH(methylene)}, 1633 ss (νCO), 1535 ss (δNH), 1478 m (νC=C), 1277 m {in plane bending C-H(Ar)}, 693 m {out of plane bending C-H(Ar)}  $\text{cm}^{-1}$ . Raman ( $\text{cm}^{-1}$ ): 164 (Pb-S). MS m/z 282 [ $\text{M}^+$  - Pb]; 208, 207, 206 isotopic peaks of Pb. The compound was found to be insoluble in the same solvents as compound **3**.

BDEAsOH (**14**): A solution of  $\text{NaAsO}_2$  (0.131 g, 1.00 mmol) in DI water (10 mL) was added to a stirred solution of BDETH<sub>2</sub> (1.71 g, 6.00 mmol) in 75 mL of 95% ethanol and stirred. Cloudiness appeared immediately. The reaction mixture was stirred for 7 days after which the precipitate that formed was filtered under vacuum, washed successively with DI water and ethanol, and dried in the air to yield 0.378 g (100%) of the product. Mp. 198 °C (dec). Anal. Calcd. for  $\text{C}_{12}\text{H}_{15}\text{N}_2\text{S}_2\text{O}_3\text{As}$ : C, 38.5; H, 4.04; N, 7.48. Found C, 38.1; H, 4.32; N, 7.37. IR (KBr) 3417 s (νOH), 3298 s (νNH), 3067 m {νC-H(Ar)}, 2962 m {νC-H(methylene)}, 1638 ss (νCO), 1535 ss (δNH), 1477 m (νC=C), 1263 m (in plane bending C-H(Ar)), 692 m {out of plane bending C-H(Ar)}  $\text{cm}^{-1}$ . Raman ( $\text{cm}^{-1}$ ): 379 (As-S). MS m/z 373 [ $\text{M}^+$  - H], 282 [ $\text{M}^+$  - AsOH], and 208 (base peak, product of intramolecular cyclization with loss of a fragment). The compound was found insoluble in the same solvents as compound **3**, except for dimethylsulfoxide.

BDET-Hg and *n*-BuLi. To BDET-Hg (0.242 g, 0.500 mmol) was added 25 mL of dry THF and 25 mL of hexanes and stirred under nitrogen for 30 minutes. To the resulting suspension was syringed 0.40 mL (1.0 mmol) of *n*-BuLi (2.5 M in hexane) and stirred under nitrogen for 3 days. The solid left in the reaction flask (0.237 g, 98%) was filtered under vacuum and dried in the air to yield a white solid which was found to be identical to BDET-Hg by IR and melting point. The supernatant kept in the freezer did not yield any solid even after 18 months. Reflux of the reaction mixture over 48 hrs did not produce different results.

#### **Reactions between BDET-M (M = Cd, Hg) and C<sub>2</sub>H<sub>5</sub>MgBr**

BDET-Cd and C<sub>2</sub>H<sub>5</sub>MgBr. To BDET-Cd (0.197 g, 0.500 mmol) was added 20 mL of dry THF and 20 mL of dry hexane and stirred under nitrogen for 30 minutes. To the resulting suspension was syringed 1.0 mL (1.0 mmol) of C<sub>2</sub>H<sub>5</sub>MgBr (1.0 M in THF) and stirred under nitrogen for 48 hrs. The solid left in the reaction flask (0.193 g, 97%) was filtered under vacuum and dried in the air to yield a white solid which was found to be identical to BDET-Cd by IR and melting point. The supernatant kept in the freezer did not yield any solid even after 18 months. Reflux of the reaction mixture over 48 hrs did not produce different results.

BDET-Hg and C<sub>2</sub>H<sub>5</sub>MgBr. To BDET-Hg (0.483 g, 1.00 mmol) was added 25 mL of dry THF and 25 mL of dry hexane and stirred under nitrogen for 30 minutes. To the resulting suspension was syringed 2.0 mL (2.0 mmol) of C<sub>2</sub>H<sub>5</sub>MgBr (1.0 M in THF) and stirred under nitrogen for 3 days. The solid left in the reaction flask (0.472 g, 98%) was filtered under vacuum and dried in the air to yield a white solid, which was found to be identical to BDET-Hg by IR and melting point. The supernatant kept in the freezer did

not yield any solid even after 18 months. Reflux of the reaction mixture over 48 hrs did not produce different results.

### **Reactions between BDET-M ( M = Cd, Hg, Pb) and Bu<sub>2</sub>Mg**

BDET-Cd and Bu<sub>2</sub>Mg. To BDET-Cd (0.198 g, 0.500 mmol) was added 25 mL of dry THF and 25 mL of dry hexane and stirred under nitrogen for 2 hrs. To the resulting suspension was syringed 1.0 mL (1.0 mmol) of Bu<sub>2</sub>Mg (1.0 M in heptane) and stirred under nitrogen for 48 hrs. The solid left in the reaction flask (0.193 g, 97%) was filtered under vacuum and dried in the air to yield a white solid which was found to be identical to BDET-Cd by IR and melting point. The supernatant kept in the freezer did not yield any solid even after 18 months. Reflux of the reaction mixture over 48 hrs did not produce different results.

BDET-Hg and Bu<sub>2</sub>Mg. To BDET-Hg (0.242 g, 0.500 mmol) was added 25 mL of dry THF and 25 mL of hexanes and stirred under nitrogen for 2 hrs. To the resulting suspension was syringed 1.0 mL (1.0 mmol) of Bu<sub>2</sub>Mg (1.0 M in heptane) and stirred under nitrogen for 48 hrs. The solid left in the reaction flask (0.232 g, 96%) was filtered under vacuum and dried in the air to yield a white solid which was found to be identical to BDET-Hg by IR and melting point. The supernatant kept in the freezer did not yield any solid even after 18 months. Reflux of the reaction mixture over 48 hrs did not produce different results.

BDET-Pb and Bu<sub>2</sub>Mg. To BDET-Pb (0.245 g, 0.500 mmol) was added 25 mL of dry THF and 25 mL of hexanes and stirred under nitrogen for 2 hrs. To the resulting suspension was syringed 1.0 mL (1.0 mmol) of Bu<sub>2</sub>Mg (1.0 M in heptane) and stirred under nitrogen for 48 hrs. The solid left in the reaction flask (0.239 g, 97%) was filtered

under gravity and dried in the air to yield a yellow solid which was found to be identical to BDET-Pb by IR and melting point. The supernatant kept in the freezer did not yield any solid even after 18 months. Reflux of the reaction mixture over 48 hrs did not produce different results.

### 2.6.3 Leaching Studies

Two 100 mL aqueous solutions (100 ppm) of each of the metal salts of mercury, lead, and cadmium were prepared using deionized water. To these were added equivalent amounts (1:1) of BDETH<sub>2</sub> solution in 95% ethanol. The reaction mixtures were stirred for 1 hr, the resulting precipitates were filtered under gravity, and dried overnight in the air. The precipitates were transferred into Erlenmeyer flasks followed by addition of 100 mL of deionized water. The flasks were divided into two categories. pH of one category of flasks (labeled A) was adjusted to 1 and the other category (labeled B) to 3 by adding concentrated HCl. The pH were measured by pHTestr™ (Sigma-Aldrich). 10 mL aliquots from each of the two different categories of flasks were syringed into tubes for metal concentration measurements. Contents of all the flasks were stirred (using magnetic stir bars). 10 mL aliquots were syringed into tubes after 7, 14 and 28 days and saved for metal concentration measurements.

Metal concentrations of the Cd, and Pb solutions were measured at the Environmental Research and Training Laboratory (ERTL), University of Kentucky using a Varian Vista-Pro CCD Simultaneous Inductively Coupled Argon Plasma Optical Emission Spectrometer (ICP-OES). In this technique, the liquid sample is sprayed into an argon plasma where the dissolved metals are excited to emit their characteristic

ultraviolet and visible radiation. The radiation is dispersed by a grating monochromator and detected with photomultiplier tubes. Radiation wavelength is used to identify the element and radiation intensity is used to determine its concentration. ICP-OES measures elements in the concentration range of 1 ppb (part-per-billion) to 1000 ppm (parts-per-million) or more.

Mercury levels of the samples were determined using cold vapor atomic absorption spectrophotometry (CVAAS) on a CETAC Technologies M-6000A Mercury Analyzer, using EPA methods.<sup>166</sup> Digestion of the samples was performed following EPA methods (7470) for mercury detection in liquid waste. This involves using an aqua regia solution under heat, followed by the addition of potassium permanganate and potassium persulfate under heat. Finally, the excess potassium permanganate is reduced using a sodium chloride-hydroxylamine sulfate solution.

## CHAPTER 3

### Attempted Alkylaluminumation

#### 3.1 Overview

One of the problems faced in this work was that no crystal suitable for X-ray crystallographic study could be grown from BDET-metal compounds. An X-ray crystallographic study would have unambiguously established the structures of the metal compounds prepared. So, the BDET-M compounds were treated with a variety of reagents like *n*-BuLi, C<sub>2</sub>H<sub>5</sub>MgBr and Bu<sub>2</sub>Mg etc. under different conditions in order to prepare compounds soluble in common laboratory solvents, but none of the reactions yielded any product which could be solubilized; the products were unreacted BDET-M compounds. Therefore, it was decided to attempt an alkylaluminumation of BDET-M across the C=O bond using AlMe<sub>3</sub> and create potentially soluble compounds. The hypothetical product of alkylaluminumation of BDET-M is shown in figure 3.1.

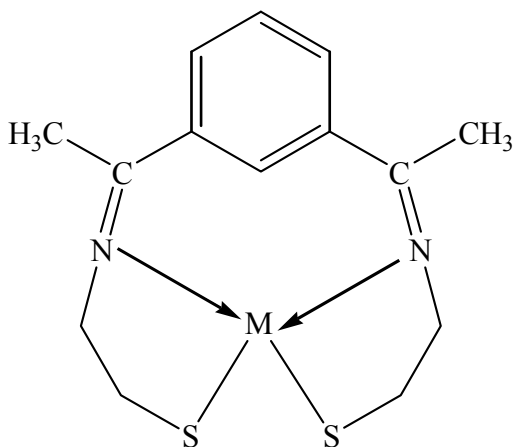


**Figure 3.1.** Hypothetical product of reaction between BDET-M and AlMe<sub>3</sub>

Alkylaluminumation of an imine (N=C) has been reported in the literature.<sup>167</sup> The unusual alkylaluminumation of an imine bond in a heptadentate Schiff-base ligand made from salicylaldehyde and bis(2-aminoethyl)ethylenediamine resulted when 3 equiv. of AlMe<sub>3</sub> was added. The reaction is shown below (Figure 3.2).<sup>167</sup>

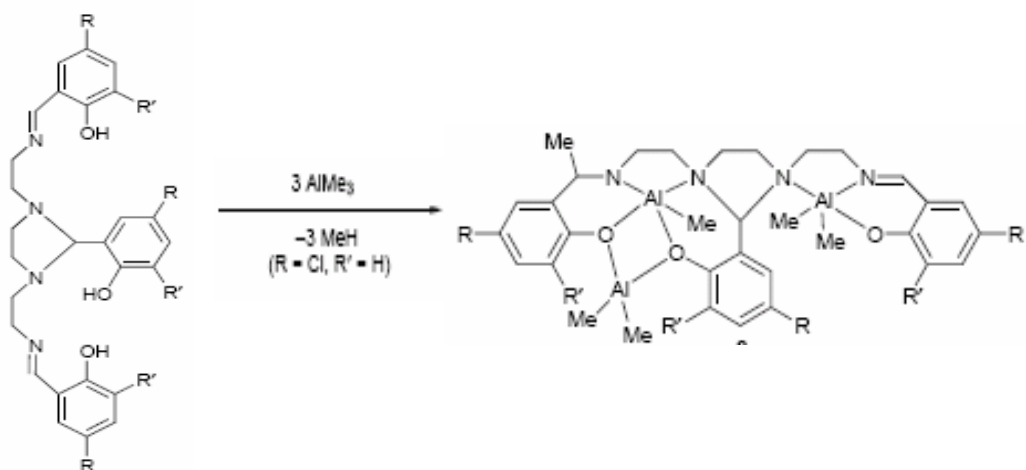


**Figure 3.2.** Alkylaluminumation of a Schiff-base ligand.<sup>167</sup>

Trimethylaluminum has been shown to add to carbonyl compounds, such as in benzophenone.<sup>168</sup> Equation 30 illustrates the reaction between trimethylaluminum and benzophenone in diethyl ether. It was, thus, possible that trimethylaluminum will add to the carbonyl carbons of BDETH<sub>2</sub>.



However, attempts to alkylaluminumate BDET-M compounds under different reaction conditions failed. So, it was decided to combine BDETH<sub>2</sub> with Al(CH<sub>3</sub>)<sub>3</sub>. It was

hypothesized the reaction would yield either a) a product of alkylaluminum or b) form a chelate. The hypothetical products of the reaction are shown below in figure 3.3.

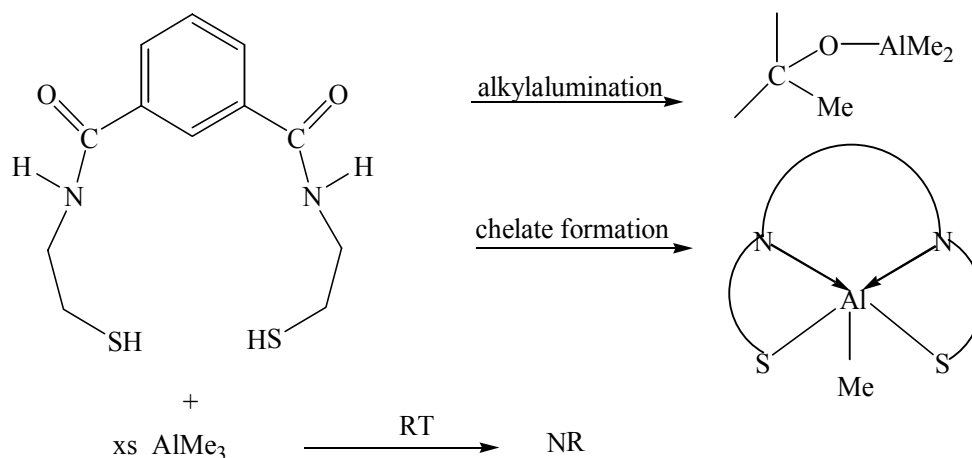
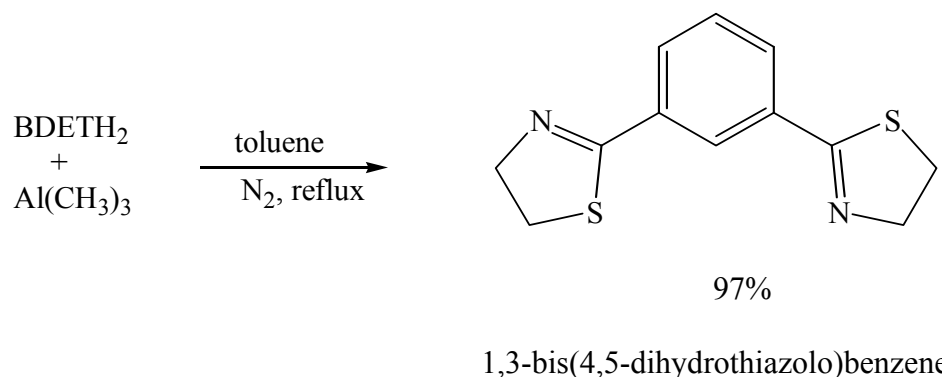


**Figure 3.3.** Hypothetical products of the reaction between BDETH<sub>2</sub> and Al(CH<sub>3</sub>)<sub>3</sub>

## 3.2 Synthesis and characterization

### 3.2.1 Synthesis

1,3--bis(4,5-dihydrothiazolo)benzene (**15**) resulted when BDETH<sub>2</sub> was treated with excess AlMe<sub>3</sub> under reflux for 48 hrs in toluene (scheme 3.1). The compound was brownish with a melting point of 211- 214 °C, and yield of 97%. No reaction occurred when BDETH<sub>2</sub> was combined with excess AlMe<sub>3</sub> at room temperature. Compound **15** was characterized by IR, <sup>1</sup>H NMR, EA, mass spectroscopy, and X-ray crystallography. This compound was prepared first by Jerrod Delcamp while conducting research in CHE 450G.<sup>169</sup>



**Scheme 3.1.** Reaction between BDETH<sub>2</sub> and Al(CH<sub>3</sub>)<sub>3</sub>.

Although the synthesis of 1,3-bis(4,5-dihydrothiazolo)benzene is being reported herefor the first time, this type of cyclization is not unprecedented. In the literature there is evidence of intramolecular amino-thiol cyclization, i.e. intramolecular ring formation in compounds containing –NH and –SH functionalities (Figure 3.4).<sup>170</sup> Since BDETH<sub>2</sub> possesses both –NH and –SH functionalities at appropriate distances for the formation of five-membered rings, it was decided to treat BDETH<sub>2</sub> with AlMe<sub>3</sub> under various reaction conditions. No reaction took place when BDETH<sub>2</sub> was treated with AlMe<sub>3</sub> at room temperature, but five-membered rings were formed when BDETH<sub>2</sub> was treated with AlMe<sub>3</sub> in toluene under reflux. It is likely that reflux activated the substrate, BDETH<sub>2</sub>.

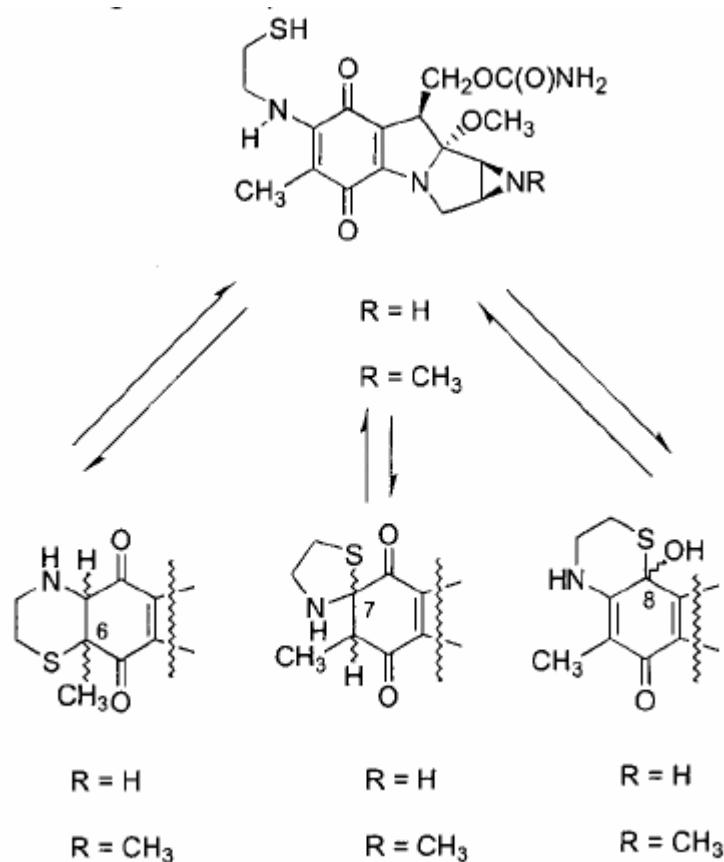


**Figure 3.4.** Amino-thiol cyclization.<sup>170</sup>

It has also been reported that reaction of L-cysteine ethyl ester hydrochloride with carbon disulfide in the presence of triethylamine in  $CH_2Cl_2$  at room temperature yielded a five-membered ring.<sup>171</sup> Similarly, esterification of L-(*R*)-cysteine followed by reaction with phosphoryl chloride and 2 moles of triethylamine, yielded cyclic phosphoramidothiolic chloride,<sup>172</sup> a five membered ring.

### 3.2.2 Characterization

The IR bands corresponding to the amide I (carbonyl) and amide II (N-H bending), and S-H stretching at 1640, 1542, and 2557  $cm^{-1}$ , respectively that are present

in the spectrum for BDETH<sub>2</sub> were absent in the spectrum for the new compound indicating that all of BDETH<sub>2</sub> was used up in the reaction. The bands at 1432 and 666 cm<sup>-1</sup> correspond to C-N and C-S stretching.

<sup>1</sup>H NMR (99% CS<sub>2</sub> and 1% CDCl<sub>3</sub>; 400 MHz) signals at δ 8.23 ppm (s, 1H), 7.92 ppm (d, J=7.4 Hz, 2H), and 7.44 ppm (t, J=7.6 Hz, 1H) correspond to the aromatic protons, whereas signals at δ 4.48 ppm (t, J=8.4Hz, 4H), and 3.44 ppm (t, J=8.4 Hz, 4H) correspond to the methylene protons in the five-membered rings.

The EI mass spectrum had the following significant peaks (m/z): 248 [M<sup>+</sup>], 220 [M<sup>+</sup> - CH<sub>2</sub>CH<sub>2</sub>], 188 [M<sup>+</sup> - NSCH<sub>2</sub>] confirming the molecular mass of the product.

Elemental analysis data showed that the calculated and experimental values for C, H, and N completely matched each other.

Single crystals of **15** suitable for study by X-ray crystallography were obtained from CS<sub>2</sub>. Crystal structure of the compound is shown below (Figure 3.5). The compound consists of a central benzene ring connected to two five membered rings in a symmetrical fashion. It crystallizes in the monoclinic space group C 2/c. The crystallographic data are presented in table 3.1.

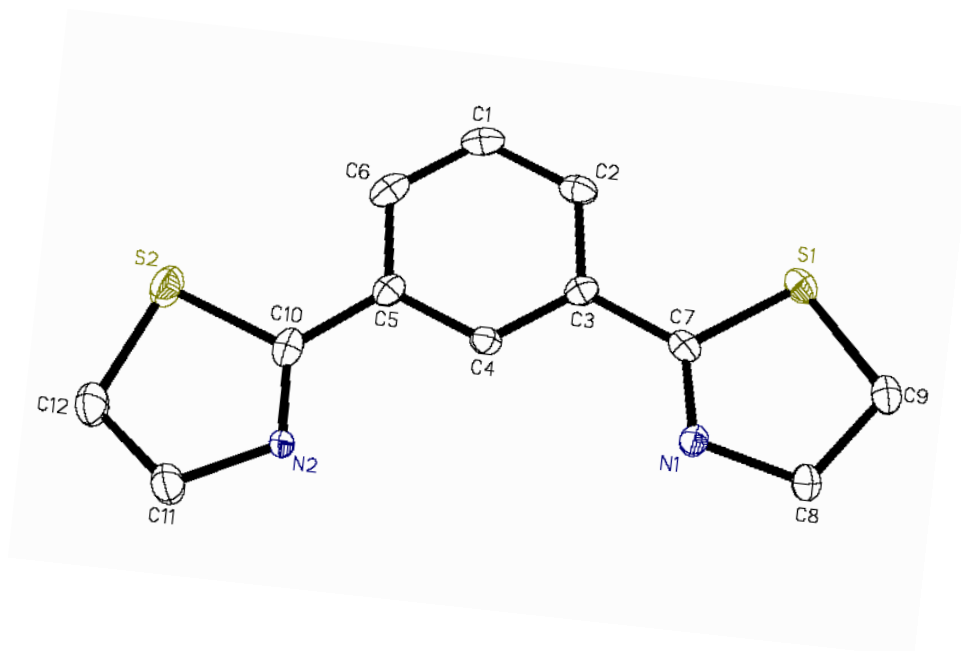


**Figure 3.5.** Crystal structure of 1,3-bis(4,5-dihydrothiazolo)benzene

**Table 3.1.** Crystallographic table for compound **15**.

formula	$C_{12}H_{12}N_2S_2$
formula weight	248.36
crystal group	monoclinic
space group	$C 2/c$
$a$ (Å)	23.5183(6)
$b$ (Å)	6.8439(2)
$c$ (Å)	14.5880(5)
$\alpha$ (degree)	90.00
$\beta$ (degree)	107.1923(11)
$\gamma$ (degree)	90.00
$V$ (Å <sup>3</sup> )	2243.12(12)
$Z$	8
$T$ (K)	90.0(2)
Radiation	Mo $K\alpha$ ( $\lambda = 0.71073$ Å)

### 3.3 Experimental

#### 3.3.1 General considerations.

All chemicals were purchased from commercial sources and used without further purification. Solvents were of reagent grade. Elemental analyses were carried out at the Center for Applied Energy Research (CAER) at the University of Kentucky. Infrared spectra were recorded as KBr disks, using a Nicolet 320 FTIR spectrophotometer.  $^1\text{H}$  NMR spectra were run on a Varian INOVA 400 MHz instrument and  $^{13}\text{C}$  NMR spectra were run on a Varian Gemini 200 MHz instrument. A Finnigan Incos 50 Quadrupole instrument was used for recording EI mass spectra. Single-crystal X-ray diffraction measurements were made using a Nonius KappaCCD machine with a sealed-tube molybdenum X-ray source.

#### 3.3.2 Synthesis

$\text{C}_{12}\text{H}_{12}\text{N}_2\text{S}_2$  (**15**): To a stirred suspension of BDETH<sub>2</sub> (0.43 g, 1.5 mmol) in 10 mL of dry toluene was added, dropwise and under glove box conditions, 0.11 g (1.5 mmol) of  $\text{Al}(\text{CH}_3)_3$  in dry toluene. The Schlenk flask was then removed from the glove box and refluxed for 2 days under standard Schlenk line conditions. Toluene was evaporated off to yield 0.36 g (97%) of the product (white powder). Mp. 211-214 °C. Anal. Calcd. for  $\text{C}_{12}\text{H}_{12}\text{N}_2\text{S}_2$ : C, 37.8; H, 7.6; N, 5.7. Found: C, 37.8; H, 7.6; N, 5.7. IR (KBr) 3028 m { $\nu\text{C-H}(\text{Ar})$ }, 2942 m { $\nu\text{C-H}(\text{methylene})$ }, 2846 m { $\nu\text{C-H}(\text{methylene})$ }, 1574 m ( $\nu\text{C}=\text{C}$ ), 1432 m ( $\nu\text{C-N}$ ), 916 m {out of plane bending  $\text{CH}(\text{aliph})$ }, 796 m {out of plane bending  $\text{C-H}(\text{Ar})$ }, 687 m {out of plane bending  $\text{C-H}(\text{Ar})$ }, 666 w ( $\nu\text{C-S}$ )  $\text{cm}^{-1}$ .  $^1\text{H}$

NMR (CS<sub>2</sub> [99%], CDCl<sub>3</sub> [1%], 400 MHz)  $\delta$  8.23 (s, ArH, 1H), 7.92 (d, ArH, 2H), 7.44 (t, ArH, 1H), 4.48 (t, -NCH<sub>2</sub>, 4H), 3.44 (t, -SCH<sub>2</sub>, 4H). MS  $m/z$  = 248 [M<sup>+</sup>], 220 [M<sup>+</sup> - CH<sub>2</sub>CH<sub>2</sub>], 188 [M<sup>+</sup> - NSCH<sub>2</sub>].

### 3.4 Conclusions

Efforts to alkylaluminum BDET-M compounds by combining them with Al(CH<sub>3</sub>)<sub>3</sub> under different reaction conditions failed due to the poor basicity of the C=O groups. However, a new compound, 1,3-bis(4,5-dihydrothiazolo)benzene formed when BDETH<sub>2</sub> was combined with AlMe<sub>3</sub> in toluene under reflux. The new compound was characterized by IR, NMR, MS, EA, and single crystal X-ray diffraction. This reaction demonstrated that presence of -NH and -SH functionalities at appropriate distances and appropriate reaction conditions results in a cyclic product. The reaction is triggered by the attack of the thiol sulfur on the carbonyl carbon, followed by removal of a water molecule to form a C=N bond. The mechanism, in its simplified form, can be shown as in Figure 3.6.

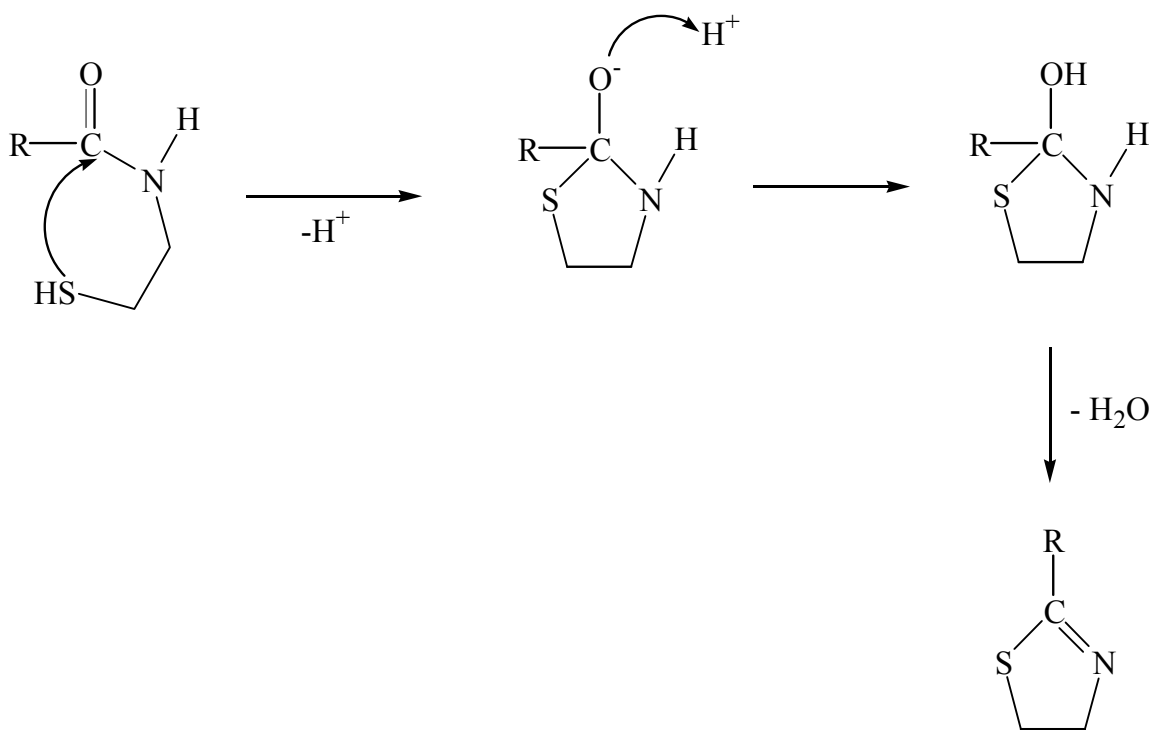


**Figure 3.6.** Simplified mechanism for the formation of 1,3-bis(4,5-dihydrothiazolo)-Benzene

## CHAPTER 4

### *N,N'*-Bis(2-mercaptoethyl)oxalamide (MOA)

#### 4.1 Overview

BDETH<sub>2</sub> is very effective in binding divalent heavy metals. However, its application remains a problem because of its insolubility in water and other solvents. So, attempts were made to prepare a hydroxyl analogue, and amino- and halo-derivatives of BDETH<sub>2</sub> which might lead to more soluble compounds. But those attempts were not successful. It was thought that other dithiol compounds, especially those with shorter carbon chains, may have better solubility characteristics. Efforts made in this direction resulted in the synthesis of a dithiol compound, *N,N'*-bis(2-mercaptoethyl)oxalamide (MOA). Although this compound was first reported by Brenner et al.,<sup>173</sup> a new synthetic procedure was devised in this study. Although it has been reported that MOA is capable of binding Tc species,<sup>173</sup> there is no evidence in the literature of its effectiveness in binding main group heavy metals. In this study a series of reactions was run to see the effectiveness of MOA in binding the heavy metals Cd, Hg and Pb. The compounds of MOA were characterized by different techniques including IR, Raman, EA, mass spectroscopy and TGA.

#### 4.2 Synthesis and characterization

##### 4.2.1 Synthesis

*N,N'*-Bis(2-mercaptoethyl)oxalamide, compound **16**, was synthesized by reacting oxalyl chloride with cysteamine hydrochloride (Scheme 4.1). Off-white powders were obtained; M.p. 108-110 °C, yield 65%.



In a typical reaction an aqueous salt solution of a metal was added to an ethanolic solution of MOA. Precipitates formed immediately. Compounds **17** (MOA-Cd) and **18** (MOA-Hg) were white, while compound **19** (MOA-Pb) was yellow.

Yields of the products ranged from 67% for compound **17** to 100% for compound **19**.

The compounds were found to be very stable in air, light, and water. None possessed well defined melting points and decomposed at temperatures ranging from 218 °C to 226 °C. They were found to be insoluble in common laboratory solvents, showing again, a similarity to BDETH<sub>2</sub>.

#### 4.2.2 Characterization

MOA was fully characterized spectroscopically. In the infrared spectrum (KBr pellet) the bands at 3297, 2554, and 1689 cm<sup>-1</sup> were attributed to N-H stretching ( $\nu_{\text{NH}}$ ), S-H stretching ( $\nu_{\text{SH}}$ ), and C=O stretching ( $\nu_{\text{C=O}}$ ), respectively. In the <sup>1</sup>H NMR the amide protons were shown as a broad singlet at 7.72 ppm, while the sulfhydryl protons exhibited a triplet at 1.52 ppm. In the <sup>13</sup>C NMR the signals at 162.1, 43.4, and 24.5 corresponded to the carbonyl carbon, methylene carbon adjacent to the amide nitrogen, and the methylene carbon next to the sulfhydryl group respectively. Mass spectroscopy signals at  $m/z$  207, 104 and 61 may be attributed to the  $[\text{M}^+ - \text{H}]$ ,  $[\text{M}^+ - \text{CONHCH}_2\text{CH}_2\text{SH}]$ , and  $-\text{CH}_2\text{CH}_2\text{SH}$  peaks, respectively. The base peak at  $m/z$  131 may be attributed to a product of intramolecular cyclization (with loss of a fragment) initiated by the attack of a nucleophilic S atom on the carbon of an amido group. The structure of the product is shown below (Figure 4.1).

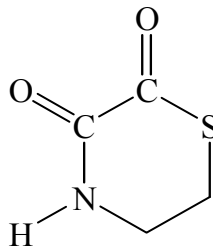


**Figure 4.1.** Product of intramolecular cyclization of MOA

In contrast to the  $\text{AlMe}_3$ -induced cyclization of  $\text{BDETH}_2$  where the attack was on the nearest carbonyl carbon of the amide group, here the attack was by a nucleophilic thiol on the farthest carbonyl carbon of the amide group.

Infrared spectroscopy data obtained for compounds **17**, **18** and **19** show that the peak at  $2554\text{ cm}^{-1}$  due to S-H stretching ( $\nu\text{SH}$ ) is absent from their spectra indicating that the protons of the thiol groups in MOA were displaced by the metals and the metals formed bonds with the S atoms.

Raman spectroscopy exhibited metal-sulfur stretches for all of the compounds. For example, the band at  $242\text{ cm}^{-1}$  in compound **17** was attributed to Cd-S. This is similar to values found in the literature for  $\nu\text{Cd-S}$  in tetrahedral cadmium compounds like  $\text{Cd}(\text{TAA})_2$  (TAA= monothioacetylacetonate)<sup>142</sup> and  $[\text{Cd}(\text{Et}_2\text{dtc})_2]_2$  ( $\text{Et}_2\text{dtc}$  = diethyldithiocarbamate).<sup>143</sup> However, this value is higher than that obtained for BDET-Cd. This may be due to the lower mass of MOA-Cd compared to BDET-Cd. The band at  $308\text{ cm}^{-1}$  for compound **18** can be attributed to a linear Hg-S bond. Such values are very similar to values for linear Hg-S bonds reported in the literature.<sup>144</sup> For example, for the Hg-S bands in  $\text{Hg}(\text{SMe})_2$  are  $297$ ,<sup>145</sup>  $295$ ,<sup>146</sup> and  $298$ <sup>147</sup>  $\text{cm}^{-1}$ . Again, this value is higher than the value found for BDET-Hg which may be attributed to the lighter

mass of MOA-Hg compared to its BDET analogue. The band at  $256\text{ cm}^{-1}$  for compound **19** was assigned to  $\nu\text{Pb-S}$ . These values are similar to values for  $\nu\text{Pb-S}$  reported in the literature for tetrahedral lead compounds like  $(\text{C}_6\text{H}_5)_3\text{PbSC}_6\text{H}_5$ .<sup>148</sup> As in the case of Cd and Hg compounds, this value is higher than that of its BDET analogue.

No solution NMR experiments could be performed with these compounds due to their lack of solubility in NMR solvents. Similarly, single crystal X-ray analysis could not be performed since no appropriate solvent was found to grow crystals suitable for study.

In the EI mass spectroscopic data for MOA-Cd the peak at  $m/z$  206 corresponds to  $[\text{M}^+ - \text{Cd}]$  while the peaks at 112, 111, and 110 correspond to the isotope peaks of Cd. In the spectrum for MOA-Hg peaks at  $m/z$  202 - 198 correspond to the isotopic peaks of Hg. The peak at 206 corresponds to  $[\text{M}^+ - \text{Hg}]$ . Similarly, in the spectrum for MOA-Pb peaks at  $m/z$  208, 207, and 206 correspond to the isotope peaks of Pb. The peak at 206 corresponds to  $[\text{M}^+ - \text{Pb}]$ .

Thermogravimetric analysis (TGA) was conducted under atmospheric conditions at a heating rate of  $10\text{ }^\circ\text{C}$  per minute. The thermogram for **17** shows that the compound is fairly stable up to  $97\text{ }^\circ\text{C}$  after which it begins to lose weight. The observed weight loss of 3.2% (between  $97$  and  $241\text{ }^\circ\text{C}$ ) indicates that half of a molecule of water of hydration may be present in the compound. However, the absence of broad bands at  $3415$  ( $\nu\text{OH}$ ) and  $1642\text{ cm}^{-1}$  ( $\delta\text{HOH}$ ) in the IR spectrum and results of elemental analysis do not support this assumption. The other weight losses for MOA-Cd indicate that the compound decomposes without producing any stable intermediates. The thermogram for **18** shows that the compound is very stable up to  $163\text{ }^\circ\text{C}$ . No distinct plateau was

observed in the thermogram indicating that the product decomposed without producing any stable intermediate. The observed weight losses of 26.03% (between 163 and 273 °C), 16.82% (between 273 °C and 313 °C), 20.74% (between 313 and 370 °C), and 28.92% (between 370 and 556 °C) did not correspond to any structural feature of the compound; they simply indicate that the compound decomposes without producing any intermediates. The thermogram for **19** shows that the compound is fairly stable up to 168 °C after which it begins to lose weight. The weight losses observed indicate that the compound decomposes without producing any stable intermediate.

Elemental analyses clearly indicated that the formulations MOA-M (M = Cd, Hg, Pb) are correct. For **17** (anal. calcd for C<sub>6</sub>H<sub>10</sub>N<sub>2</sub>S<sub>2</sub>O<sub>2</sub>Cd) the experimental values agreed very well with that of the calculated ones. While the calculated values for C, H, and N were 22.6%, 3.16%, and 8.79%, the corresponding experimental values were 22.7%, 3.54%, 7.98% respectively. The elemental analysis data found experimentally for compounds **18** and **19** also agree well with the calculated values (see Experimental Section).

## 4.3 Experimental

### 4.3.1 General considerations

All chemicals were purchased from commercial sources and used without further purification. Solvents were of reagent grade. The following reagent grade materials were used for the synthesis of MOA and its metal compounds: 1) oxalyl chloride (99% purity), 2) 2-mercaptoethylamine hydrochloride (98% purity), 3) triethylamine (99%

purity), 4)  $\text{Cd}(\text{CH}_3\text{COO})_2 \cdot 2\text{H}_2\text{O}$  (99%), 5)  $\text{HgCl}_2$  (99.5%), 6)  $\text{Pb}(\text{CH}_3\text{COO})_2 \cdot 3\text{H}_2\text{O}$  (99%); all were purchased from Aldrich.

Elemental analyses were carried out at the Center for Applied Energy Research (CAER), University of Kentucky. Infrared spectra were recorded, as KBr disks, using a Nicolet 320 FTIR spectrophotometer.  $^1\text{H}$  NMR spectra were run on a Varian INOVA 400 MHz instrument and  $^{13}\text{C}$  NMR spectra were run on a Varian Gemini 200 MHz instrument. A Finnigan Incos 50 Quadrupole instrument was used for recording EI mass spectra.

#### 4.3.2 Syntheses

$\{\text{HSCH}_2\text{CH}_2\text{NHC(O)}\}_2$  (**16**). To a stirred solution of  $\text{HSCH}_2\text{CH}_2\text{NH}_2 \cdot \text{HCl}$  (4.99 g, 44.0 mmol) in 150 mL of  $\text{CHCl}_3$  was added 4.50 mL of  $\text{Et}_3\text{N}$  (3.27 g, 32.0 mmol) and stirred for 10 minutes. To the resulting reaction mixture was added a solution of  $\text{C}_2\text{Cl}_2\text{O}_2$  (1.72 mL; 2.54 g, 20.0 mmol) in 5 mL of  $\text{CHCl}_3$  and stirred for 10 minutes. Then another portion (4.50 mL) of  $\text{Et}_3\text{N}$  was added to the reaction mixture and stirred for 4 hrs. The reaction mixture was extracted with DI water (200 mL + 100 mL + 100 mL), the organic layer dried over anhydrous  $\text{MgSO}_4$ , and solvent removed under vacuum to yield 2.69 g (65%) of the product. Mp. 108-110 °C. IR (KBr) 3297 w (vNH), 2933 m {vC-H(methylene)}, 2554 m (vSH), 1689 ss (vCO), 1533 ss ( $\delta\text{NH}$ ), 1076 m (vC-S)  $\text{cm}^{-1}$ .  $^1\text{H}$  NMR ( $\text{CDCl}_3$ , 400 MHz)  $\delta$  1.52 (t, SH, 2H), 2.78 (m,  $\text{CH}_2\text{SH}$ , 4H), 3.60 (m,  $-\text{NHCH}_2$ , 4H), 7.72 (s,  $-\text{CONH}$ , 2H).  $^{13}\text{C}$  NMR ( $\text{CDCl}_3$ , 200 MHz)  $\delta$  162.1 (CO), 43.4 ( $\text{NHCH}_2$ ), 24.5 ( $\text{CH}_2\text{S}$ ). Anal. Calcd. for  $\text{C}_6\text{H}_{12}\text{N}_2\text{O}_2\text{S}_2$ : C, 34.6; H, 5.81; N, 13.5.

Found: C, 35.2; H, 5.90; N, 13.5. MS m/z 207 [ $M^+ - H$ ], 131 (base peak, result of intramolecular cyclization with loss of a fragment), 104 [ $M^+ - CONHCH_2CH_2SH$ ], 61 [ $-CH_2CH_2SH$ ].

MOA-Cd (**17**). A solution of  $Cd(CH_3COO)_2 \cdot 2 H_2O$  (0.27 g, 1.0 mmol) in DI water (10 mL) was added to a stirred solution of MOA (0.21 g, 1.0 mmol) in 60 mL of 95% ethanol. A white precipitate formed immediately which was filtered under vacuum and dried in the air to yield 0.22 g (67%) of the product. Mp. 226 °C (dec). Anal Calcd. for  $C_6H_{10}N_2S_2O_2Cd$ : C, 22.6; H, 3.16; N, 8.79. Found C, 22.7; H, 3.54; N, 8.97. IR (KBr) 3303 m ( $\nu NH$ ), 2928 s ( $\nu C-H$ (methylene)), 1655 ss ( $\nu CO$ ), 1509 ss ( $\delta NH$ ), and 1020 m ( $\nu C-N$ )  $cm^{-1}$ . Raman ( $cm^{-1}$ ) 242 (Cd-S). MS m/z 206 [ $M^+ - Cd$ ]. The compound was found insoluble in water, methanol, ethanol, water/methanol, water/ethanol, dimethylsulfoxide, dimethylsulfoxide/water, dimethylformamide, acetone, ethyl acetate, tetrahydrofuran, diethyl ether, acetonitrile, acetonitrile/water, chloroform, dichloromethane, hexanes, toluene, nitrobenzene, nitromethane, carbon disulfide, 10% acetic acid, etc.

MOA-Hg (**18**). A solution of  $HgCl_2$  (0.27 g, 1.0 mmol) in DI water (20 mL) was added to a stirred solution of MOA (0.21 g, 1.0 mmol) in 60 mL of 95% ethanol. A white precipitate formed immediately which was filtered under vacuum and dried in the air to yield 0.33 g (81%) of the product. Mp. 218 °C (dec). Anal Calcd. for  $C_6H_{10}N_2S_2O_2Hg$ : C, 17.7; H, 2.48; N, 6.89. Found C, 17.2; H, 2.25; N, 6.41. IR (KBr) 3279 s ( $\nu NH$ ), 2933 m ( $\nu C-H$ (methylene)), 1651 ss ( $\nu CO$ ), 1521 ss ( $\delta NH$ ), and 1021 m ( $\nu C-N$ )  $cm^{-1}$ . Raman ( $cm^{-1}$ ): 308  $cm^{-1}$  (Hg-S). MS m/z 206 [ $M^+ - Hg$ ]; 198, 199, 200,

202 isotopic peaks of Hg. The compound was found insoluble in the same solvents as compound **17**.

MOA-Pb (**19**). A solution of  $\text{Pb}(\text{CH}_3\text{COO})_2 \cdot 3 \text{H}_2\text{O}$  (0.38 g, 1.0 mmol) in DI water (10 mL) was added to a stirred solution of MOA (0.21 g, 1.0 mol) in 60 mL of 95% ethanol. A yellow precipitate formed immediately which was filtered under vacuum and dried in the air to yield 0.41 g (100%) of the product. Mp. 223 °C (dec). Anal Calcd. for  $\text{C}_6\text{H}_{10}\text{N}_2\text{S}_2\text{O}_2\text{Pb}$ : C, 17.4; H, 2.44; N, 6.78. Found C, 17.7; H, 2.42; N, 6.62. IR (KBr) 3271 s ( $\nu\text{NH}$ ), 2963 m { $\nu\text{CH}(\text{methylene})$ }, 1649 ss ( $\nu\text{CO}$ ), 1523 ss ( $\delta\text{NH}$ ), and 1026 m ( $\nu\text{C-N}$ )  $\text{cm}^{-1}$ . Raman ( $\text{cm}^{-1}$ ): 256 (Pb-S). MS m/z 206 [ $\text{M}^+ - \text{Pb}$ ]; 206, 207, 208 (isotopic peaks of Pb). The compound was found insoluble in the same solvents as compound **17**.

#### 4.4 Conclusions

A dithiol compound, MOA, has been synthesized and characterized by different techniques including IR, NMR, EA, and mass spectroscopy. Although the compound was not soluble in water, it was moderately soluble in dimethylsulfoxide, dimethylformamide, and tetrahydrofuran and slightly soluble in methanol and ethanol (less than BDETH<sub>2</sub>). In this regard the compound was similar to BDETH<sub>2</sub>. However, the synthesis of this compound has been proven to be clean and less troublesome than that of BDETH<sub>2</sub>. The formation of sticky masses in the separatory funnel during the extraction makes the synthesis of BDETH<sub>2</sub> lengthy and troublesome.

A series of metal compounds of MOA has been prepared and characterized by IR, Raman, EA, and Mass spectroscopy. However, single crystal X-ray crystallographic study could not be performed because of their insolubility in common laboratory

solvents. Based on results of current investigations and the evidence presented in the literature it is likely that the compounds are polymeric. It is possible that MOA-Hg (**18**) has a linear geometry around Hg. The geometry around Cd and Pb in MOA-Cd (**17**) and MOA-Pb (**19**) may be four-coordinate and tetrahedral. Figure 4.2 illustrates the proposed structures for compounds **17**, **18** and **19**.

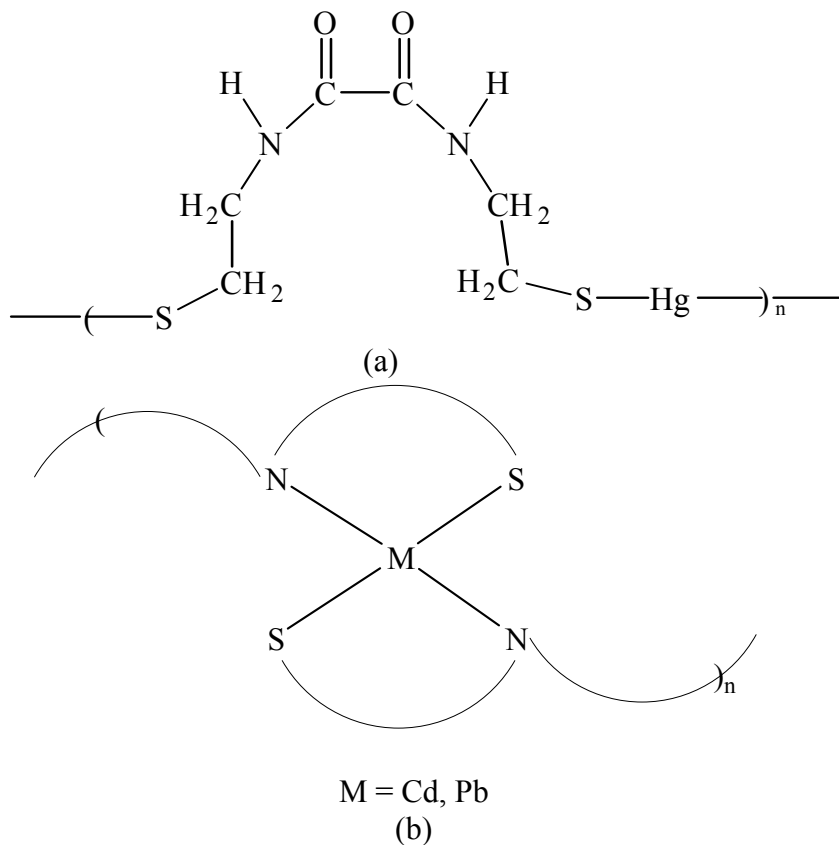


**Figure 4.2.** Structures of MOA-Metal Compounds: (a) MOA-Hg, (b) MOA-M (M = Cd, Pb)

It is possible that reactions of MOA-M compounds with *n*-BuLi, C<sub>2</sub>H<sub>5</sub>MgBr, Bu<sub>2</sub>Mg and NaHSO<sub>3</sub> may yield products, by attacking the carbonyl group present in them, soluble in common laboratory solvents. This will facilitate growth of crystals suitable for single crystal X-ray analysis.

## CHAPTER 5

### Metal Compounds of Dithiothreitol (DTT)

#### 5.1 Overview

Since the metal compounds of BDETH<sub>2</sub> and MOA were insoluble in common laboratory solvents, crystals suitable for single crystal X-ray crystallography could not be grown. The coordination environment around the metal centers in those compounds remain largely undetermined although it is possible that they are polymeric.

It is known that threo-1,4-dimercaptobutane-2,3-diol or dithiothreitol (DTT), commonly known as Cleland's reagent,<sup>174</sup> is a dithiol compound readily soluble in water. The molecular structure of its reduced form is shown below (Figure 5.1).

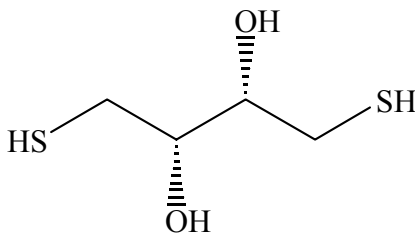


**Figure 5.1.** Dithiothreitol.(DTT)

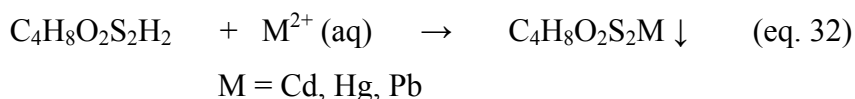
The most common use of DTT is as a reducing or "deprotecting" agent for thiolated DNA. Due to air oxidation, DTT is a relatively unstable compound whose useful life can be extended by refrigeration and handling in an inert atmosphere. In the literature it has been reported that it is capable of binding with heavy metals such as Cd and Pb.<sup>175</sup> But there is no report of any characterization or structure elucidation of the compounds that DTT makes when it binds these metals. The present study was undertaken to prepare some main group metal compounds of DTT and characterize them

with particular focus on their solubility behavior and crystal structures. It turned out that the DTT-Metal compounds are also insoluble in common laboratory solvents. Efforts to grow crystals suitable for single crystal X-ray crystallography remained unsuccessful. Attempts to prepare alkali metal salts of DTT yielded a disulfide. Structure of the disulfide was established by single crystal X-ray crystallography. The present chapter will describe the preparation and characterization of the DTT-Metal compounds.

## 5.2 Synthesis and characterization

### 5.2.1 Synthesis

The syntheses of the main group metal complexes of DTT were accomplished by one general method (equation 32). This is very similar to the method described in the literature where DTTCd and DTTPb were prepared by adding 10 mL of a 1.0 M solution of the metal ion to 10 mL of a water solution of DTT.<sup>175</sup>



In a typical reaction an aqueous salt solution of a metal was added to an aqueous solution of DTT. Precipitates formed immediately. Compounds **20** (DTT-Cd) and **21** (DTT-Hg) were white, while compound **22** (DTT-Pb) was yellow. Yields of the products ranged from 88% for compound **22** to 100% for compound **21**. The compounds were found to be very stable in air, light, and water. DTTCd, DTTHg and DTTPb decomposed at 208 °C, 148 °C and 162 °C, respectively. The values are different from those reported in the literature (DTTCd and DTTPb decomposed between 230 °C – 240 °C and 145 °C,

respectively).<sup>174</sup> This may be due to the post-synthetic treatments that they were subjected to in the previous work (dissolution of the precipitates in concentrated HCl followed by neutralization with KOH and finally washing with water, 95% ethanol and anhydrous diethyl ether). They were found to be insoluble in common laboratory solvents. In the literature, however, it was reported that DTTCd dissolved in both strongly acidic and basic solutions, while DTTPb dissolved in strongly acidic solutions as well as in solutions containing an excess of lead acetate.

Syntheses of the alkali metal compounds of DTT were attempted by combining aqueous solutions of DTT with aqueous solutions of alkali metal hydroxides, NaOH and KOH. Precipitates appeared only after 7 days of continuous stirring. But upon filtration almost nothing remained on the filter paper. The supernatant was allowed to stand at room temperature for 7 days to yield crystals which proved to be a disulfide (by single crystal X-ray crystallography), formed by the oxidation of DTTH<sub>2</sub>. Yield of the crystals was 50%. Equation 33 illustrates the formation of the disulfide.



### 5.2.2 Characterization

Infrared spectroscopy data obtained for all three main group metal compounds of DTT (**20**, **21** and **22**) showed that the peak at 2565 cm<sup>-1</sup> due to S-H stretching (νSH) was absent from their spectra indicating that the protons of the thiol groups in DTT were displaced by the metals and the metals formed bonds with the S atoms. The peak at 2565 cm<sup>-1</sup> due to S-H stretching (νSH) was also absent in the infrared spectra of the disulfide

(compound **23**) indicating that the protons of the thiol groups were removed. A very weak peak at  $490\text{ cm}^{-1}$  indicated the presence of a disulfide bond in the compound. Raman spectroscopy exhibited metal-sulfur stretches for compounds **20** and **21**, but no discernible peak was detected for compound **22**. The stretches at  $182\text{ cm}^{-1}$  in compound **20** and at  $329\text{ cm}^{-1}$  for compound **21** were attributed to the Cd-S and the linear Hg-S bonds. They are very similar to values for Cd-S bond in compounds with tetrahedral geometry around Cd<sup>142,143</sup> and linear Hg-S bonds reported in the literature.<sup>144</sup>

In the EI mass spectrum of compound **20** the peak at  $m/z$  152 corresponds to  $[M^+ - \text{Cd}]$ . No isotopic peaks of Cd were observed. In the mass spectrum of compound **21** the peak at  $m/z$  152 corresponds to  $[M^+ - \text{Hg}]$ , while the peaks at  $m/z$  198, 199, 200, and 202 correspond to the isotopic peaks of Hg. In the mass spectrum of compound **22** the peak at  $m/z$  152 corresponds to  $[M^+ - \text{Pb}]$ , while the peaks at  $m/z$  206, 207, and 208 correspond to the isotopic peaks of Pb.

No solution NMR experiment could be performed with compounds **20-22** due to their insolubility in NMR solvents. Similarly, single crystal X-ray analysis of compounds **20-22** could not be performed since no appropriate solvent was found to grow crystals suitable for study. Crystal structure of any DTT-M compound has not been reported in the literature. Crystals of compound **23** (Figure 5.2) were formed after the stirred reaction mixture containing the aqueous solutions of DTT and the aqueous solutions of the alkali metal hydroxides were left undisturbed for a week. The compound crystallized in the monoclinic space group P 21/c. The crystallographic data for compound **23** are presented in table 5.1.

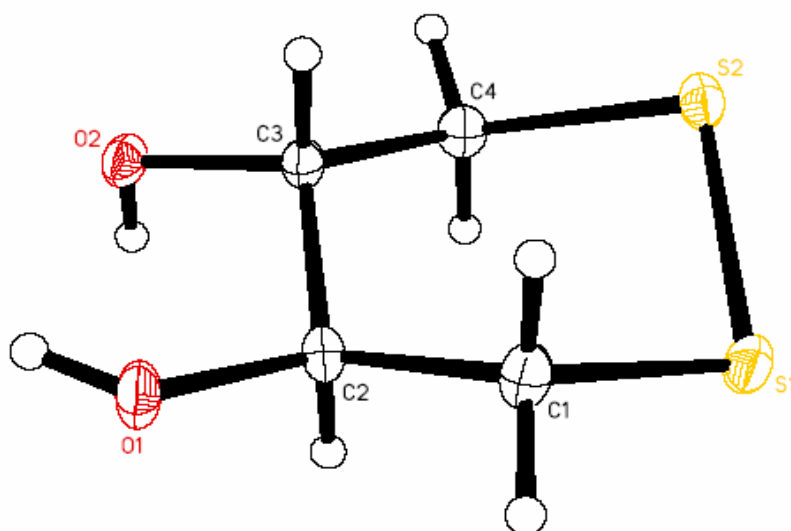


**Figure 5.2.** Crystal structure of the disulfide from DTT.

**Table 5.1.** Crystallographic data for compound **23**.

formula	C <sub>4</sub> H <sub>8</sub> O <sub>2</sub> S <sub>2</sub>
formula weight	152.24
crystal group	monoclinic
space group	P 21/c
a (Å)	9.6566(3)
b (Å)	8.3959(3)
c (Å)	8.1217(3)
α (degree)	90.00
β (degree)	104.9815(16)
γ (degree)	90.00
V (Å <sup>3</sup> )	636.09(4)
Z	4
Radiation	MoKα (λ = 0.71073)

Thermogravimetric analysis (TGA) was carried out under atmospheric conditions at a heating rate of 10 °C per minute. The thermogram for **20** shows that the compound is fairly stable up to 81.4 °C after which it begins to lose weight. The observed weight losses of 1.73% (between 81.4 and 193.3 °C) and 39.55% (between 193.3 and 293.9 °C)

for DTT-Cd indicate that the compound decomposes without producing any stable intermediates. The thermogram for **21** shows that the compound is very stable up to 143 °C. The observed weight loss of 65.1% (between 199.8 and 401.4 °C) indicates that elemental Hg and SO<sub>2</sub> formed as a result of heating of DTT-Hg. The thermogram for **22** shows that the compound is fairly stable up to 124 °C after which it begins to lose weight. The observed weight losses of 26.3% (between 198 and 230.3 °C) and 3.33% (between 203.3 and 272.9 °C) indicate that the compound decomposes without producing any stable intermediate.

Elemental analyses clearly indicated that the formulations DTT-Cd, DTT-Hg and DTT-Pb are correct. For **20** (anal. calcd for C<sub>4</sub>H<sub>8</sub>O<sub>2</sub>S<sub>2</sub>Cd) the experimental values agreed very well with that of the calculated ones. While the calculated values for C, and H were 18.2%, and 3.05% the corresponding experimental values were 17.7%, and 3.38% respectively. The elemental analysis data found experimentally for the other compounds, DTT-Hg and DTT-Pb, also agree well with the calculated values (see Experimental Section).

### 5.3 Experimental

#### 5.3.1 General considerations

All chemicals were purchased from commercial sources and used without further purification. Solvents were of reagent grade. The following reagent grade materials were used for the preparation of DTT- metal compounds: 1) Dithiothreitol (99%), 2) Cd(CH<sub>3</sub>COO)<sub>2</sub> · 2 H<sub>2</sub>O (99%), 3) HgCl<sub>2</sub> (99.5%), 4) Pb(CH<sub>3</sub>COO)<sub>2</sub> · 3 H<sub>2</sub>O (99%), 5) KOH (98%); all were purchased from Aldrich.

Elemental analyses were carried out at the Center for Applied Energy Research (CAER), University of Kentucky. Infrared spectra were recorded, as KBr disks, using a Nicolet 320 FTIR spectrophotometer. Raman spectra were recorded at the Center for Applied Energy Research, University of Kentucky using a Nicolet FT-Raman 906 spectrometer ESP instrument. A Finnigan Incos 50 Quadrupole instrument was used for recording EI mass spectra. Thermogravimetric analyses were carried out in the air at a rate of 10 °C per minute on a TA instruments TGA 2950 thermogravimetric analyzer.

### 5.3.2 Synthesis

DTT-Cd (**20**). A solution of  $\text{Cd}(\text{CH}_3\text{COO})_2 \cdot 2 \text{H}_2\text{O}$  (0.53 g, 2.0 mmol) in DI water (10 mL) was added to a stirred solution of DTT (0.31 g, 2.0 mmol) in 5 mL of DI water. A white precipitate formed immediately which was filtered under vacuum and dried in the air to yield 0.48 g (91 %) of the product. Mp. 208 °C (dec). Anal Calcd. for  $\text{C}_4\text{H}_8\text{O}_2\text{S}_2\text{Cd}$ : C, 18.2; H, 3.05. Found C, 17.7; H, 3.38. IR (KBr) 3346 m (νOH), 2916 s {νC-H(methylene)}, 1630 m (δHOH), and 1036 m (νC-O)  $\text{cm}^{-1}$ . Raman ( $\text{cm}^{-1}$ ) 182 (Cd-S). MS m/z 152 [ $\text{M}^+$  - Cd]. The compound was found insoluble in water, methanol, ethanol, water/methanol, water/ethanol, dimethylsulfoxide, dimethylsulfoxide/water, dimethylformamide, acetone, ethyl acetate, tetrahydrofuran, diethyl ether, acetonitrile, acetonitrile/water, chloroform, dichloromethane, hexanes, toluene, nitrobenzene, nitromethane, carbon disulfide, 10% acetic acid, etc.

DTT-Hg (**21**). A solution of  $\text{HgCl}_2$  (1.36 g, 5.00 mmol) in DI water (20 mL) was added to a solution of DTT (0.77 g, 5.0 mol) in 10 mL of DI water. A white precipitate formed immediately which was filtered under vacuum and dried in the air to yield 1.91 g

(100%) of the product. Mp. 148 °C (dec). Anal Calcd. for  $C_4H_8O_2S_2Hg$ : C, 13.6; H, 2.29. Found C, 13.4; H, 2.67. IR (KBr) 3385 s ( $\nu OH$ ), 2915 m  $\{\nu C-H(\text{methylene})\}$ , 1630 m ( $\delta HOH$ ), and 1036 m ( $\nu C-O$ )  $cm^{-1}$ . MS m/z 152 [ $M^+ - Hg$ ]; 198, 199, 200, 202 (isotopic peaks of Hg). Raman ( $cm^{-1}$ ): 329  $cm^{-1}$  (Hg-S). The compound was found insoluble in the same solvents as compound **20**.

DTT-Pb (**22**). A solution of  $Pb(CH_3COO)_2 \cdot 3 H_2O$  (0.76 g, 2.0 mmol) in DI water (10 mL) was added to a solution of DTT (0.31 g, 2.0 mmol) in 5 mL of DI water. A yellow precipitate formed immediately which was filtered under vacuum and dried in the air to yield 0.63 g (88%) of the product. Mp. 162 °C (dec). Anal Calcd. for  $C_4H_8O_2S_2Pb$ : C, 13.4; H, 2.24. Found C, 13.3; H, 2.61. IR (KBr) 3405 s ( $\nu OH$ ), 2902 m  $\{\nu CH(\text{methylene})\}$ , 1631 m ( $\delta HOH$ ), and 1034 m ( $\nu C-O$ )  $cm^{-1}$ . MS m/z 152 [ $M^+ - Pb$ ]; 206, 207, 208 (isotopic peaks of Pb). The compound was found insoluble in the same solvents as compound **20**.

$C_4H_8O_2S_2$  (**23**). A solution of KOH (0.28 g, 5.0 mmol) in DI  $H_2O$  (10 mL) was added to a solution of DTT (0.38 g, 2.5 mmol) in 5 mL of DI water and stirred for 7 days after which some white precipitates seemed to form. A very insignificant amount of solid remained on the filter paper when the reaction mixture was filtered. The supernatant was allowed to stand at room temperature for 7 days to yield 0.19 g (50%) of colorless crystals. Mp. 111-112 °C. IR (KBr) 3430 s ( $\nu OH$ ), 2956 m  $\{\nu CH(\text{methylene})\}$ , 1630 m ( $\delta HOH$ ), 1034 m ( $\nu C-O$ ), 490 vw ( $\nu S-S$ )  $cm^{-1}$ . MS m/z 152 [ $M^+$ ].

## 5.4 Conclusions

A series of DTT-metal compounds (**20-22**) was prepared by combining aqueous solutions of dithiothreitol (DTT) with appropriate aqueous solutions of metals salts. The metal compounds have been characterized by Mp, IR, Raman, MS, and elemental analysis. However, none of the compounds were soluble in common laboratory solvents. So, solution NMR could not be performed. Also, crystals suitable for single crystal X-ray crystallographic study could not be grown. Based on the evidence presented above, it is likely that compounds are polymeric. It is possible that DTT-Hg has a linear geometry like BDET-Hg and MOA-Hg. Similarly, in DTT-Cd and DTT-Pb the geometry around the central metal atoms are four-coordinate and tetrahedral as in the cadmium and lead compounds of BDETH<sub>2</sub> and MOA. The following structures (Figure 5.3) are proposed for the DTT-Metal compounds.

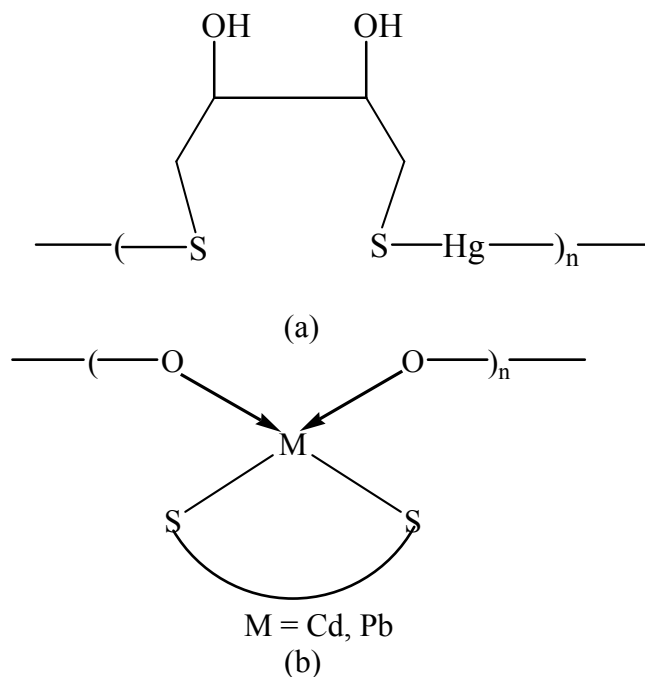


**Figure 5.3.** Proposed structures for DTT-Metal compounds: (a) DTT-Hg, (b) DTT-M (M = Cd, Pb).

## CHAPTER 6

### *N*-Mercaptoethylfuroylamide (MFA)

#### 6.1 Overview

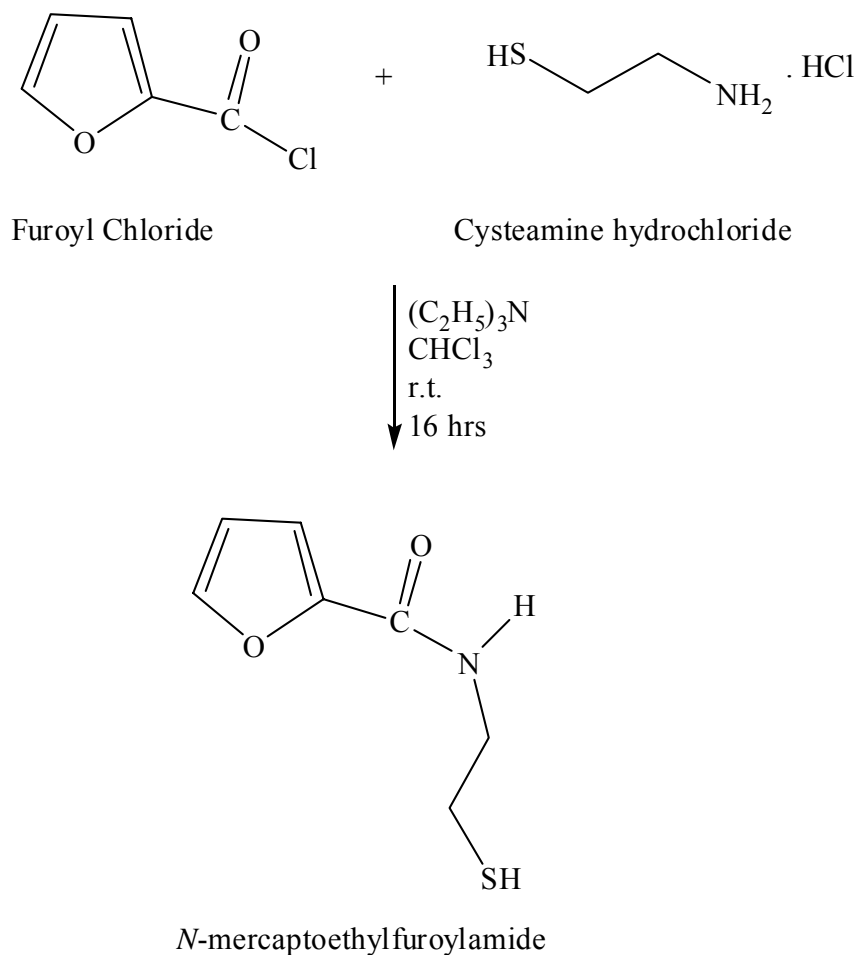
BDETH<sub>2</sub> and other dithiols have proven effective in binding heavy metals. But most of them are insoluble in water limiting their application. Although monothiols have been known to chelate heavy metals in biological systems,<sup>176,177</sup> there has been no report of systematic investigations of monothiols in heavy metal remediation. It was thought that any thiol with a small number of carbon atoms and containing an oxygen atom with lone pairs of electrons in the structure may be soluble in water. So, it was decided to design and develop a monothiol capable of binding heavy metals in the aqueous environment. Efforts made in this direction resulted in the successful synthesis of a monothiol ligand, *N*-mercaptoethylfuroylamide (MFA). There is no report in the literature of its synthesis or its use in heavy metal remediation. In this study a series of reactions were run to see the effectiveness of MFA in binding heavy metals like Cd, Hg and Pb. The compounds of MFA were characterized by different techniques including IR, NMR, EA, mass spectroscopy, and TGA.

#### 6.2 Synthesis and characterization

##### 6.2.1 Synthesis

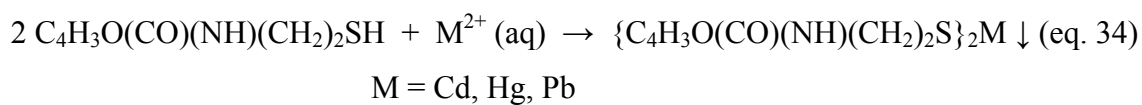
*N*-mercaptoethylfuroylamide (MFA), compound **24**, was synthesized by combining furoyl chloride with cysteamine hydrochloride (Scheme 6.1). Light brown powders were obtained; M.p. 112-116 °C, yield 89 %. MFA was found to be moderately

soluble in tetrahydrofuran, chloroform, dimethylsulfoxide and dimethylformamide and slightly soluble in methanol, ethanol, and acetonitrile.



**Scheme 6.1.** Synthesis of *N*-mercaptoethylfuroylamide (MFA).

The syntheses of the metal complexes of MFA were accomplished by one general method (equation 34).



In a typical reaction one equivalent of an aqueous salt solution of a metal was added to a solution of MFA (two equivalents) in THF and stirred. Precipitates were observed to form after 12 hours of stirring. Stirring was stopped after 48 hours and the reaction mixtures filtered to yield solid products. Compounds **25** (MFA-Cd), **26** (MFA-Hg) and **27** (MFA-Pb) were light brown. Yields of the products ranged from 35% for compound **25** to 38% for compound **27**. The compounds were found to be stable in air, light, and water. Compounds **25**, **26** and **27** melted at 142-144 °C, 134-136 °C and 122-125 °C respectively. They were found to be moderately soluble in DMSO and DMF and very slightly soluble in CHCl<sub>3</sub>, a characteristic totally different from the metal compounds of the dithiol ligands including BDETH<sub>2</sub>.

### 6.2.2 Characterization

MFA was fully characterized spectroscopically. In the infrared spectrum (KBr pellet) the bands at 3260, 2573, and 1644 cm<sup>-1</sup> were attributed to N-H stretching ( $\nu_{\text{NH}}$ ), S-H stretching ( $\nu_{\text{SH}}$ ), and C=O stretching ( $\nu_{\text{C=O}}$ ), respectively. In the <sup>1</sup>H NMR the amide protons were shown as a broad singlet at 6.84 ppm, while the sulfhydryl protons exhibited a triplet at 1.64 ppm. In the <sup>13</sup>C NMR the signals at 158.9 ppm corresponded to the carbonyl carbon; the signals at 148.2, 144.3, 114.7, 112.5 were due to the ring carbons; the methylene carbons were displayed at 38.1 and 27.6 ppm. Mass spectroscopy signals at m/z 171, 170, 138, 95 (base peak) and 67 were attributed to M<sup>+</sup>, [M<sup>+</sup> - H], [M<sup>+</sup> - SH], [M<sup>+</sup> - NHCH<sub>2</sub>CH<sub>2</sub>SH] and [M<sup>+</sup> - CONHCH<sub>2</sub>CH<sub>2</sub>SH] respectively.

Infrared spectroscopy data obtained for compounds **25**, **26** and **27** show that the peak at 2573 cm<sup>-1</sup> due to S-H stretching ( $\nu_{\text{SH}}$ ) is absent from their spectra indicating that

the protons of the thiol groups in MFA were displaced by the metals and the metals formed bonds with the S atoms. In the  $^1\text{H}$  NMR spectra of all compounds the signal (three lines) for the amide proton was seen at around 8.50 ppm. This shift in position of the amido proton is probably a result of coordination of the amido nitrogen with the metal. The three lines probably are due to splitting of the proton by the quadrupolar nitrogen atom ( $I = 1$ ). The signals for the ring protons were displayed between 6.60 and 7.83 ppm. There was no signal due to the sulfhydryl proton since it was displaced by the metal. In the  $^{13}\text{C}$  NMR spectra the signals at around 157.9 ppm were due to the carbonyl carbon. The signals between 147.9 and 111.7 ppm were due to the ring carbons; the methylene carbons were seen as a single line at 37.6 ppm.

In the EI mass spectra for compounds **25**, **26** and **27** the base peak at  $m/z$  95 was due to the fragment obtained after the cleavage of the C-N bond to the right of the carbonyl carbon. The peak at  $m/z$  67 was due to the fragment formed after the cleavage of the C-C bond joining the carbonyl carbon with the ring. For compound **25** the isotopic peaks of Hg were observed between  $m/z$  202 and 198.

Attempts to grow crystals of compounds **25**, **26** and **27** did not succeed. So, no single crystal X-ray analysis could be performed.

Thermogravimetric analysis (TGA) was conducted under atmospheric conditions at a heating rate of 10 °C per minute. The thermogram for **25** shows that the compound is fairly stable up to 236 °C after which it begins to lose weight. Absence of any distinct plateau in the thermogram indicates that the compound decomposed without producing any stable intermediates. This is quite similar to the behavior of the cadmium compounds of the dithiols including BDETCd. The observed weight losses of 82.97%

(between 236 and 329 °C) and 12.69% (between 329 and 558 °C) do not correspond to any structural feature of the compound. Similarly, the thermogram for **26** shows that the compound is fairly stable up to 190 °C at which point it begins to lose weight. But no distinct plateau was observed in the thermogram indicating that the product decomposed without producing any stable intermediate. The observed weight losses of 70.4% (between 190 and 321 °C), 17.1% (between 329 and 459 °C), and 7.75% (between 459 and 572 °C) do not correspond to any structural feature of the compound. This behavior agrees very well with that of the mercury dithiol compounds discussed previously. The thermogram of **27** shows that the compound is very stable up to 246 °C after which it begins to lose weight. No distinct plateau was observed in the thermogram indicating that the MFA-Pb compound decomposed without producing any stable intermediate. The observed weight losses of 76.61% (between 246 and 322 °C), 5.92% (between 322 and 471 °C), and 7.28% (between 471 and 529 °C) do not correspond to any structural feature of the compound. This is consistent with the dithiol-Pb compounds discussed previously.

## 6.3 Experimental

### 6.3.1 General considerations

All chemicals were purchased from commercial sources and used without further purification. Solvents were of reagent grade. The following reagent grade materials were used for the synthesis of MFA and its metal compounds: 1) 2-furoyl chloride (98% purity), 2) 2-mercaptoethylamine hydrochloride (98% purity), 3) triethylamine (99% purity), 4)  $\text{Cd}(\text{CH}_3\text{COO})_2 \cdot 2 \text{H}_2\text{O}$  (99% purity), 5)  $\text{HgCl}_2$  (99.5% purity), 6)

$\text{Pb}(\text{CH}_3\text{COO})_2 \cdot 3 \text{H}_2\text{O}$  (99% purity). All except 2-furoyl chloride were purchased from Aldrich; 2-furoyl chloride was purchased from TCI America.

Elemental analyses were carried out at the Center for Applied Energy Research (CAER), University of Kentucky. Infrared spectra were recorded, as KBr disks, using a Nicolet 320 FTIR spectrophotometer.  $^1\text{H}$  NMR spectra were run on a Varian INOVA 400 MHz instrument and  $^{13}\text{C}$  NMR spectra were run on a Varian Gemini 200 MHz instrument. A Finnigan Inco 50 Quadrupole instrument was used for recording EI mass spectra.

### 6.3.2 Synthesis

$\text{C}_4\text{H}_3\text{OC}(\text{O})\text{NHCH}_2\text{CH}_2\text{SH}$  (**24**). To a stirred solution of  $\text{HSCH}_2\text{CH}_2\text{NH}_2 \cdot \text{HCl}$  (2.49 g, 22.0 mmol) in 100 mL of  $\text{CHCl}_3$  was added 3.00 mL of  $\text{Et}_3\text{N}$  (2.18 g, 19.2 mmol) and stirred for 10 min. To the resulting reaction mixture was added, dropwise, a solution of  $\text{C}_4\text{H}_3\text{OC}(\text{O})\text{Cl}$  (1.98 mL; 2.61 g, 20.0 mmol) in 5 mL of  $\text{CHCl}_3$  and stirred for 10 minutes. Then another portion (3.00 mL) of  $\text{Et}_3\text{N}$  was added to the reaction mixture and stirred for 16 h. The reaction mixture was extracted with DI water (150 mL + 100 mL + 100 mL), the organic layer dried over anhydrous  $\text{MgSO}_4$ , and solvent removed under vacuum to yield 3.05 g (89%) of the product. Mp. 112-114 °C. IR (KBr) 3260 m ( $\nu\text{NH}$ ), 3086 s { $\nu\text{C-H}(\text{Ar})$ }, 2907 m { $\nu\text{C-H}(\text{methylene})$ }, 2573 w ( $\nu\text{SH}$ ), 1644 m ( $\nu\text{CO}$ ), 1545 m ( $\delta\text{NH}$ ), 608 m ( $\nu\text{CS}$ )  $\text{cm}^{-1}$ .  $^1\text{H}$  NMR ( $\text{CDCl}_3$ , 400 MHz)  $\delta$  1.64 (t, SH, 1H), 2.92 (m,  $\text{CH}_2\text{SH}$ , 2H), 3.76 (m,  $-\text{NHCH}_2$ , 2H), 6.48 (t, ArH, 1H), 6.84 (s,  $-\text{CONH}$ , 1H), 7.11 (d, ArH) and 7.42 (d, ArH, 1H).  $^{13}\text{C}$  NMR ( $\text{CDCl}_3$ , 200 MHz)  $\delta$  158.7 (CO), 143.7 (ArC), 115.8 (ArC), 114.5 (ArC), 111.7 (ArC), 38.1 ( $\text{CH}_2$ ), 27.6 ( $\text{CH}_2$ ). Anal. Calcd. for

C<sub>7</sub>H<sub>9</sub>NO<sub>2</sub>S: C, 49.1; H, 5.23; N, 8.18. Found: C, 49.3; H, 5.35; N, 8.27. MS m/z 171 [M<sup>+</sup>], 170 [M<sup>+</sup> - H], 138 [M<sup>+</sup> - SH], 95 [M<sup>+</sup> - NHCH<sub>2</sub>CH<sub>2</sub>SH], 67 [M<sup>+</sup> - CONHCH<sub>2</sub>CH<sub>2</sub>SH].

MFA-Cd (**25**). A solution of Cd(CH<sub>3</sub>COO)<sub>2</sub> · 2 H<sub>2</sub>O (0.17 g, 0.63 mmol) in DI water (10 mL) was added to a stirred solution of MFA (0.21 g, 1.3 mmol) in 20 mL of THF. Very light brown precipitate seemed to form after stirring the reaction mixture for 2 hours. The reaction mixture was kept stirring for 48 hours after which the precipitate was filtered under vacuum and dried in the air to yield 0.11 g (36%) of the product. Mp. 136-138 °C. Anal Calcd. for C<sub>14</sub>H<sub>16</sub>N<sub>2</sub>O<sub>4</sub>S<sub>2</sub>Cd: C, 37.1; H, 3.56; N, 6.19. Found C, 37.3; H, 3.58; N, 6.17. IR (KBr) 3250 m (νNH), 3079 s {νC-H(Ar)}, 1644 ss (νCO), 1550 m (δNH), and 607 s (νC-S) cm<sup>-1</sup>. <sup>1</sup>H NMR (d-DMSO, 400 MHz) δ 2.92 (m, CH<sub>2</sub>SH, 2H), 3.50 (m, -NHCH<sub>2</sub>, 2H), 6.62 (m, ArH, 1H), 7.08(d, ArH), 7.83 (d, ArH, 1H), and 8.52 (t, -CONH, 1H). <sup>13</sup>C NMR (d-DMSO, 200 MHz) δ 157.9 (CO), 147.8 (ArC), 145.1, 113.5 (ArC), 111.9 (ArC), 37.6 (CH<sub>2</sub>). MS m/z 341 [M<sup>+</sup> - Cd], 138 [C<sub>4</sub>H<sub>3</sub>O(C=O)NHCH<sub>2</sub>CH<sub>2</sub>], 95 (base peak) [C<sub>4</sub>H<sub>3</sub>O(C=O)]. The compound was found to be insoluble in water, but slightly soluble in dimethylsulfoxide and dimethylformamide, and very slightly soluble in chloroform.

MFA-Hg (**26**). A solution of HgCl<sub>2</sub> (0.34 g, 1.3 mmol) in DI water (20 mL) was added to a stirred solution of MFA (0.43 g, 2.5 mmol) in 20 mL of THF. A very light brown precipitate appeared after one hour of stirring. The reaction mixture was stirred for 48 hours after which the solid was filtered under vacuum and dried in the air to yield 0.24 g (35%) of the product. Mp. 142-144 °C. Anal Calcd. for C<sub>14</sub>H<sub>16</sub>N<sub>2</sub>O<sub>4</sub>S<sub>2</sub>Hg: C, 31.1; H, 2.98; N, 5.18. Found C, 31.2; H, 2.95; N, 5.23. IR (KBr) 3259 m (νNH), 3081 s

{ $\nu$ C-H(Ar)}, 2943 m { $\nu$ C-H(methylene)}, 1644 ss ( $\nu$ CO), 1547 ss ( $\delta$ NH), and 607 m ( $\nu$ C-S)  $\text{cm}^{-1}$ .  $^1\text{H}$  NMR (d-DMSO, 400 MHz)  $\delta$  2.92 (m,  $\text{CH}_2\text{SH}$ , 2H), 3.76 (m,  $-\text{NHCH}_2$ , 2H), 6.60 (dd, ArH, 1H), 7.11 (d, ArH) 7.83 (d, ArH, 1H) and 8.51 (t,  $-\text{CONH}$ , 1H).  $^{13}\text{C}$  NMR (d-DMSO, 200 MHz)  $\delta$  158.7 (CO), 148.1, 143.7 (ArC), 115.8 (ArC), 114.5 (ArC), 38.1 ( $\text{CH}_2$ ). MS m/z 341 [ $\text{M}^+ - \text{Hg}$ ], 198, 199, 200, 202 isotopic peaks of Hg, 138 [ $\text{C}_4\text{H}_3\text{O}(\text{C}=\text{O})\text{NHCH}_2\text{CH}_2$ ], 95 (base peak) [ $\text{C}_4\text{H}_3\text{O}(\text{C}=\text{O})$ ]. The compound has the same solubility properties as that of compound **25**.

MFA-Pb (**19**). A solution of  $\text{Pb}(\text{CH}_3\text{COO})_2 \cdot 3 \text{H}_2\text{O}$  (0.38 g, 1.0 mmol) in DI water (10 mL) was added to a stirred solution of MOA (0.21 g, 1.0 mol) in 60 mL of 95% ethanol. A slightly off-white precipitate formed after 4 hours of stirring. The reaction mixture was stirred for 48 hours after which the off-white precipitate was filtered under vacuum and dried in the air to yield 0.41 g (100%) of the product. Mp. 122-125  $^\circ\text{C}$ . Anal Calcd. for  $\text{C}_{14}\text{H}_{16}\text{N}_2\text{O}_4\text{S}_2\text{Pb}$ : C, 30.7; H, 2.95; N, 5.12. Found C, 31.1; H, 2.92; N, 5.16. IR (KBr) 3253 m ( $\nu$ NH), 3080 m { $\nu$ CH(Ar)}, 1644 ss ( $\nu$ CO), 1549 ss ( $\delta$ NH), and 607 m ( $\nu$ C-S)  $\text{cm}^{-1}$ .  $^1\text{H}$  NMR (d-DMSO, 400 MHz)  $\delta$  2.91 (m,  $\text{CH}_2\text{SH}$ , 2H), 3.51 (m,  $-\text{NHCH}_2$ , 2H), 6.61 (dd, ArH, 1H), 7.08 (d, ArH, 1H), 7.82 (d, ArH) and 8.50 (t,  $-\text{CONH}$ , 1H).  $^{13}\text{C}$  NMR (d-DMSO, 200 MHz)  $\delta$  157.9 (CO), 147.9 (ArC), 145.1 (ArC), 113.5 (ArC), 111.7 (ArC), 37.1 ( $\text{CH}_2$ ). MS m/z 341 [ $\text{M}^+ - \text{Pb}$ ]; 138 [ $\text{C}_4\text{H}_3\text{O}(\text{C}=\text{O})\text{NHCH}_2\text{CH}_2$ ], 95 (base peak) [ $\text{C}_4\text{H}_3\text{O}(\text{C}=\text{O})$ ]. The compound has the same solubility properties as that of compound **25**.

## 6.4 Conclusions

A monothiol compound, *N*-mercaptoethylfuroylamide (MFA), has been synthesized and characterized by different techniques including IR, NMR, and mass spectroscopy. Although the compound was not soluble in water, it was moderately soluble in dimethylsulfoxide, dimethylformamide and tetrahydrofuran and slightly soluble in methanol, ethanol and CHCl<sub>3</sub>. In this regard MFA was similar to the dithiol compounds discussed previously. The synthesis of MFA took a longer time than for the dithiol compounds.

A series of metal compounds of MFA has been prepared. However, precipitates did not form immediately after the mixing of the solution of the ligand with that of the metal salts; the reaction mixtures had to be stirred at least 24 hours to complete the reactions. It is very different from what was observed when aqueous solutions of metal salts were combined with the solutions of the dithiols. In cases with dithiols, precipitates formed immediately after the solutions were mixed and most reactions were complete within an hour or so. Whereas in the cases of the dithiol-metal compounds the yields were at least 60%, reaching 100% in some cases, the product yields were only between 35 and 38% for the MFA-metal compounds.

The MFA-metal compounds were characterized by IR, NMR, Mass spectroscopy and TGA. The compounds were moderately soluble in DMSO and slightly soluble in CHCl<sub>3</sub>. However, no single crystals suitable for X-ray crystallographic study could be grown.

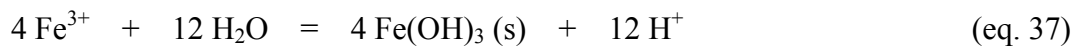
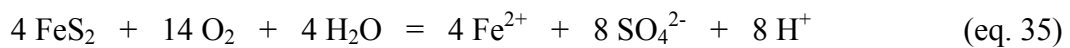
## CHAPTER 7

### Mineral Coating Study

#### 7.1 Overview

Acid mine drainage (AMD) is a serious environmental problem adversely affecting over 23,000 km of surface water in the United States of America.<sup>178</sup> This is prevalent in the areas which are situated close to coal refuse piles that have accumulated as a result of coal cleaning processes. Somerset, Pennsylvania houses many such piles containing hundreds of tons of refuse coal. Among others, pyritic minerals are left in the waste piles on the surface when the coal is taken to market after cleaning. Although several kinds of pyritic minerals are known, only iron pyrite (FeS<sub>2</sub>) is commonly found in association with coal.

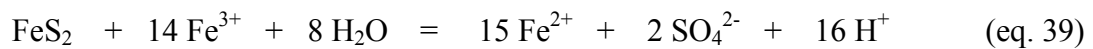
Exposure of pyrites to atmospheric oxygen, moisture, and a group of acidiphilic bacteria capable of oxidizing iron and sulfur gives rise to the formation of sulfuric acid.<sup>179,180</sup> The following equations (35-38) represent the most important chemical-biological processes responsible for the production of acidic water.<sup>179,180</sup>



The overall reaction is:



Pyritic oxidation can also occur in the presence of ferric ions (equation 39):



Every year the U.S. mineral processing industry generates over  $3 \times 10^7$  metric tons of residue and waste that contain hazardous material and other by-products.<sup>181</sup> Many of these by-products are sulfides of problematic elements like Hg, Pb and As. Sulfides are a very important class of minerals because the majority of the metals in the minerals exist in this form.<sup>182</sup> A substantial quantity of these ore minerals is found directly on the surface of the earth, and these surface minerals often release toxic metals into the environment due to changes in climate and through oxidation of the sulfur. Also, minerals found in coal contain sulfides of iron (pyrite,  $\text{FeS}_2$ ), and oxides of aluminum, silicon, calcium, magnesium, and sodium.<sup>183,184</sup> The relative concentrations of the minerals depend mainly on the geological location of the coal seam, and vary from place to place. The leaching of iron and consequent production of sulfuric acid is the basis for acid mine drainage, a global and potentially unending problem. Thus, sulfide minerals are a significant source of environmental contamination since the minerals are continuously made soluble as more and more water passes through the material.

Also, there are between 20,000 and 50,000 abandoned mines in the United States which produce acid mine drainage (AMD) that affect hundreds of water reservoirs.<sup>178,185</sup> On average an abandoned mine necessitates the treatment of approximately 3 million cubic meters of AMD each year.<sup>186</sup>

Many methods have been proposed to control acid mine drainage problems. They include physical methods such as mine sealing, water diversion, improved mining technologies, constructed wetlands and land reclamation.<sup>187</sup> But most generate problematic secondary wastes. In recent years several studies have demonstrated the ability of wetlands to remove acidity, sulfate and iron from moderate acid drainage.<sup>188</sup>

One alternative approach involves destruction of the bacteria responsible for pyrite oxidation.<sup>189</sup> This was achieved by using the anionic surfactant, sodium lauryl sulfate (SLS), as a bactericide for *T. ferrooxidans*.<sup>190</sup> It was observed that all concentrations (25 mg/L, 50 mg/L, 75 mg/L and 100 mg/L) of SLS reduced sulfate production for the first 12 days. However, after 12 days the 75 mg SLS/L stimulated sulfur formation. On the other hand, the 25- and 50-mg SLS/L concentrations reduced sulfate formation over the 26-day period. Use of 100 mg SLS/L completely inhibited sulfate formation for the first 12 days and significantly reduced it for the remaining 14 days. So, use of optimum doses of SLS is very important for the success of this method.

Metal precipitation is the most common AMD mitigation technique. This involves neutralization of the acidic water with lime, limestone, soda ash or caustic soda.<sup>98</sup> This method has several drawbacks including the need for continuous high doses of alkali. It also requires the removal of the secondary wastes including ferric hydroxide. And these techniques involve high costs and low effectiveness.<sup>98</sup>

Chemical methods have also been developed to treat the coal waste directly and prevent metal release. One of the first chemical methods is known as microencapsulation. In microencapsulation potassium hydrogen phosphate ( $K_2HPO_4$ ) or silica-based compounds create a ferric phosphate or ferric silica complex around the pyrite that prevents oxidation.<sup>191,192</sup> Treatment with an oxidizing agent, such as peroxide, is required prior to the introduction of  $K_2HPO_4$  for this method to be effective. In the case of phosphate minerals, formation of ferrous phosphate complexes renders the phosphate source inactive and thus reducing the overall effectiveness of this process.<sup>193</sup>

Another shortcoming of this method is that for optimal results it is necessary to maintain pH values greater than 4.<sup>194</sup>

The oxidation of pyrite can be effectively inhibited by coating it with an inert hydrophobic layer of sodium oleate.<sup>187</sup> It was found that sodium oleate coating on the surface of coal pyrites virtually removed oxidation of pyrite and subsequent acid production both in moist air and aqueous solution.

Pyrite oxidation can be suppressed by coating the coal with a layer of 8-hydroxyquinoline.<sup>195</sup> The 8-hydroxyquinoline combines with the surface  $\text{Fe}^{3+}$  on the pyrite suppressing both chemical and biological oxidation leading to decreased release of metals and acidic water to the environment. However, since the iron 8-hydroxyquinoline complex is decomposed by strong acid, this approach is likely to be effective only for fresh tailing piles before AMD and the associated low pH is generated.<sup>195</sup>

At pH 6 pyrite coating by silicates and lipids can effectively prevent oxidative destruction of pyrites.<sup>196</sup> However, at lower pH environments, which is common in AMD sites, only lipids may be effective since silicate coating cannot be established at  $\text{pH} < 3$ .

It is evident from the above discussion that although some of the methods and technologies including phosphate and silica based coatings are capable of inhibiting acid mine drainage to some extent, they are ineffective at ambient pH ranges and are not capable of controlling high sulfur discharges. So, it was decided to investigate the effectiveness of BDETH<sub>2</sub> or its sodium salt in inhibiting acid mine drainage by coating the surface of coal with it. Since thiol based compounds have a tendency to form iron-sulfur clusters in biological systems, the disodium salt of BDETH<sub>2</sub> will utilize its terminal

sulfur groups to covalently coordinate to the lattice of the ferrous atom in the polyhedral cubic structure of pyrite, thereby prohibiting oxidation of the ferrous atoms. Equation 40 shows the theoretical reaction between BDETNa<sub>2</sub> and an oxidized pyrite surface:<sup>10</sup>



Furthermore, BDETNa<sub>2</sub> is capable of utilizing its aromatic hydrophobic tail to repel water at the pyrite surface to reduce the leaching of other metals present in the coal.

A BDETNa<sub>2</sub> coating is capable of reducing metal leaching significantly in solutions of pH 3.0 and 6.5.<sup>10</sup> It was determined that for the pH 3.0 and 6.5 solutions the leached iron concentrations were 36-fold and 135-fold greater in the uncoated samples than the BDET<sup>2-</sup> samples. The results for the other metals like Cu, Mn, Ni, Zn, Cd, and Pb are similar. CVAA determinations showed that leached mercury in both the coated and uncoated samples fell below the CVAA detection limit. Table 7.1 summarizes the results of reduction in leaching of metals present in coal as a result of BDET-coating.<sup>10</sup>

**Table 7.1.** Heavy metal leaching of coal samples, uncoated and BDET-coated.<sup>10</sup>

Metal	pH	Metal concentration (ppm) 15 days	
		Uncoated	Coated
Fe	3.0	241	6.78
Fe	6.5	131	0.973
Cu	3.0	1.95	0.012
Cu	6.5	0.461	< 0.009 <sup>a</sup>
Mn	3.0	3.62	0.542
Mn	6.5	1.003	0.329
Ni	3.0	1.75	0.997
Ni	6.5	0.573	0.075
Zn	3.0	5.012	0.384
Zn	6.5	3.79	0.877
Pb	3.0	< 0.020 <sup>a</sup>	< 0.020 <sup>a</sup>
Pb	6.5	0.011	< 0.002 <sup>a</sup>
Hg	3.0	< 0.0005 <sup>b</sup>	< 0.0005 <sup>b</sup>
Hg	6.5	0.006	< 0.005 <sup>a</sup>
Cd	3.0	< 0.008 <sup>a</sup>	< 0.008 <sup>a</sup>
Cd	6.5	0.018	< 0.008 <sup>a</sup>

<sup>a</sup> Concentration fell below the ICP-OES method detection limit

<sup>b</sup> Concentration fell below the CVAA method detection limit

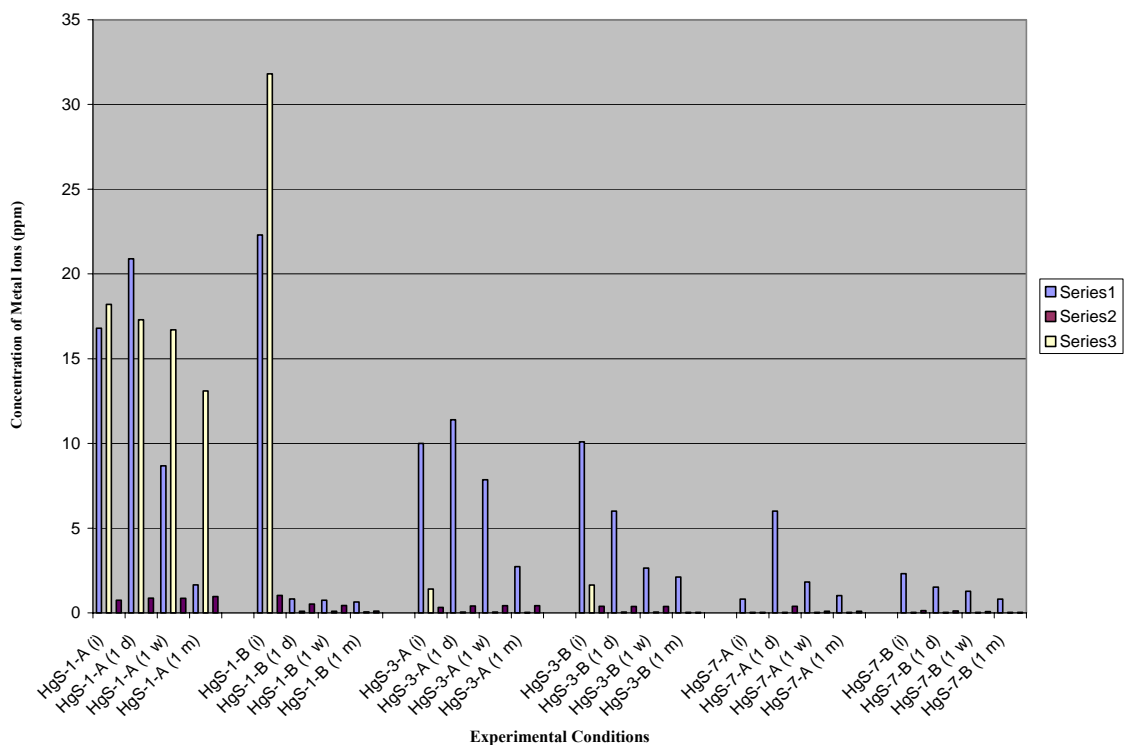
Coating of coal by BDETH<sub>2</sub> effectively reduces metal leaching from coal. It is thought that the BDET coating is covalent. This chapter will describe how BDETH<sub>2</sub> inhibits leaching of the minerals under varying pH over extended periods of time by forming a covalent surface coating to the metals in the mineral.

## 7.2 Results and Discussion

### 7.2.1 Cinnabar

Cinnabar is an extremely insoluble solid<sup>197</sup> with a solubility product of  $10^{-36.8}$ . The presence of high (7 mM) sulfide concentrations at pH > 6 or elemental sulfur can dissolve cinnabar by forming soluble aqueous complexes. The presence of Fe<sup>3+</sup> in acid

mine waters ( $\text{pH} < 2.0$ ) has also been shown to release mercury through oxidation of cinnabar. Nevertheless, the uncoated samples (A) did not leach sufficient Hg to be detected. However, many other metals readily leached from cinnabar, since the mineral is not of 100% purity. As can be seen in Figure 7.1, at pH 1 the dissolved concentration of Fe and Mn show virtually no change in concentration over a one month period in untreated sample A. In coated sample B, Fe drops from a concentration of 31.80 ppm to 0.10 ppm in just 24 hours and reduces down to 0.06 ppm over a one month period. The initial concentration of Mn is reduced by 50%, and continues to drop over the one month period. Al drops over time in uncoated sample A, likely due to oxidation to  $\text{Al}_2(\text{SO}_4)_3$ , while in coated sample B the concentration is immediately reduced to less than 1ppm in 24 hours where it is maintained for the duration of the experiment. At pH 3, again coated sample B is reduced faster than sample A. Uncoated sample A even shows trends in leaching for Al and Mn initially. At pH 7, in uncoated sample A, all three metals have an increase in leaching at the 24 hour period, while in coated sample B, the increase in leaching is greatly inhibited for Al and Mn, while Fe still maintains a reduced concentration. The other metal impurities in the cinnabar leaching experiment are negligible.



i – initial; d – day; w – week; m – month; A – uncoated mineral; B – coated mineral  
 1, 3, 7 – pH values  
 Series 1 – Al; Series 2 – Mn; Series 3 - Fe

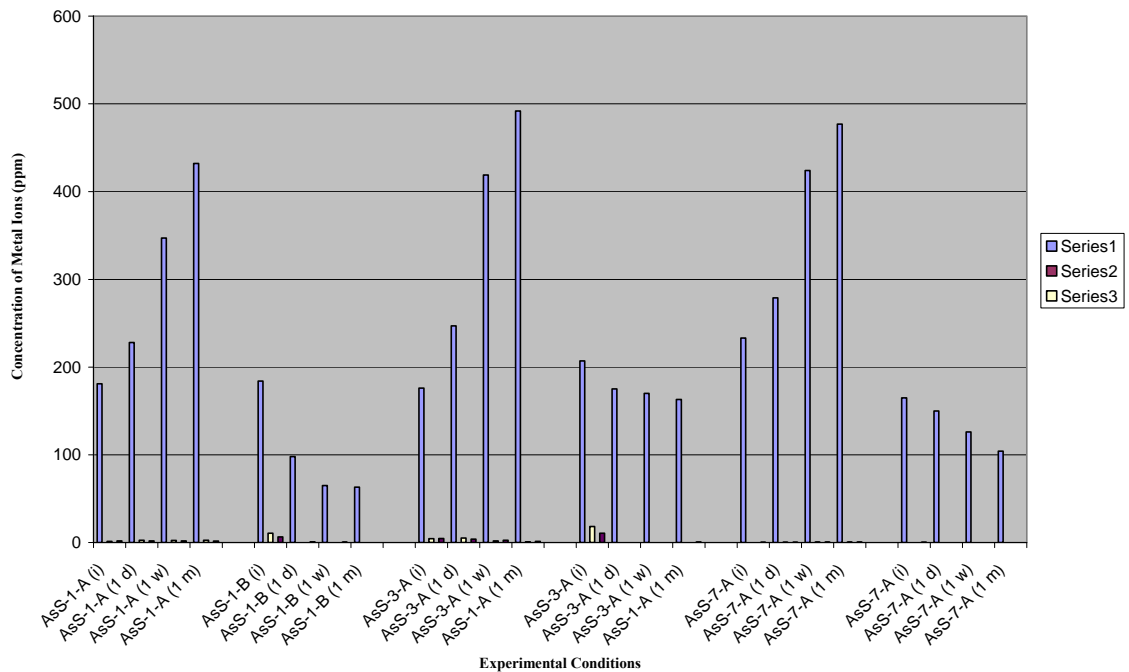
**Figure 7.1.** ICP Analysis for Cinnabar (HgS) Leaching Study

### 7.2.2 Realgar

Realgar, one of many traditional Chinese medicines used to treat carbuncles, boils, insect and snake-bites, etc., is soluble in water.<sup>198</sup> In acid solutions of realgar up to 0.63% As is soluble. Dissolution of realgar produces  $As^{3+}$ .

For  $AsS$ , only three metals, As, Fe, and Mn, are released from the mineral sample (Figure 7.2). At pH 1, uncoated sample A shows an increase in concentration for all three metals over the initial baseline concentration. For coated sample B, Fe and Mn show negligible leaching despite the baseline concentrations of 10.70 ppm (Fe) and 6.43

ppm (Mn) determined prior to coating. The uncoated samples released increased amounts of As throughout the time period at each pH. The coated samples released much less As than the baseline determined before coating. The effect is more dramatic at pH 1 where the leached As is only 50% of the baseline. Interestingly, this level of reduction was not replicated at pH 3, or 7. It is possible that at these pH levels oxidation generates  $\text{H}_2\text{AsO}_3^-$  which can abstract the thiol protons from BDETH<sub>2</sub>, thus making it unavailable for covalent binding with the metal. Thus, the combined effect of the ligand coating and low pH improves leaching inhibition.



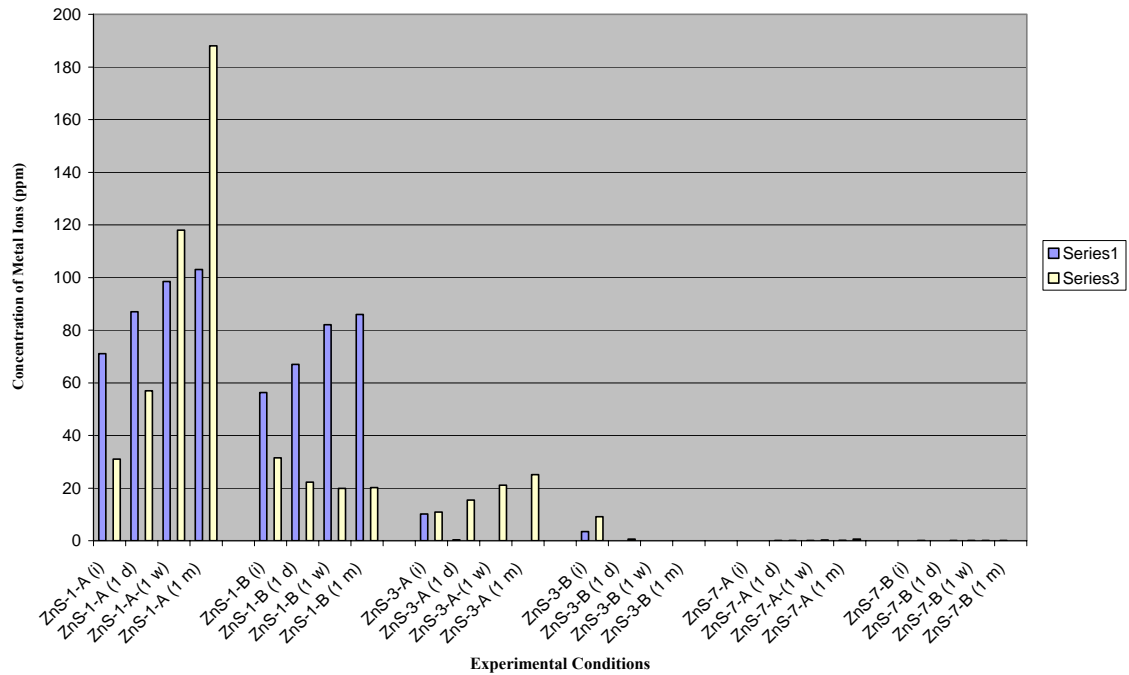
i – initial; d – day; w – week; m – month; A – uncoated mineral; B- coated mineral  
 1, 3, 7 – pH values  
 Series 1- As; Series 2 – Fe; Series 3 - Mn

**Figure 7.2.** ICP Analysis for Realgar (AsS) Leaching Study

### 7.2.3 Sphalerite

ZnS is soluble in acid generating  $\text{Zn}^{2+}$  (aq) and  $\text{H}_2\text{S}$  in the process.<sup>199</sup> Elemental sulfur is formed in the absence of sulfur-oxidizing bacteria. Dissolution of ZnS decreases with increase in pH.

With ZnS, only Fe and Zn show the greatest leaching although the presence of other elements was detected (Figure 7.3). At pH 1, in uncoated sample A, Zn follows the trend of increasing concentration through one month. Coated sample B has a baseline concentration of 31.50 ppm and after coating drops down to ~ 20.00 ppm where it is maintained for the duration of the experiment. In contrast at pH 1, Fe shows continual leaching in uncoated sample A; in coated sample B it continues to leach, but not as significantly. At pH 3, Zn follows the same trend in uncoated sample A, with an increase in leaching from 10.90 ppm to 25.10 ppm, while in coated sample B the level is reduced to 0.63 ppm within 24 hours compared to the baseline concentration of 9.16 ppm. At pH 3 for Fe, both samples show an immediate drop in concentration; this is probably due to a rapid oxidation and precipitation of the Fe as hydrous oxide. As mentioned in chapter 1 at pH > 2, red brown gelatinous hydrous oxides are formed.<sup>13</sup> At pH 7, Zn again shows a steady increase in concentration in uncoated sample A, while coated sample B shows a steady drop to the detectable limit for Zn. Neither uncoated sample A nor coated sample B has enough iron present at pH 7 to make a good comparison.



i – initial; d – day; w – week; m – month; A – uncoated mineral; B – coated mineral.  
 1, 3, 7 – pH values  
 Series 1 – Fe; Series 3 - Zn

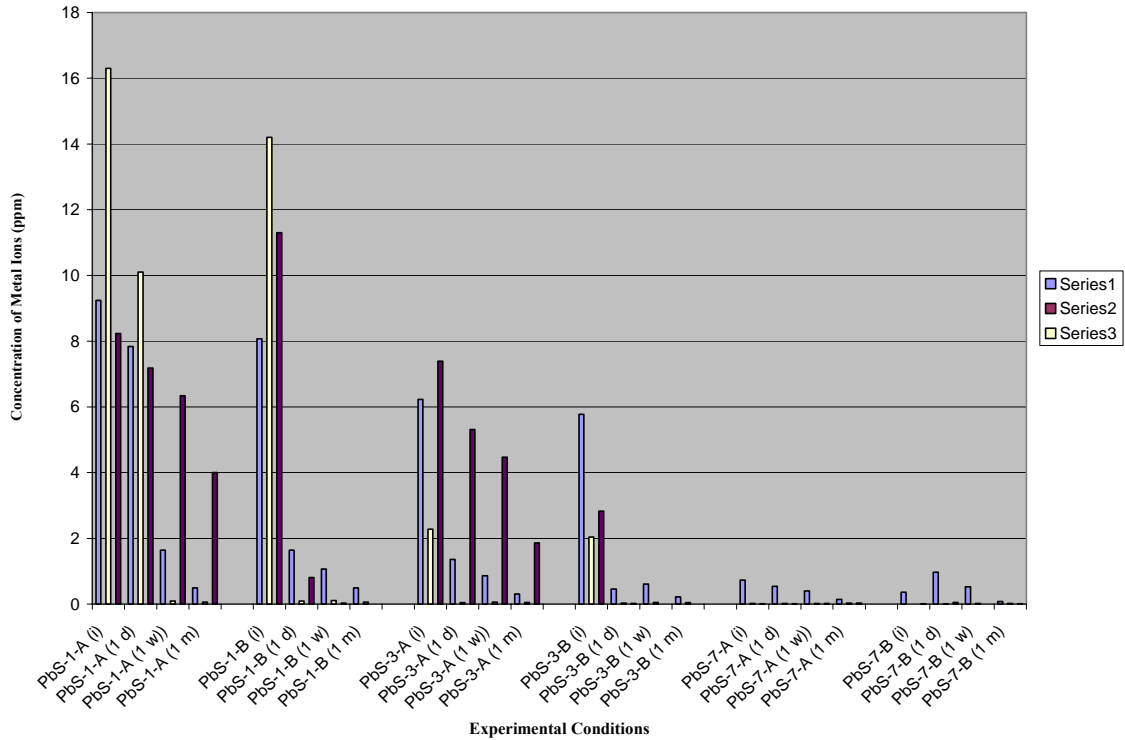
**Figure 7.3.** ICP Analysis for Sphalerite (ZnS) Leaching Study

#### 7.2.4 Galena

The dissolution mechanism of galena (PbS) is not very clear.<sup>200</sup> A wide variety of mechanisms have been proposed for this process in the literature. It has been reported that in acidic aerobic media, dissolution proceeds with the formation of  $H_2SO_4$  and  $Pb^{2+} \cdot 6 H_2O$ .

At pH 1, three metals, Al, Fe, and Pb, showed significant leaching from galena (Figure 7.4). However, their concentration, in both coated and uncoated samples, reduced over time. Reduction in concentration in the uncoated samples may be attributed to the oxidation and precipitation of the metals as oxides and hydroxides. At pH 3, only

Al and Pb showed significant leaching. Again, concentration of the metals, in both coated and uncoated samples, decreased over time, probably due to oxidation and precipitation of the metals. At pH 7, none of the metals showed any significant leaching.



i – initial; d – day; w – week; m – month; A – uncoated mineral; B – coated mineral.  
1, 3, 7 – pH values  
Series 1 – Al; Series 2 – Pb; Series 3 - Fe

**Figure 7.4.** ICP Analysis for Galena (PbS) Leaching Study

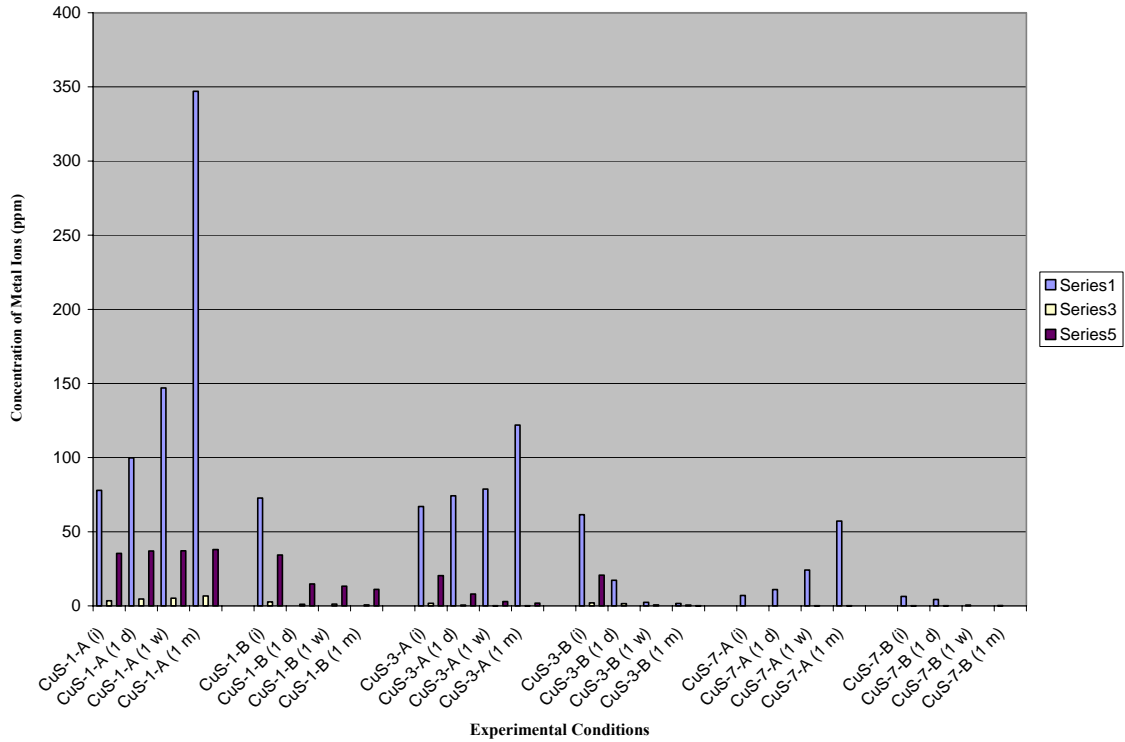
### 7.2.5 Covellite

In acidic media covellite dissolves with the formation of  $\text{Cu}^{2+}(\text{aq})$  and  $\text{HS}^{-}(\text{aq})$ .<sup>201</sup>

Its solubility product  $K_{\text{sp}} = 10^{-21.39}$  at 0.2 M NaCl.

Three metals, Cu, Fe, and Al, show significant leaching from CuS (Figure 7.5). At pH 1 in uncoated sample A, Cu shows a tremendous amount of leaching, starting at 77.90 ppm and after 30 days reaching 347.00 ppm with a consistent increasing trend. It is quite

expected since in acidic environments ( $\text{pH} < 7$ ),  $\text{Cu}^{2+}$  is the dominant species (see chapter 1). In coated sample B, Cu begins at 72.70 ppm and after just 24 hours is reduced to below detectable limits, where it is maintained for the duration of the leaching experiment. Fe and Al have similar profiles, but neither Fe nor Al leach as much in uncoated sample A. In coated sample B, however, concentrations are reduced significantly; Fe drops from 34.30 ppm down to 14.80 ppm after just 24 hours. After one month Fe continued to drop to 11.20 ppm, maintaining that no leaching occurred. Al showed similar results with uncoated sample A, leaching consistently throughout the duration of the study and coated sample B remaining at almost negligible values. At pH 3, the Cu in uncoated sample A increases by a factor of two in just one month, while in coated sample B values begin at 61.60 ppm and drop to 1.70 ppm over one month. At pH 3, the Fe in uncoated sample A gradually drops from 20.50 ppm to 1.85 ppm over one month, may be due to oxidation of Fe forming hydrous oxides. Coated sample B drops from 20.70 ppm to below detectable limits within one month. Al follows the same trend as Fe, with the Al in uncoated sample A gradually dropping from 1.78 ppm to 0.11 ppm over a one month period and no leaching occurring with coated sample B. At pH 7, Cu shows increase in concentration in uncoated sample A over one month, Cu starts at 7.14 ppm and ends at 57.20 ppm. In coated sample B, Cu slowly drops from 6.40 ppm to 0.33 ppm over the 30 day period.



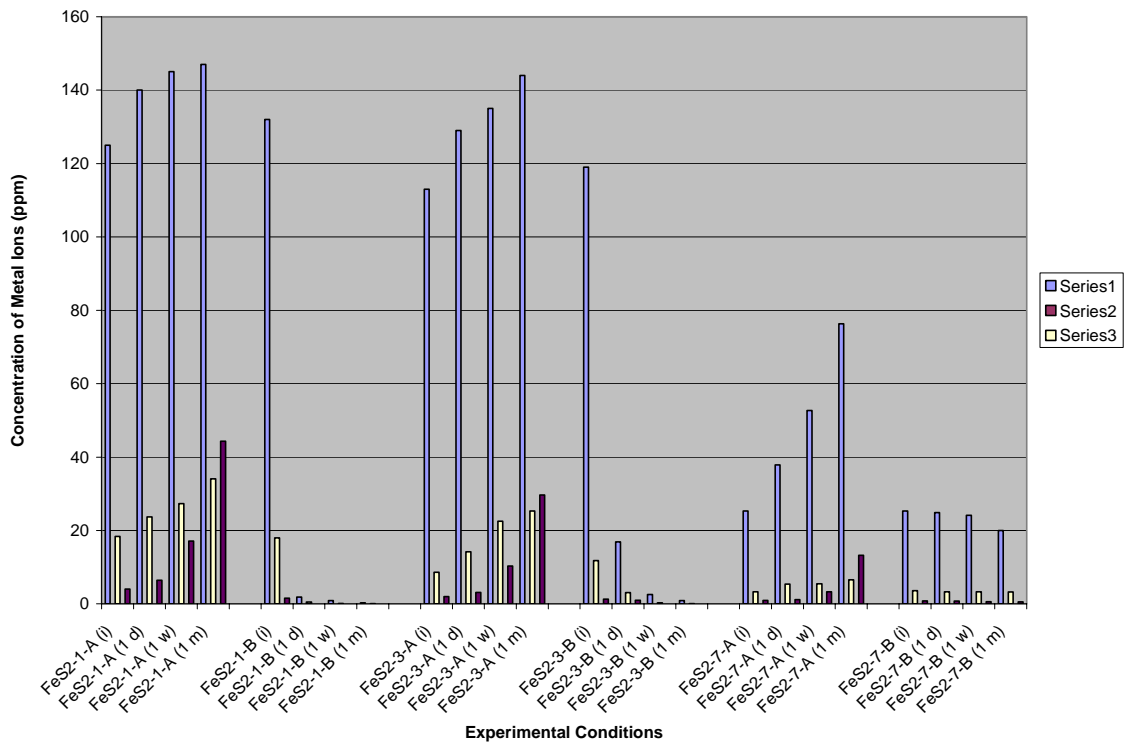
i – initial; d – day; w – week; m – month; A – uncoated mineral; B – coated mineral  
 1, 3, 7 – pH values  
 Series 1 – Cu; Series 3 – Al; Series 5 - Fe  
**Figure 7.5.** ICP Analysis for Covellite (CuS) Leaching Study

### 7.2.6 Pyrite

Pyrite, the most abundant sulfide mineral, accompanies almost all sulfide and many non-sulfide minerals including coal. It oxidizes relatively easily generating  $\text{H}_2\text{SO}_4$  and  $\text{FeSO}_4$ .  $\text{Fe}_2(\text{SO}_4)_3$  is generated if excess  $\text{O}_2$  is available. When pH of the surrounding aqueous phase increases above 5.5, ferric sulfate hydrolyzes to ferric hydroxide.<sup>202</sup> Dissolution of  $\text{FeS}_2$  in the acidic media generates  $\text{Fe}^{2+}(\text{aq})$  and  $\text{H}_2\text{S}$ .

As shown in Figure 7.6, in the leaching study for pyrite ( $\text{FeS}_2$ ), all metals follow the trend of uncoated sample A at all three pHs continuing to leach throughout the duration of the experiment, while with coated sample B no more leaching occurs. Quite

expectedly Fe shows significant leaching at all three pHs. At pH 1, the Fe in uncoated sample A increased from 125.00 ppm to 147.00 ppm over a one month period. But it decreased from 132.00 ppm to 0.30 ppm in coated sample B. At pH 3, the Fe in uncoated sample A increased from 113.00 ppm to 144.00 ppm over a one month period, but in coated sample B it decreased from 119.00 ppm to 0.89 ppm over the same period of time. At pH 7, concentration of Fe in uncoated sample A increased three fold (starting at 25.30 ppm and ending at 76.30 ppm) over a one month period, but in coated sample B it showed a gradual decrease in concentration (starting at 25.30 ppm and ending at 20.00 ppm). The results show that BDETH<sub>2</sub> can effectively reduce and maintain low levels of divalent heavy metal concentrations.



i – initial; d – day; w – week; m – month; A – uncoated mineral; B – coated mineral  
1, 3, 7 – pH values

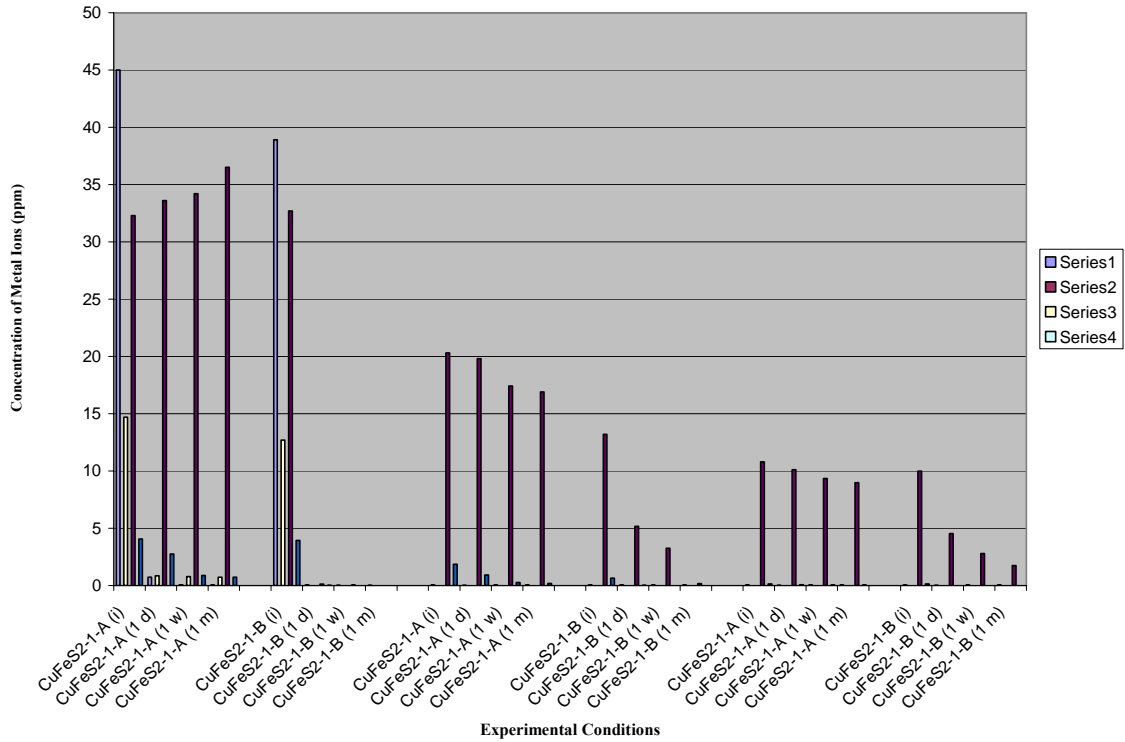
Series 1 – Fe; Series 2 – Cu; Series 3 – Pb

**Figure 7.6.** ICP Analysis for Pyrite (FeS<sub>2</sub>) Leaching Study

### 7.2.7 Chalcopyrite

Dissolution of chalcopyrite generates  $\text{Cu}^{2+}$ ,  $\text{Fe}^{2+}$ ,  $\text{SO}_4^{2-}$ .<sup>203</sup> Elemental sulfur,  $\text{CuS}$  and non-stoichiometric  $\text{FeCuS}_2$  have been reported as solid reaction products.

As is evident from Figure 7.7, chalcopyrite ( $\text{CuFeS}_2$ ) provided different results. There are four significant metals at pH 1 (Cu, Fe, Mn, and Zn), but two metals at pH 3 (Mn and Zn) and only one metal at pH 7 (Mn). At pH 1, with uncoated sample A all four metals begin the process at relatively high concentrations; Cu and Fe readily decrease to much lower values (0.84 and 0.73 ppm respectively) after 24 hours, where they are maintained throughout 30 days (likely due to oxidation, presumably generating  $\text{Fe}^{3+}$  and  $\text{Cu}^{2+}$ ). Concentration of Mn and Zn decreased slowly over 30 days. In coated sample B, all four metals drop to below detectable limits within 24 hours where the concentrations are maintained and no leaching occurs. At pH 3, both Mn and Zn show the same trend with uncoated sample A, slowly decreasing concentration, while in coated sample B, a drastic drop in concentration occurs within just 24 hours. At pH 7, while in uncoated sample A the concentration of Mn decreased slowly over 30 days, in coated sample B it showed a two fold decrease in concentration within 24 hours with further reduction in concentration occurring during the remainder of the experiment.



i – initial; d – day; w – week; m – month; A – uncoated mineral; B – coated mineral  
 1, 3, 7 – pH values  
 Series 1- Fe; Series 2 – Mn; Series 3 – Cu; Series 4 - Zn  
**Figure 7.7.** ICP Analysis for Chalcopyrite (CuFeS<sub>2</sub>) Leaching Study

### 7.3 Examination of the BDET-coated mineral surface

It has been reported in the literature that organosulfur compounds bond strongly to many metal and metal sulfide surfaces and form monolayer films.<sup>204</sup> Formation of oriented monolayers of dialkyl sulfides such as {CH<sub>3</sub>(CH<sub>2</sub>)<sub>15</sub>S}<sub>2</sub> on gold was shown by Nuzzo et al.<sup>205</sup> Subsequent studies characterized various aspects of these monolayers such as the nature of the interaction of organosulfur compounds with gold (dissociative vs molecular adsorption).<sup>206-208</sup> Recently the use of X-ray absorption spectroscopy (XAS) and X-ray photoelectron spectroscopy (XPS) to characterize the chemical interaction between gold surfaces and monolayers derived from a dithiol monomer and

related disulfide-containing polyamides was reported.<sup>8</sup> It was determined that most of the monomeric dithiols adsorb through a single thiol end while the disulfide-containing precursors attach to the surface through both sulfurs.

The nature of the sulfur-metal bonds that formed after the minerals were coated with the dithiol ligand, BDETH<sub>2</sub> were explored by X-ray photoelectron spectroscopy (XPS).

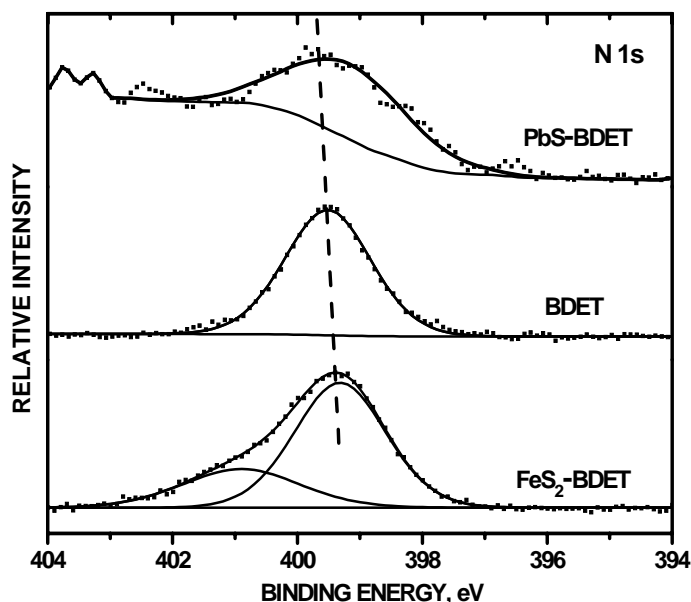
Pyrite and galena were chosen as representative examples of open-shell and closed-shell mineral sulfides to see how changes in electronic configuration in metals affect the binding efficacy with BDETH<sub>2</sub>. This work was conducted in collaboration with Dr. C. Chusuei, Department of Chemistry, Missouri University of Science & Technology, Rolla, Missouri..

A markedly thicker BDET overlayer is observed on the pyrite as compared to galena under identical preparation conditions following the mineral coating procedure. The XPS signals from BDET after binding are more pronounced on the FeS<sub>2</sub> surface than on PbS. The XPS data shows electron density donation from the ligand atoms (N and S) in BDET to the metal in FeS<sub>2</sub>, but not in PbS. The core level BE shifts along with fwhm (full width at half maximum) in parentheses are summarized in Table 7.2. Figure 7.8 shows the N 1s stackplot (emanating from BDET) comparing the two bare mineral surfaces with unbound BDET. The N 1s at 399.5 eV signifies the N atoms in the unbound BDET. Upon interaction with FeS<sub>2</sub>, a second oxidation state appears at 400.9 eV. The higher BE denotes N bonding to the Fe where electron density is extracted from the BDET.

**Table 7.2:** XPS Core Level Shifts of Mineral Sulfides Binding with BDET (eV)

Sample	S 2p				Fe 2p		Pb 4f		N 1s	
PbS- BDET	161.0 (0.99)	162.1 (0.85)	163.4 (1.80)	164.8 (1.80)	.....	.....	137.8 (1.21)	142.7 (1.26)	399.1 (2.23)	.....
PbS	160.7 (1.00)	161.9 (0.99)	.....	.....	.....	.....	137.5 (1.23)	142.4 (1.27)	.....	.....
BDET	161.8 (1.13)	163.3 (1.36)	164.5 (1.46)	.....	.....	.....	.....	.....	399.5 (1.61)	.....
FeS <sub>2</sub> - BDET	163.5 (1.95)	164.8 (2.74)	167.0 (2.99)	.....	706.2 (2.95)	718.6 (4.00)	.....	.....	399.3 (1.72)	400.9 (2.21)
FeS <sub>2</sub>	159.8 (1.51)	162.5 (1.14)	163.7 (0.82)	164.8 (1.92)	706.8 (1.01)	719.7 (1.76)	.....	.....	.....	.....

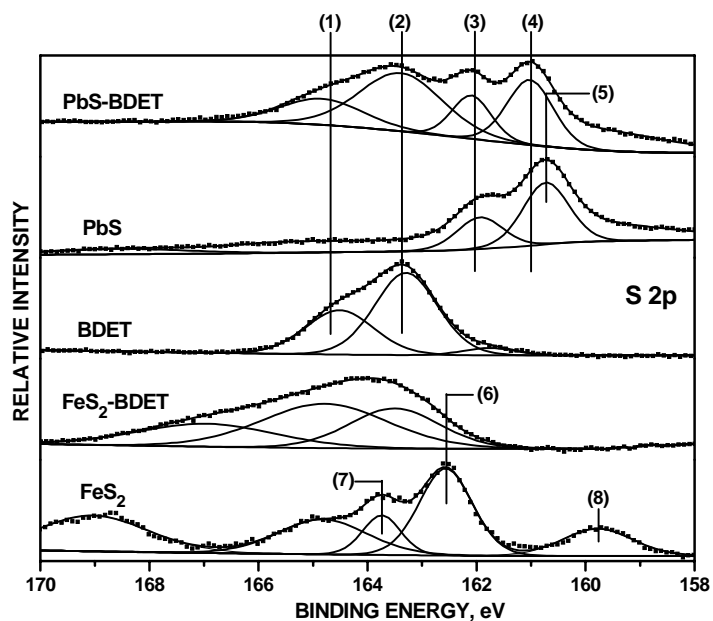
In binding to PbS, the N 1s BE exhibits a  $-0.4$  eV shift indicative of an increase in electron density. Marked differences are especially observed in the S 2p core level indicating binding interactions between the sulfide and BDET that occurs predominantly through binding between the S and metal atoms, but not involving any interaction with the N atoms within BDET. This configuration is reminiscent of sulfur-gold bond formation in monolayers derived from the BDET molecule tethered to gold through two terminal sulfurs, forming surface attached loops.<sup>8,209</sup> Based on the fact that changes were observed only in the S 2p BE positions and virtually no change in the N 1s positions, we postulate that BDET attaches to the metal surfaces through both sulfurs forming a loop.



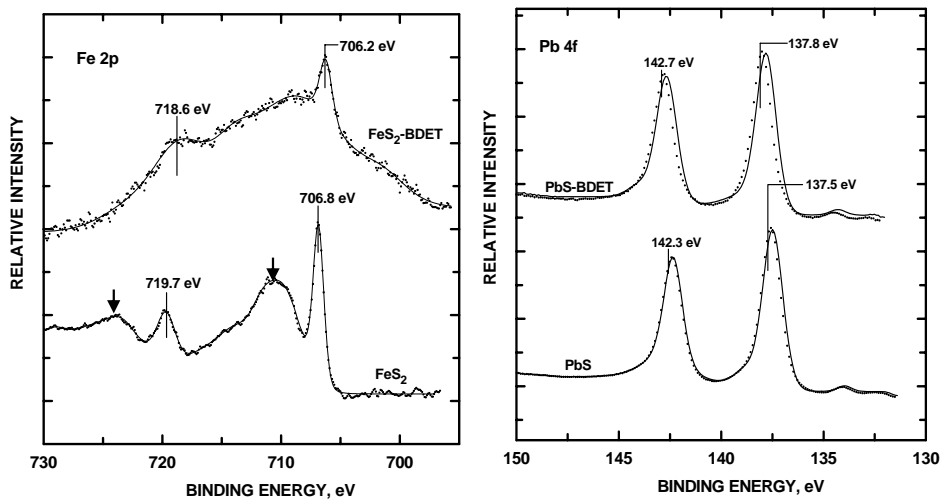
**Figure 7.8.** Photoelectron spectra of the N 1s orbital of (a) BDET ;(b) coordinated to PbS and (c) coordinated to FeS<sub>2</sub>.

Figure 7.9 shows the S 2p core levels of the coated (FeS<sub>2</sub>-BDET, PbS-BDET) and uncoated (FeS<sub>2</sub>, PbS) mineral sulfide surfaces and uncomplexed BDET. In Figure 7.9, peaks (1) and (2) at S 2p BE at 164.6 and 163.4 eV denoting oxidation states of S atoms within the BDET uncomplexed ligand are in excellent agreement with binding energies reported in the literature; positions at 163.4 and 164.6 eV correspond to the S 2p<sub>3/2</sub> and 2p<sub>1/2</sub> spin orbit coupled peak for the S in BDET,<sup>8,210</sup> at a BE position typical of dithiols.<sup>211,212</sup> Likewise, peaks (3) and (4) in the PbS-BDET, at 161.0 and 162.1 eV, are the S 2p<sub>3/2</sub> and 2p<sub>1/2</sub> orbits that match BE values observed in the literature for PbS.<sup>213</sup> The S 2p spectrum of the PbS-BDET reveals contributions of all of the states, peaks (1) - (4), emanating from both PbS and BDET. Furthermore, since peaks (1)- (4) were all observed for the PbS-BDET complex, it would appear that BDET allowed photoelectrons from the underlying PbS to penetrate through the BDET coating. Peaks (3) and (4) from

PbS was clearly observable due to either: (i) the fact that the BDET coating was thin (less than  $\sim 50$  Å-thick) and/or (ii) BDET covered the underlying PbS in a non-contiguous manner, e.g. forming islands rather than a complete monolayer. The observation of the PbS through the BDET coating suggests that the coating binds weakly to PbS. In addition, a BE shift is observed from S 2p = 160.7 and 161.9 eV in PbS to lower BEs at 161.0 and 162.1 eV in PbS-BDET, indicating an increase in electron density to the S atoms in PbS upon coordination with BDET, suggestive of electron density being withdrawn from the Pb. This interpretation is supported by the corresponding increase in BE of the Pb 4f<sub>7/2</sub> and 4f<sub>5/2</sub> orbitals from 137.5 and 142.4 eV of the unbound PbS to 137.8 and 142.7 eV in the PbS-BDET complex, respectively (Figure 7.10; right-hand panel). Furthermore, the S 2p oxidation states of PbS at 163.3 and 164.5 eV increased to 163.4 and 164.8 eV after binding to BDET in forming the BDET-PbS complex. Hence, when BDET binds to PbS, electron density is withdrawn from the metal.



**Figure 7.9.** Photoelectron spectra of the S 2p orbital of fresh (a) PbS; (b) FeS<sub>2</sub>; (c) unbound BDET; and the complexes of (d) PbS-BDET; and (e) FeS<sub>2</sub>-BDET.



**Figure 7.10.** Photoelectron spectra of (a) Fe 2p orbitals (left-hand panel) bound and unbound to BDET; and (b) the Pb 4f orbitals (right-hand panel).

In contrast, BDET binds FeS<sub>2</sub> more completely. The contribution of peaks (6)-(8) from the underlying FeS<sub>2</sub> is not apparent in the FeS<sub>2</sub>-BDET peak envelope. Intensity from peak (7) may be contributing to the FeS<sub>2</sub>-BDET lineshape but is not clearly resolved. The overall S 2p lineshape of the FeS<sub>2</sub>-BDET complex is similar to that of the uncomplexed BDET (Figure 7.9), which is due to more complete coverage of BDET to the FeS<sub>2</sub> as compared to PbS. The markedly greater BDET coverage and binding to the pyrite is a result of electron density donation from the S atoms in BDET to the open-shell Fe 2p electronic configuration. In contrast, PbS has a closed-shell configuration that hampers the donation to the metal; hence, the opposite trend of electron withdrawal from the metal is observed (*vide supra*). This conclusion is supported by the observed core level shifts of the Fe 2p orbitals comparing the complexed and uncomplexed pyrite powders. The BE peak positions at 706.8 and 719.7 eV of the bare pyrite surface match with those reported in the literature.<sup>214,215</sup> A decrease in electron density in the Fe 2p orbitals after binding with BDET is evident (Figure 7.10; left-hand panel) as the Fe 2p<sub>3/2</sub> and 2p<sub>1/2</sub> orbitals shift from 706.8 and 719.7 eV to 706.2 and 718.6 eV, respectively, after complexation to form FeS<sub>2</sub>-BDET. Shake-up satellite features in transition metal 2p orbitals typically arise from unpaired 3d electrons.<sup>216</sup> The features arise from unpaired electrons excited to a discrete state after relaxation during the photoionization process (i.e. final state effects). Pyrite, in which the Fe has a formal +2 charge and is tetrahedrally coordinated to the S atoms, exhibits an open shell electronic configuration. The shake-up satellite features in the Fe 2p at 716.2 and 709.5 eV (denoted by the arrows) of the pyrite diminishes greatly after complexation with BDET, indicating an

open-shell to closed-shell transition as a result of the complexation, i.e. as electron density is being donated from the S to the Fe (Figure 7.10: left-hand panel).

It is likely that electron density donation (from S and N in the BDET) results in a closed-shell configuration, leading to reduced shake-up. It implies that electron density from the BDET sulfur is transferred to the Fe in the pyrite structure. The attachment of various groups to Fe varies the relative intensities of the shake-up satellites depending upon the ligand-to-metal or metal-to-ligand electronic transfer.<sup>217</sup> This interpretation is consistent with the Fe 2p BE decrease and S 2p BE increase after complexation as well as the disappearance of the satellites as FeS<sub>2</sub> coordinates with BDET. In contrast, PbS, having a closed-shell electronic configuration<sup>218</sup> (evident by the absence of shake-up satellites in the Pb 4f orbitals) does not exhibit any electron density increase after complexation with BDET (Figure 7.10: right-hand panel). A slight increase in the S 2p BE is also observed. Corresponding shifts in the S 2p peaks for FeS<sub>2</sub> could not be observed due to greater attenuation by the S atoms in BDET. The greater attenuation further signifies greater binding interaction of BDET to FeS<sub>2</sub> relative to PbS at equivalent BDET-mineral sulfide complex formations.

## 7.4 Experimental

### 7.4.1 General considerations

All reagents were purchased from commercial sources and were used as received. BDETH<sub>2</sub> was synthesized following the procedure outlined in Chapter 2. The minerals, cinnabar (HgS), pyrite (FeS<sub>2</sub>), chalcopyrite (CuFeS<sub>2</sub>), covellite (CuS), galena (PbS),

realgar (AsS), and sphalerite (ZnS), were obtained from D. J. Minerals in Butte, MT and were between 79 - 87% pure.

#### 7.4.2 Sample Preparation

Each sample (10 cm x 7 cm x 7 cm) was rinsed with distilled water to remove any excess residue and allowed to dry. They were broken up with a sledge hammer and BICO Chipmunk Jaw Crusher, which reduced their size to approximately 6 mm or less. They were then pulverized to a size of 60 mesh using a BICO Vibratory Ring Pulverizer. An amount of 20 g of finely powdered sulfide-mineral was added to three 250 mL beakers containing 150 mL of distilled water. Each beaker contained a solution with a different pH, acidified using trace metal grade hydrochloric acid. Each test was carried out in duplicate and averaged (Figures 7.1 – 7.7).

After each mineral was placed into the appropriately acidified water, a sample was taken at three days to determine initial baseline concentration. The samples were studied in two categories: uncoated samples (A) and samples (B) that were coated with calculated amounts of BDETH<sub>2</sub> based on the concentration of divalent heavy metals present in solution found in the initial ICP analysis.

The contents of the beakers were stirred for the duration of the experiment.

The beakers were kept open to the air at all times in an effort to mimic the natural environment as closely as possible. The experiments were performed at room temperature. 10 mL aliquots of samples from each container were filtered through Nalgene-Syringe filters (25 mm, 0.2 µm pore size) purchased from Fisher Scientific.

Samples were prepared separately for the different time periods meaning that aliquots were drawn out from different beakers at different times.

#### 7.4.2.1 Coating of the Minerals

Weighed amounts of each powdered mineral were put in Erlenmeyer flasks with 100 mL of DI H<sub>2</sub>O in each of them followed by the addition of stoichiometric amounts of BDETH<sub>2</sub>. The contents of the flask were stirred for 24 hours after which the solids were filtered and dried in the air for 24 hours.

#### 7.4.3 Analytical Techniques

Metal concentrations, except for mercury, were determined using a Varian Vista-Pro CCD Simultaneous Inductively Coupled Argon Plasma Optical Emission Spectrometer (ICP-OES). Mercury levels of the samples were determined using cold vapor atomic absorption spectrophotometry (CVAAS) on a CETAC Technologies M-6000A Mercury Analyzer, using EPA methods.<sup>166</sup> Digestion of the samples was performed following EPA methods (7470) for mercury detection in liquid waste.

X-ray photoelectron spectra (XPS) were acquired at the University of Missouri-Rolla using an ion-pumped Kraton Axis 165 system with a hemispherical analyzer. The base pressure of the chamber was  $\sim 1 \times 10^{-10}$  Torr. A Mg K<sub>α</sub> anode ( $h\nu = 1253.6$  eV) was used which was operating at 15 kV and 300 Watts and had a pass energy of 20 eV for high resolution scans. The powder samples were mounted using double-sided tape (Scotch 3M) and outgassed in a load-lock prior to introduction into the analysis chamber. The C 1s core level at 284.7 eV was used for binding energy correction due to

charging.<sup>219,220</sup> A 70:30 Gaussian: Lorentzian lineshape and a Shirley background subtraction were used to curvefit the spectra.<sup>221</sup>

## 7.5 Conclusions

By continuously monitoring the aqueous effluents by ICP-OES it was determined that the BDETH<sub>2</sub> ligand adheres to the metals in the sulfide mineral to prevent leaching. There was no free ligand causing metal precipitation. An important discovery was the fact that BDETH<sub>2</sub> could be administered by dissolution in EtOH and adding this solution to the leaching solution. This greatly simplifies the procedure as well as dramatically reducing the material cost.

Sulfides are a very important class of minerals, primarily because they contain some of the most toxic heavy metals available. Metal leaching from these minerals in water is caused by acid dissolution of the metal ions. It has been shown previously that metal ions in solution are bound by BDETH<sub>2</sub> to produce insoluble non-leaching precipitates.

In the present study the affinity of BDETH<sub>2</sub> for heavy metals was used to bind the metals at the mineral surface. This has been corroborated by the study on the stability of BDET-metal compounds. The results of XPS study confirmed that covalent bonds are formed between the S atoms of BDETH<sub>2</sub> and the metal ions.

Enhanced binding of BDET to the mineral sulfide is accompanied by electron donation to the metal as opposed to extraction from it. The results suggest that BDET interactions with mineral sulfides having an open shell electronic configuration (opposed to a closed one) would result in an enhanced coating of the mineral surface, and hence

improved heavy metal leaching remediation ability. Electronic structure may be an important variable for evaluating BDET's binding efficacy to a host of mineral sulfide systems, e.g. covellite (CuS) having an open shell versus chalcocite (Cu<sub>2</sub>S) having a closed shell configuration.

For the soft metal minerals where there is appreciable natural leaching the BDET has a dramatic effect. For the hard metal-containing minerals such as ZnS prevention is moderate to satisfactory. This proves the hypothesis that BDET containing soft thiol groups form covalent bonds with the soft metals at the surface of the minerals.

It may be possible to prevent AMD through the binding of the metals in the coal which contains among others pyrite (FeS<sub>2</sub>), marcasite (FeS<sub>2</sub>), chalcopyrite (CuFeS<sub>2</sub>), galena (PbS) and sphalerite (ZnS). This could be achieved by spraying BDET onto dry mine walls before allowing the mine to fill with water. This technique will also be effective in preventing acid mine drainage from 'coal-slurry deposits' or CSDs. It is known that CSDs contain significant quantities of pyrite.

BDET has the unique characteristic of being insoluble in water but capable of being added to water as a solution in EtOH. Thus, BDET will not only bind the soft metals in the coal, it will also provide a water insoluble coating on the coal. Figure 7.11 illustrates the covalent binding of BDET<sup>2-</sup> with Fe present in pyrite.

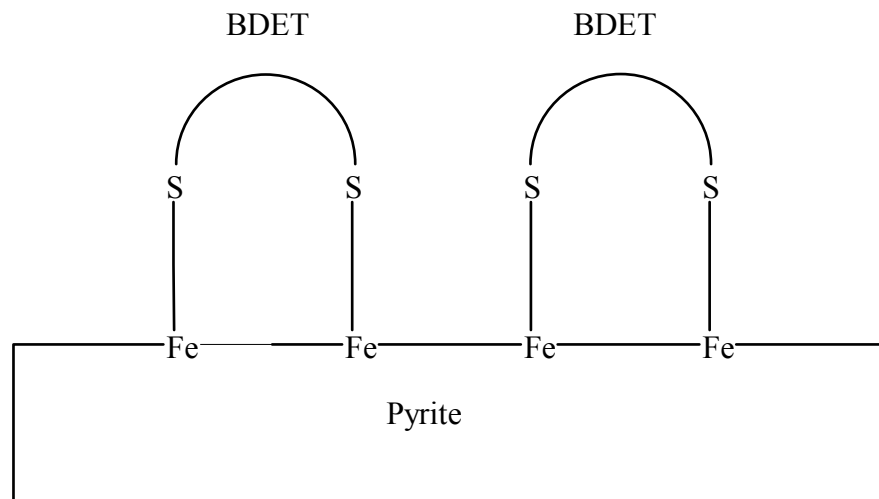


**Figure 7.11.** Postulated covalent bonding between BDET<sup>2-</sup> and FeS<sub>2</sub>

## CHAPTER 8

### Conclusions and Suggestions for Future Work

#### 8.1 Conclusions

Benzene-1,3-diamidoethanethiol (BDETH<sub>2</sub>), a ligand capable of binding divalent heavy metals efficiently, has been synthesized and characterized. Its application in binding divalent heavy metals in industrial effluents, sulfide minerals, coals, etc. has been demonstrated. A wide range of metal compounds including BDETLi<sub>2</sub>, BDETNa<sub>2</sub>, BDETK<sub>2</sub>, BDETMg, BDETFe, BDETCO, BDETNi, BDETCu, BDETAsOH, BDETSn, BDETCd, BDETHg, and BDETPb has been synthesized and characterized. The metal compounds of BDET have sharp melting points indicating that they are pure. Thermogravimetric analysis indicated that the compounds are thermally stable and do not contain any water molecule in the compounds. Solubility studies indicated that they are insoluble in water and other common laboratory solvents indicating that the compounds may be polymeric. Leaching studies performed with BDET-Cd, BDET-Hg and BDET-Pb indicate that they are very stable to harsh acidic conditions.

Attempts to derivatize BDET-Metal compounds by combining them with *n*-BuLi, C<sub>2</sub>H<sub>5</sub>MgBr and Bu<sub>2</sub>Mg failed. Also, efforts to alkylaluminate the BDET-Metal compounds by combining them with Al(CH<sub>3</sub>)<sub>3</sub> was not successful. These indicate that the N-H groups in the BDET-Metal compounds have low acidity and the C=O groups possess low Lewis basicity.

A new cyclic compound, 1,3-bis(4,5-dihydrothiazolo)benzene resulted when BDETH<sub>2</sub> was combined with AlMe<sub>3</sub> in toluene under reflux. This reaction establishes the fact that presence of SH and NH functionalities in BDETH<sub>2</sub> gave rise to amino-thiol cyclization.

A mineral coating study indicated that BDETH<sub>2</sub> can prevent leaching of metals from sulfur-containing minerals. Surface study carried out to examine the metal-sulfur bonding on BDET-coated minerals indicated the presence of covalent bonding between BDET and the mineral surfaces.

Another dithiol compound, namely, *N,N'*-bis(2-mercaptoethyl)oxalamide (MOA), has been synthesized and characterized. Three metal compounds of MOA have also been synthesized and characterized. This re-emphasises the fact that dithiol compounds are very effective in binding heavy metals and thus are important tools for heavy metal remediation. Efforts made to solubilize the MOA-metal compounds did not succeed as well. The products of the reactions are, as in the case with BDET-M compounds, unreacted MOA-M compounds.

A series of metal compounds of dithiothreitol (DTT), a water-soluble dithiol compound, has been prepared and characterized. This, again, proves that dithiol compounds may be used for removing heavy metals from the environment. However, it should be mentioned here that DTT is very sensitive to air and light. Also, this compound is relatively expensive. These facts will limit its use in heavy metal remediation.

A monothiol compound, *N*-mercaptoethylfuroylamide (MFA), has been synthesized and characterized. Three main group heavy metal compounds have also been prepared and characterized. It demonstrated that a bidentate chelate was not necessary to precipitate heavy metals from water. The ligand or its metal compounds are not soluble in water. The metal compounds, however, are moderately soluble in dimethylsulfoxide and dimethylformamide and slightly soluble in chloroform.

The results of study with MOA, DTT, and MFA demonstrated that BDET is not unique in its ability to form water insoluble precipitates. The insolubility was due to metal-sulfur bonding and the likely formation of a polymeric compound with bridging S-M  $\cdots$ S groups.

A complete understanding of the chemistry of the metal-ligand precipitates has been attained. This information can now be used for industrial application of precipitating different metals in the water environment.

## 8.2 Future Work

Since attempts to synthesize a water-soluble analogue of BDETH<sub>2</sub> did not prove successful, future work should be directed at preparing this elusive compound. A different methodology should be employed to successfully achieve this goal. It seems likely that the desired product may be obtained by converting the hydroxyl group into an ester group, and then treating it with cysteamine hydrochloride since it is assumed that the presence of the hydroxyl group is hindering the reaction.

Renewed efforts should be undertaken to metallate BDETH<sub>2</sub> and its metal compounds by changing the reaction conditions. However, the task seems to be a huge one since attempts to run the reactions using both polar and non-polar solvents failed. Also, attempts to run them at room temperature and under reflux failed.

The coordination environment of Hg in BDET-Hg has been successfully established using XAFS. It will be very exciting if the coordination environment of the metals in the other BDET-M compounds, especially the main group and transition metal elements, are also found out using XAFS. Although XAFS can be used to identify any

element in the periodic table, its use has so far been limited to the heavier ones. Single crystal X-ray analysis will not be possible since the compounds are insoluble in common laboratory solvents.

It will be very interesting to find out how BDETH<sub>2</sub> reacts with other divalent metals like Ca, Sr, Ba, Zn, etc. Although Ca, Sr and Ba are not considered environmental hazards, investigation of the reactivity of BDETH<sub>2</sub> towards these elements will help to understand the chemistry of BDETH<sub>2</sub> better. Therefore, efforts should be made to prepare other metal compounds of BDETH<sub>2</sub> and fully characterize them.

Although industrial applications for precipitating different metals such as Fe, Co, Ni, Pb, Zn, Hg, As can now be addressed (for internal water treatment) toxicity data is needed for remediation applications. So, efforts should be made to collect toxicity data on the BDET-Metal compounds.

Future endeavours should be directed at growing crystals of *N,N'*-bis(2-mercaptoethyl)oxalamide (MOA) suitable for single crystal X-ray spectroscopy since it has been found that MOA is moderately soluble in THF and slightly soluble in CH<sub>3</sub>OH and C<sub>2</sub>H<sub>5</sub>OH.

Investigations should be carried out to find out the efficacy of MOA in binding heavy metals in industrial effluents, and in preventing acid mine drainage. Although MOA and BDETH<sub>2</sub> share common features in their chemical behaviors, synthesis of MOA has proven to be less troublesome than BDETH<sub>2</sub>. It is likely that industrial production of MOA will be cheaper than that of BDETH<sub>2</sub>.

Efforts should be continued to grow crystals of MFA and its metal compounds so that their structures can be established unambiguously. Investigations may be carried out

to find out if MFA is capable of binding heavy metals in industrial effluents or in the aqueous environments. Attempts may also be made to synthesize water-soluble monothiol compounds.

## References

1. Matlock, M. M.; Howerton, B. S.; Atwood, D. A. *J. Hazard. Mater.* **2001**, *B84*, 73.
2. Matlock, M. M.; Howerton, B. S.; van Aelstyn, M. A.; Henke, K. R.; Atwood, D. A. *Water Res.* **2003**, *37*, 579.
3. Matlock, M. M.; Howerton, B. S.; van Aelstyn, M. A.; Nordstrom, F. L.; Atwood, D. A. *Environ. Sci. Technol.* **2002**, *36*, 1636.
4. Matlock, M. M.; Howerton, B. S.; Robertson, J. D.; Atwood, D. A. *Ind. Eng. Chem. Res.* **2002**, *41*, 5278.
5. Matlock, M. M.; Howerton, B. S.; Atwood, D. A. *Water Res.* **2002**, *36*, 4757.
6. Matlock, M. M.; Howerton, B. S.; Atwood, D. A. *Adv. Environ. Res.* **2003**, *7*, 347.
7. Matlock, M. M.; Howerton, B. S.; Atwood, D. A. *Ind. Eng. Chem. Res.* **2002**, *41*, 1579.
8. Vance, A. L.; Wiley, T. M.; Nelson, A. J.; van Buuren, T.; Bostedt, C.; Terminello, L. J.; Fox, G. A. *Langmuir* **2002**, *18*, 8123-8125
9. Matlock, M. M.; Howerton, B. S.; Atwood, D. A. (University of Kentucky, Lexington, KY) . U.S. Patent No. 6,586, 600; July 1, 2003.
10. Matlock, M. M.; Howerton, B. S.; Atwood, D. A. *Adv. Environ. Res.* **2003**, *7*, 495-501.
11. Bunce, N. *Environmental Chemistry*, 2<sup>nd</sup> edition; Wuerz Publishing Ltd.:Winnipeg, Canada, 1994.

12. (a) Pearson, R. G. *J. Am. Chem. Soc.* **1963**, 85, 3553. (b). Pearson, R. G.; Songstad, J. *J. Am. Chem. Soc.* **1967**, 89, 1827-1836.
13. Spiro, G.T.; Stigliani, W.M. *Chemistry of the Environment*, 2nd ed.; Prentice-Hall, Inc.: Upper Saddle River, NJ, 2003.
14. King, R. B. *Inorganic Chemistry of Main Group Elements*; Wiley-VCH: New York, 1995.
15. Huang, R.; Lee, T. *Toxicol. Appl. Pharmacol.* **1996**, 136, 243-249
16. Patterson, T. J.; Ngo, M.; Aronov, P. A.; Reznikova, T. V.; Green, P. G.; Rice, R. H. *Chem. Res. Toxicol.* **2003**, 16, 1624-1631.
17. Morrison, G. M. P.; Batley, G. E.; Florence, T. M. *Chem. Britain* **1989**, 791-796.
18. Jones-Lee, A.; Lee, F. G. *Remediation* **2005**, 33-41.
19. Stumm, W.; Morgan, J. J. *Aquatic Chemistry: Chemical Equilibria and Rates in Natural Waters*; Wiley: New York, 1996.
20. Cotton, A. F.; Wilkinson, G.; Murillo, C. A.; Bochmann, M. *Advanced Inorganic Chemistry*, 6<sup>th</sup> edition; John Wiley & Sons, Inc., 1999.
21. Rashid, M. A.; Leonard, J. D. *Chem. Geol.* **1973**, 11, 89-97.
22. Manahan, S. E. *Environmental Chemistry*, 7<sup>th</sup> edition; CRC Press LLC., 2000.
23. Belliveau, B. H.; Trevors, J. T. *Appl. Organomet. Chem.* **1989**, 3, 283-294.
24. Rabenstein, D. *Acc. Chem. Res.* **1978**, 11, 100-107.
25. D'Itri, P. A.; D'Itri, F. D. *Mercury Contamination: A Human Tragedy*; Wiley: New York, 1977.

26. Driscoll, C. T.; Yan, C.; Schofield, C. L.; Munson, R.; Holsapple, J. *Environ. Sci. Technol.* **1994**, *28*, 136A-143A.
27. Snoeyink, V. L.; Jenkins, D. *Water Chemistry*; John Wiley and Sons: New York, 1980.
28. <http://www.lef.org/protocols/prtcl-156.shtml>
29. Liu, C.; Huang, Y.; Naismith, N.; Economy, J. *Environ. Sci. Technol.* **2003**, *37*, 4261.
30. US Environmental Protection Agency, Mercury Study Report to Congress: Overview. <http://www.epa.gov/airprog/oar/mercover.html> (accessed June 2003).
31. Hutchinson, A. R.; Atwood, D. A. *J. Chem. Crystallogr.* **2003**, *33*, 631.
32. Patterson, J.; Gasca, E.; Wang, Y. *Water Sci. Technol.* **1994**, *29*, 275.
33. Yu, Q.; Matheickal, J.; Yin, P.; Kaewsarn, P. *Water Res.* **1999**, *33*, 1534.
34. Smuleac, V.; Butterfield, D. A.; Sikdar, S. K.; Varma, R. S.; Bhattacharyya, D. *J. Membr. Sci.* **2005**, *251*, 169.
35. Roundhill, D. M. *J. Chem. Educ.* **2004**, *81*, 275.
36. Salt, D. E.; Blaylock, M.; Kumar, N. P. B. A.; Dushenkov, V.; Ensley, B. D.; Chet, I.; Raskin, I. *Bio/technology* **1995**, 468-474.
37. Kumar, N. P. B. A.; Dushenkov, V.; Motto, H.; Raskin, I. *Environ. Sci. Technol.* **1995**, *29*, 1232-1235.
38. (a) Huang, J. W.; Chen, J.; Berti, W. R.; Cunningham, S. D. *Environ. Sci. Technol.* **1997**, *31*, 800-805. (b) Blaylock, M. J.; Salt, D. E.; Dushenkov, S.;

- Zakharova, O.; Gussman, C.; Kapulnikov, Y.; Ensley, B.D.; Raskin, I. *Environ. Sci. Technol.* **1997**, *31*, 860-865.
39. Dushenkov, V.; Kumar, N. P. B. A.; Motto, H.; Raskin, I. *Environ. Sci. Technol.* **1995**, *29*, 1239-1245.
40. Meagher, R. B. *Curr. Opin. Plant Biol.* **2000**, *18*, 23.
41. Macek, T.; Mackova, M.; Kas, J. *Biotechnol. Adv.* **2000**, *18*, 23.
42. Riddle, S. G.; Tran, H. H.; Dewitt, J. G.; Andrews, J. C. *Environ. Sci. Technol.* **2002**, *36*, 1965.
43. Halberg, R. O.; Larsson, C. *Aquat. Geochem.* **1999**, *5*, 269.
44. Rugh, C. L. *In Vitro Cell Dev. Biol. Plant* **2001**, *37*, 321.
45. Pilon-Smits, E.; Pilon, M. *Trends Plant Sci.* **2000**, *5*, 235.
46. Nelson, E. A.; Specht, W. L.; Knox, A. S. *Engineering in Life Sciences* **2006**, *6*, 26-30.
47. Jindal, R.; Samorkhom, N. *Practical Periodical of Hazardous, Toxic, and Radioactive Waste Management* **2005**, *9*, 173-178.
48. Jianguo, L.; Yuan, D.; Hai, X.; Deke, W.; Jiankuan, X. *J. Hazard. Mater.* **2007**, *147*, 947-953.
49. von Canstein, H.; Li, Y.; Timmis, K. N.; Deckwer, W. D.; Wagner-Dobler, I. *Appl. Environ. Microbiol.* **1999**, *65*, 5279.
50. Wagner-Dobler, I. *Appl. Microbiol. Biotechnol.* **2003**, *62*, 124.
51. Pan-Hou, H.; Kiyono, M.; Kawase, T.; Omura, T.; Endo, G. *Biol. Pharm. Bull.* **2001**, *24*, 1423.

52. Chen, S.; Kim, E.; Shuler, M. L.; Wilson, D. B. *Biotechnol. Prog.* **1998**, *14*, 667.
53. Pérez-Rama, M.; Alonso, J. A.; Lopez, C. H.; Vaamonde, E. T. *Bioresour. Technol.* **2002**, *84*, 265-270.
54. Matsunga, T.; Takeyama, H.; Nakao, T.; Yamazawa, A. *J. Biotechnol.* **1999**, *70*, 33-38.
55. Huang, C. P.; Blankenship, D.W. *Water Res.* **1984**, *18*, 37-46.
56. Gash, A. E.; Spain, A. L.; Dysleski, L. M.; Flaschenriem, C. J.; Kalaveshi, A.; Dorhout, P. K.; Strauss, S. H. *Environ. Sci. Technol.* **1998**, *32*, 1007.
57. Hollerman, W.; Holland, L.; Ila, D.; Hensley, J.; Southworth, G.; Klasson, T.; Taylor, P.; Johnston, J.; Turner, R. *J. Hazard. Mater.* **1999**, *B68*, 193.
58. Jyotsna, G.; Kadirvelu, K.; Rajagopal, C. *Environ. Technol.* **2004**, *25*, 141.
59. Orham, Y.; Buyukgungo, H. *Water Sci. Technol.* **1993**, *28*, 247.
60. Bailey, S.; Olin, T.; Bricka, M.; Adrian, D. *Water Res.* **1999**, *33*, 2469.
61. Wafwoyo, W.; Seo, C.; Marshall, W. *J. Chem. Technol. Biotechnol.* **1999**, *74*, 1117.
62. Chamarthy, S.; Seo, C.; Marshall, W. *J. Chem. Technol. Biootechnol.* **2001**, *76*, 593.
63. Kumar, P.; Dara, S. *J. Polym. Sci.* **1981**, *19*, 397.
64. Okieimen, F.; Orhornoro, F. *Int. J. Environ. Anal. Chem.* **1986**, *24*, 319.
65. Said, O.; Shalmor, M.; Egila, J. *Bioresource Technol.* **1993**, *43*, 63.
66. Metwally, M.; Metwally, N.; Samy, M. *J. Appl. Ploym. Sci.* **1994**, *52*, 61.

67. Valenzuela-Calahorro, C.; Bernalte-Garcia, A.; Preciado-Barrera, C.; Bernalte-Garcia, M.; Gomez-Corso, M.; *Bioresour. Technol.* **1993**, *44*, 229.
68. Brezny, R.; Paszner, L.; Micko, M.; Uhrin, D. *Holzforschung* **1988**, *42*, 369.
69. Srivastava, S.; Singh, A.; Sharma, A. *Environ. Technol.* **1994**, *15*, 353.
70. Aoyama, M.; Honma, S.; Kassi, A.; Iseda, Y.; Nakajima, A.; Sakaguchi, T. *Holzforschung* **1991**, *45*, 75.
71. Freer, J.; Baeza, J.; Maturana, H.; Palma, G. *J. Chem. Technol.* **1989**, *46*, 41.
72. Alves, M.; Gonzales, B. C.; Guedes de Carvalho, R.; Castanheira, J.; Sol, P. M.; Vasconcelos, L. *Water Res.* **1993**, *27*, 1333.
73. Palma, G.; Freer, J.; Baeza, J. *Water Res.* **2003**, *37*, 4974.
74. Dujardin, M. C.; Vaze, C.; Vroman, I. *React. Funct. Polym.* **2000**, *43*, 123.
75. Hoell, W. H.; Bartosch, C.; Zhao, X.; He, S. *Zhong. Huan. Gong. Xue.* **2003**, *13*, 77.
76. Xuan, Z.; Gang, Z.; Jianlong, W.; Guichun, Y. *Water Environ. Res.* **2005**, *77*, 212.
77. Monteagudo, J. M.; Ortiz, M. J. *J. Chem. Technol. Biotechnol.* **2000**, *75*, 767-772.
78. Mattigod, S. V.; Skaggs, R.; Fryxell, G. E. 9<sup>th</sup> Annual Industrial Wastes Technical and Regulatory Conference; San Antonio, TX, USA; Apr. 13-16, 2003. Water Environment Federation, Alexandria, Virginia, USA, p94.
79. Li, Y. -H.; Ding, J.; Luan, Z. K.; Di, Z. C.; Zhu, Y. F.; Xu, CL.; Wui, D. H.; Wei, B. Q. *Carbon* **2003**, *41*, 2787-2792.
80. Colvin, V.L. *Nature Biotechnol.* **2003**, *10*, 1166-1170.

81. Huang, S.; Franz, K. J.; Arnold, E. H.; Devenyi, J.; Fish, R. H. *Polyhedron* **1996**, *15*, 4241.
82. Li, W.; Coughlin, M.; Albright, R. L.; Fish, R. H. *React. Funct. Polym.* **1995**, *28*, 89.
83. Huang, S.; Li, W.; Franz, K. J.; Albright, R. H. *Inorg. Chem.* **1995**, *34*, 2813.
84. Cooper, S. R. *Acc. Chem. Res.* **1988**, *21*, 141.
85. Baumann, T. F.; Reynolds, J. G.; Fox, G. A. *React. Funct. Polym.* **2000**, *44*, 111.
86. Helm, M. L.; Helton, G. P.; Van Derveer, D. G.; Grant, G. J. *Inorg. Chem.* **2005**, *44*, 5696.
87. Kostal, J.; Mulchandani, A.; Chen, W. *Macromolecules* **2001**, *34*, 2257-2261.
88. Prabhukumar, G.; Matsumoto, M.; Mulchandani, A.; Chen, W. *Environ. Sci. Technol.* **2004**, *38*, 3148-3152.
89. Ramanathan, S.; Shi, W.; Rosen, B. P.; Daunert, S. *Anal. Chim. Acta* **1998**, *369*, 189-195.
90. Bontidean, I.; Berggren, C.; Johansson, G.; Csorgi, B.; Matthiasson, B.; Llyod, J. R.; Jakeman, K. J.; Brown, N. L. *Anal. Chem.* **1998**, *70*, 4162-69.
91. Kostal, J.; Prabhukumar, G.; Lao, U. L.; Chen, A.; Matsumoto, M.; Mulchandani, A.; Chen, W. *J. Nanopart. Res.* **2005**, *7*, 517-523.
92. Aguiñaga-Díaz, P. A.; Guzmán, R. Z. *Sep. Sci. Technol.* **1996**, *31*, 1483.
93. Tung, C. C.; Yang, Y. M.; Chang, C. H.; Maa, J. R. *Waste Manage.* **2002**, *22*, 695.

94. Mulligan, C. N.; Young, R. N.; Gibbs, B. F.; James, S.; Bennett, H. P. J. *Environ. Sci. Technol.* **1999**, *33*, 3812-3820.
95. Dean, J. D.; Bosqui, F. L. *Environ. Sci. Technol.* **1972**, *6*, 518.
96. Bhattacharyya, D.; Jumawan, A. B. Jr.; Grieves, R. B. *Sep. Sci. Technol.* **1979**, *14*, 441-52.
97. Skousen, J. G.; Politan, K.; Hilton, T.; Meek, A. *Green Lands* **1990**, *20*, 31-37.
98. Marchioretto, M. M.; Bruning, H.; Rulkens, W. *Sep. Sci. Technol.* **2005**, *40*, 3393-3405.
99. Matlock, M. M.; Henke, K. R.; Atwood, D. A. *J. Hazard. Mater.* **2002**, *B92*, 129.
100. State of Indiana's Data Facts Sheet,  
<http://www.state.in.us/idem/macsfactsheets/whiteriver/185>.
101. Henke, K. R.; Robertson, J. D.; Krepps, M. K.; Atwood, D. A. *Water Res.* **2000**, *34*, 3005.
102. Bailey, J. R.; Hatfield, M. J.; Henke, K. R.; Krepps, M. M.; Morris, J. L.; Otieno, T.; Simonetti, K. D.; Wall, E. A.; Atwood, D. A. *J. Organomet. Chem.* **2001**, *623*, 185.
103. Matlock, M. M.; Howerton, B. S.; Henke, K. R.; Atwood, D. A. *J. Hazard. Mater.* **2001**, *B82*, 55.
104. Smith, J. N.; Shirin, Z.; Carrano, C. J. *J. Am. Chem. Soc.* **2003**, *125*, 868-869.
105. Docrat, A.; Morlok, M. M.; Bridgewater, B. M.; Churchill, D. G.; Parkin, G. *Polyhedron* **2004**, *23*, 481-488.

106. Annibale, G.; Brandolisio, M.; Bugarcic, Z.; Cattalini, L. *Transition Met. Chem.* **1998**, *23*, 715-719.
107. Smith, J. N.; Hoffman, J. T.; Shirin, Z.; Carrano, C. J. *Inorg. Chem.* **2005**, *44*, 2012-2017.
108. Kim, C. H.; Parkin, S.; Bharara, M.; Atwood, D. A. *Polyhedron* **2002**, *21*, 225.
109. Pappas, J. A. *J. Am. Chem. Soc.* **1978**, *100*, 6023.
110. Englich, U.; Ruhlandt-Senge, K. *Coord. Chem. Rev.* **2000**, *210*, 135-179.
111. Sigel, G. A.; Power, P. P. *Inorg. Chem.* **1987**, *26*, 2819-2822.
112. Ruhlandt-Senge, K.; Englich, U.; Senge, M. O.; Chadwick, S. *Inorg. Chem.* **1996**, *35*, 5820.
113. Nakamura, A.; Ueyama, N.; Tatsumi, K. *Pure Appl. Chem.* **1990**, *62*, 1011-1020.
114. Sellmann, D.; Becker, T.; Knoch, F. *Chem. Ber.* **1996**, *129*, 509-519.
115. Niemeyer, M.; Power, P. P. *Inorg. Chem.* **1996**, *35*, 7264.
116. Ruhlandt-Senge, K. *Inorg. Chem.* **1995**, *34*, 3499-3504.
117. Teng, W.; Englich, U.; Ruhlandt-Senge, K. *Inorg. Chem.* **2000**, *39*, 3875.
118. Ellison, J. L.; Power, P. P. *Inorg. Chem.* **1994**, *33*, 4231-4234.
119. Blower, P. J.; Dilworth, J. R. *Coord. Chem. Rev.* **1987**, *76*, 121-185.
120. Krebs, B.; Henkel, G. *Angew. Chem. Intl. Ed. Engl.* **1991**, *30*, 769-788.
121. Yamamura, T.; Miyamae, H.; Katayama, Y.; Sasaki, Y. *Chem. Lett.* **1985**, 269.

122. Redinbo, M.R.; Yeates, T.O.; Merchant, S. *J. Bioenerg. Biomembr.* **1994**, *26*, 49.
123. Coucouvanis, D.; Murphy, C. N.; Kanodia, S. K. *Inorg. Chem.* **1980**, *19*, 2993.
124. Pyykkö, P. *Angew. Chem. Intl. Ed.* **2002**, *41*, 3573-3578.
125. Swenson, D.; Baenzinger, N. C.; Coucouvanis, D. *J. Am. Chem. Soc.* **1978**, *100*, 1932.
126. Bharara, M. S.; Kim, C. H.; Parkin, S.; Atwood, D. A. *Polyhedron* **2005**, *24*, 865-871.
127. Gruff, E. S.; Koch, S. A. *J. Am. Chem. Soc.* **1990**, *112*, 1245.
128. Fleischer, H. *Coord. Chem. Rev.* **2005**, *249*, 799-827.
129. Anderson, J. E.; Sawtelle, S. M.; Thompson, J. S.; Kretchmar Nguyen, S. A.; Calabrese, J. *Inorg. Chem.* **1992**, *31*, 2778-2785.
130. Hahn, E. F.; Dittler-Klingemann, A.; Lügger, T. *Z. Naturforsch* **2003**, *58b*, 1030-1033.
131. Fleischer, H.; Schollmeyer, D. *Inorg. Chem.* **2004**, *43*, 5529-5536.
132. Farrer, B. T.; McLure, C. P.; Penner-Hahn, J. E.; Pecoraro, V. L. *Inorg. Chem.* **2000**, *39*, 5422-5423.
133. Dhubhghaill, O. M. N.; Sadler, P. J. *Struct. Bonding* **1991**, *78*, 129-130.
134. Camerman, N.; Troter, J. *J. Chem. Soc.* **1964**, 219.
135. Cordes, A. W.; Gwinup, P. D.; Malmstrom, M. C. *Inorg. Chem.* **1972**, *11*, 836.
136. Dräger, M. *Z. Anorg. Allg. Chem.* **1975**, *411*, 79.

137. Bergerhoff, G.; Namgung, H. Z. *Kristallogr.* **1979**, *150*, 209.
138. Schulte, C. *Ber.* **1882**, *15*, 1955.
139. Rey, N. A.; Howarth, O. W.; Pereira-Maia, E. C. *J. Inorg. Biochem.* **2004**, *98*, 1151-1159.
140. Vickaryous, W. J.; Healey, E. R.; Berryman, O. B.; Johnson, D. W. *Inorg. Chem.* **2005**, *44*, 9247-9252.
141. Shaikh, T. A.; Bakus II, R.C.; Parkin, S.; Atwood, D. A. *J. Organomet. Chem.* **2006**, *691*, 1825-1833.
142. Shaikh, T. A.; Parkin, S.; Atwood, D. A. *J. Organomet. Chem.* **2006**, *691*, 4167-4171.
143. Siiman, O.; Titus, D. D.; Cowman, C. D.; Fresco, J.; Gray, H. B. *J. Am. Chem. Soc.* **1974**, *96*, 2353.
144. Haberkorn, R. A.; Que, L. Jr.; Gillum, W. O.; Holm, R. H.; Liu, C. S.; Lord, R. C. *Inorg. Chem.* **1976**, *15*, 2408.
145. Wright, J. G.; Nathan, M. J.; MacDonnel, F. M.; Ralston, D. M.; O'Halloran, T. V. *Prog. Inorg. Chem.* **1990**, *38*, 323.
146. Canty, A. J.; Kishimoto, R.; Deacon, G. B.; Farquharson, G. J. *Inorg. Chim. Acta* **1976**, *20*, 161.
147. Iwasaki, N.; Tomooka, J.; Toyoda, K. *Bull. Chem. Soc. Jpn.* **1974**, *47*, 1323.
148. Biscarini, P.; Fusina, L.; Nivellini, G. *J. Chem. Soc., Dalton Trans.* **1974**, 2140.

149. Epshtein, L. M.; Shubina, E. S.; Rokhlina, E. M.; Kravtsov, D. N.; Kazitsyna, L. A. *Izvest. Akad. Nauk SSR: Ser. Khimicheskayya* **1982**, 9, 2042.
150. Harris, R. K.; Sebald, A. *Magn. Reson. Chem.* **1987**, 25, 1058.
151. Sahlman, L.; Skärfstad, E. G. *Biochem. Biophys. Res. Comm.* **1993**, 196, 583-588.
152. Steel, O. J. *Biochemistry* **1997**, 36, 6885-6895.
153. Quian, S.; Eriksson, H.; Edlund, S. J. *Biochemistry* **1998**, 37, 9316.
154. Utschig, L. M.; Wright, J. G.; O'Haloran, T. V. *Methods Enzymol.* **1993**, 226, 71-97.
155. George, G. N.; Gorbaty, M. L.; Kelemen, S. R. In: *Geochemistry of Sulfur in Fossil Fuels*; ACS Symposium Series 429; American Chemical Society: Washington, DC, 1999; Chapter 12, pp 220-229.
156. Huffman, G. P.; Mitra, S.; Huggins, F. E.; Shah, N. *Energy Fuels* **1991**, 5, 574-581.
157. Vairavamurthy, A. *Spectrochim. Acta, Part A* **1998**, 54, 2009-2017.
158. Åkesson, R.; Persson, I.; Sandström, M.; Wahlgren, U. *Inorg. Chem.* **1994**, 33, 3715-3723.
159. Huggins, F. E.; Yap, N.; Huffman, G. P. *Jpn. J. Appl. Phys.* **1999**, 38, 588-591.
160. Zabinsky, S. I.; Rehr, J. J.; Ankudinov, A.; Albers, R. C.; Ellers, M. J. *Phys. Rev. B* **1995**, 52, 299.
161. Wyckoff, R. W. G. *Crystal Structures*, 2<sup>nd</sup> ed.; Wiley-Interscience: New York, 1963.

162. Qian, J.; Skyllberg, U.; Frech, W.; Bleam, P. R.; Petit, P. E. *Geol. Environ. Sci.* **1995**, *2*, 62-63.
163. George, G. N.; Pickering, I. J.; Prince, R. C.; Zhou, Z. H.; Adams, M. W. *J. Biol. Inorg. Chem.* **1996**, *1*, 226-230.
164. Claudio, S. E.; Godwin, H. A.; Magyar, J. S. *Prog. Inorg. Chem.* **2003**, *51*, 1-144.
165. Hitchcock, P. B.; Lappert, M. F.; Samways, B. J.; Weinberg, E. L. *J. Chem. Soc., Chem. Commun.* **1983**, 1492-1494.
166. Evanko, C. R.; Dzombak, D. A. Remediation of Metals-Contaminated Soils and Groundwater. Ground-Water Remediation Technologies Analysis Center, Technology Evaluation Report ,1997, 97-01.
167. Wei, P.; Atwood, D. A. *Chem. Comm.* **1997**, 1427-1428.
168. Ashby, E. C.; Laemmle, J. T. *J. Org. Chem.* **1968**, *33*, 3398-3401.
169. Atwood, D. A.; Delcamp, J.; Zaman, K. *Main Group Chem.* **2006**, *5*, 137.
170. Na, Y.; Wang, S.; Kohn, H. *J. Am. Chem. Soc.* **2002**, *124*, 4666.
171. Rufino, A. R.; Biaggio, F. C. *Tetrahedron Lett.* **2001**, *42*, 8559-8561.
172. Ali, H. M.; Mohammed, K. *Heteroat. Chem.* **1999**, *10*, 475.
173. Brenner, D.; Davison, A.; Lister-James, J.; Jones, A.G. *Inorg. Chem.* **1984**, *23*, 3793-3797.
174. Cleland, W. W. *Biochemistry* **1964**, *3*, 480-482.
175. Po, H. N.; Legg, K. D.; Kuwahara, S. S. *Anal. Lett.* **1973**, *6*, 659-665.
176. Ahammadsahib, K. I.; Ramamurthi, R.; Desai, D. *J. Biochem. Toxicol.* **1987**, *2*, 169-80.

177. Dubey, S. K.; Rai, L. C. *Biol. Metals* **1989**, 2, 55-60.
178. USDA Forest Services, 1993. Acid Mine Drainage from Mines in the Nations Forests, A Management Challenge: Program Aid, 1505, 12 pp.
179. Singer, P. C.; Stumm, W. *Science* **1970**, 167, 1121-1123.
180. Flower, T. A.; Holmes, P. R.; Crundell, F. K. *Appl. Environ. Microbiol.* **1999**, 65, 2987..
181. Berry, J. B.; Moonis, R. A.; Dole, L. R.; Ferrada, J. J.; van Dyke, J. W. *Survey of U.S. Mineral and Metal Process Residues*. Oak Ridge National Laboratory, Oak Ridge, Tenn., 2001.
182. Faure, G. *Principles and Applications of Geochemistry*, 2<sup>nd</sup> ed.; Prentice-Hall: New Jersey, 1998.
183. Gluskoter, H. J. and co-workers, Ill. State Geol. Surv. Circ., 1977, p. 499
184. Kirk-Othmer Encyclopedia of Chemical Technology. Mark, H. F.; Othmer, D. F.; Overberger, C. G.; Seaborg, G. T. eds. 3<sup>rd</sup> ed. Volume 6, John Wiley & Sons, Inc. 1979.
185. Sasowsky, I.; Foos, A.; Miller, C. *Water Res.* **2000**, 34, 2742.
186. McKinnon, W.; Choung, J. W.; Xu, Z.; Finch, J. A. *Environ. Sci. Technol.* **2000**, 34, 2576-2581.
187. Jiang, C. L.; Wang, X. H.; Parekh, B. K. *Int. J. Min. Process.* **2000**, 58, 305-318.
188. Kleinmann, R. L. P. *Eng. Min. J.* **1989**, p. 161
189. Tuttle, J. H.; Randles, C. I.; Dugan, P.R. *J. Bacteriol.* **1968**, 95, 1495.
190. Dugan, P. R. *Biotechnol. Bioeng.* **1987**, XXIX, 41-48.

191. Evangelou, V. P. *J. Environ. Qual.* **1995**, *24*, 535-542.
192. Belzile, N.; Maki, S.; Chen, Y. *Sci. Total Environ.* **1997**, *196*, 177-186.
193. Evangelou, V. P. *Ecol. Eng.* **2001**, *17*, 165-178.
194. Evangelou, V. P. *Pyrite Oxidation and its Control*. CRC Press Inc, Boca Raton, Florida, 1995..
195. Lan, Y.; Huang, X.; Deng, B. *Archiv. Environ. Contam. Toxicol.* **2002**, *43*, 168-174.
196. Kargbo, D. M.; Atallah, G.; Chatterjee, S. *Environ. Sci. Technol.* **2004**, *38*, 3432-3441.
197. Ravichandran, M. ; Aiken, G. R.; Reddy, M. M.; Ryan, J. N. *Environ. Sci. Technol.* **1998**, *32*, 3305-3311.
198. Kwan, S. Y.; Tsui, S. K.; Man, T. O. *Anal. Lett.* **2001**, *34*, 1431-1433.
199. Schippers, A.; Sand, W. *Appl. Environ. Microbiol.* **1999**, *65*, 319-32.
200. Gerson, A. R.; O'Dea, A. R. *Geochim. Cosmochim. Acta* **2003**, *67*, 813-820.
201. Shea, D.; Helz, G. R. *Geochim. Cosmochim. Acta* **1989**, *53*, 229-236.
202. Nowak, P.; Socho, R. P. *Physiochem. Prob. Min. Process* **2006**, *40*, 135-148.
203. Abraitis, P. K.; Pattrick, R. A. D.; Kellsell, G. H.; Vaughan, D. J. *Min. Mag.* **2004**, *68*, 343-351.
204. Bain, C. D.; Troughton, E. B.; Tao, Y. T.; Evall, J.; Whitesides, G. M.; Nuzzo, R. G. *J. Am. Chem. Soc.* **1989**, *111*, 321-335.
205. Nuzzo, R. G.; Allara, D. L. *J. Am. Chem. Soc.* **1983**, *105*, 4481-83.

206. Nuzzo, R. G.; Zegarski, B. R.; Dubois, L. H. *J. Am. Chem. Soc.* **1987**, *109*, 733.
207. Nuzzo, R. G.; Fusco, F. A.; Allara, D. L. *J. Am. Chem. Soc.* **1987**, *109*, 2358.
208. (a) di Gleira, K.; Hill, H. A. O.; Page, D. J.; Tew, D. G. *J. Chem. Soc., Chem. Commun.* **1986**, 460. (b) Finklea, H. O.; Robinson, L. R.; Blackburn, A.; Richter, B.; Allara, D. L.; Bright, T. B. *Langmuir* **1986**, *2*, 239.
209. Yokokawa, S.; Tamada, K.; Ito, E.; Hara, M. *J. Phys. Chem. B* **2003**, *107*, 3544-3551.
210. Scaini, M. J.; Bancroft, G. M.; Lorimer, J. W.; Maddox, L. M. *Geochim. Cosmochim. Acta* **1995**, *59*, 2733-2747.
211. Azzam, W.; Wehner, B. I.; Fischer, R. A.; Terfort, A.; Wöll, C. *Langmuir* **2002**, *18*, 7766-7769.
212. Lau, K. H. A.; Huang, C.; Yakovlev, N.; Chen, Z. K.; O'Shea, S. J. *Langmuir* **2006**, *22*, 2968-2971.
213. Nowak, P.; Laajalehto, K. *Appl. Surf. Sci.* **2000**, *157*, 101-111.
214. Pratt, A. R.; McIntyre, N. S.; Splinter, S. J. *Surf. Sci.* **1998**, *396*, 266-272.
215. Khan, S. U. M.; Baltrus, J. P.; Lai, R. W.; Richardson, A. G. *Appl. Surf. Sci.* **1991**, *47*, 355-363.
216. Rivière, J. C. *Surface Analytical Techniques*; Clarendon Press: Oxford, 1990.
217. Brant, P.; Feltham, R. D. *J. Electron Spectrosc. Related Phenom.* **1983**, *32*, 205-221.

218. Mooser, E.; Person, W. B. *Phys. Rev.* **1956**, *101*, 1608-1609.
219. Barr, T. L. *Modern ESCA*; CRC Press: Boca Raton, Florida, 1994.
220. Barr, T. L.; Seal, S. J. *Vac. Sci. Technol. A* **1995**, *13*, 1239-1246.
221. Shirley, D. A. *Phys. Rev. B* **1972**, *5*, 4709-4714.

## Vita

The author was born on January 5, 1956 in Comilla, Bangladesh. He passed the Higher Secondary Certificate examination in 1974 securing the 5<sup>th</sup> position among more than sixty thousand students. After that he went to study at the People's Friendship University in Moscow, Russia and earned a Master of Science degree in chemistry specializing in organic chemistry in June 1981. Upon return to Bangladesh he joined the Department of Chemistry, University of Dhaka, Bangladesh as a lecturer in February 1982. He was appointed assistant professor in April 1987. In 1995 he came to the USA and studied at the South Dakota School of Mines and Technology, Rapid City, South Dakota. He graduated with an MS degree in chemistry (specializing in organic chemistry) in May 1997. He obtained another MS degree in chemistry (specializing in inorganic chemistry) from Eastern Kentucky University in December 2002. He is the author of seven research articles published in different scientific journals, and three others have been submitted for publication. He got himself admitted into the doctoral program at the Chemistry Department, University of Kentucky in January 2003.

Kamruz Md Zaman